Fakultät für Medizin der Technischen Universität München
Institut für Virologie

Modulation of hypoxia by HAdV

Sawinee Janina Masser

Vollständiger Abruck der von der Fakultät für Medizin der Technischen Universität München zur Erlangung des akademischen Grades eines

Doktors der Naturwissenschaften (Dr. rer. nat.)

genehmigten Dissertation.

Vorsitzender: Prof. Dr. Dr. Stefan Engelhardt

Prüfende der Dissertation:

1. Prof. Dr. Sabrina Schreiner

2. Prof. Angelika Schnieke Ph.D.

Die Dissertation wurde am 19.05.2020 bei der Technischen Universität München eingereicht und durch die Fakultät für Medizin am 01.12.2020 angenommen.

Anhang I

Eidesstattliche Erklärung

Ich erkläre an Eides statt, dass ich die bei der promotionsführenden Einrichtung
Fakultät für Medizin

---

der TUM zur Promotionsprüfung vorgelegte Arbeit mit dem Titel:
Modulation of hypoxia by HAdV

---

in Institut für Virologie
Fakultät, Institut, Lehrstuhl, Klinik, Krankenhaus, Abteilung

unter der Anleitung und Betreuung durch: PD Dr. rer. nat. Sabrina Schreiner ohne sonstige Hilfe erstellt und bei der Abfassung nur die gemäß § 6 Ab. 6 und 7 Satz 2 angebotenen Hilfsmittel benutzt habe.

☒ Ich habe keine Organisation eingeschaltet, die gegen Entgelt Betreuerinnen und Betreuer für die Anfertigung von Dissertationen sucht, oder die mir obliegenden Pflichten hinsichtlich der Prüfungsleistungen für mich ganz oder teilweise erledigt.

☒ Ich habe die Dissertation in dieser oder ähnlicher Form in keinem anderen Prüfungsverfahren als Prüfungsleistung vorgelegt.

☐ Die vollständige Dissertation wurde in englisch veröffentlicht. Die promotionsführende Einrichtung
Fakultät für Medizin

---

hat der Veröffentlichung zugestimmt.

☒ Ich habe den angestrebten Doktorgrad noch nicht erworben und bin nicht in einem früheren Promotionsverfahren für den angestrebten Doktorgrad endgültig gescheitert.

☐ Ich habe bereits am _____ bei der Fakultät für _____

_____

der Hochschule _____

unter Vorlage einer Dissertation mit dem Thema _____

_____

die Zulassung zur Promotion beantragt mit dem Ergebnis: _____

_____

Die öffentlich zugängliche Promotionsordnung der TUM ist mir bekannt, insbesondere habe ich die Bedeutung von § 28 (Nichtigkeit der Promotion) und § 29 (Entzug des Doktorgrades) zur Kenntnis genommen. Ich bin mir der Konsequenzen einer falschen Eidesstattlichen Erklärung bewusst.

Mit der Aufnahme meiner personenbezogenen Daten in die Alumni-Datei bei der TUM bin ich

☒ einverstanden, ☐ nicht einverstanden.

München, 20.04.2020, Unterschrift

Contents

Abbrevations

μ**g**	Microgram
μ**l**	Microliter
AIDS	Acquired Immune Deficiency Syndrome
BSA	Bovine serum albumin
CAR	Coxsackievirus-adenovirus receptor
CMV	Cytomegalovirus
DAPI	4′,6-diamidino-2-phenylindole
DBP	DNA binding protein
DDR	DNA damage response
DMEM	Dulbecco's Modified Eagle Medium
DMSO	Dimethyl sulfoxide
DNA	Desoxyribonucleic acid
ds	Double-stranded
DSB	Double-strand breaks
E.coli	*Escherichia coli*
FBS	Fecal bovine serum
ffu	Fluorescent forming units
fwd	Forward
h	Hours
HAdV	Human Adenovirus
HIF-1α	Hypoxia Inducible Factor 1α
His	Histidine
HPV	Human papillomavirus
HRP	Horseradish peroxidase
IF	Immunofluorescence
IP	Immunoprecipitation

ITR	Inverted terminal repeats K Lysine
KAP1	KRAB-associated protein 1
kb	Kilobase
kbp	Kilobase pairs
kDa	Kilodalton
LB	Luria-bertani
mA	Milliampere
mg	Milligram
ml	Milliliter
MLTU	Major late transcription unit
MOI	Multiplicity of infection
MRN	Mre11-Rad50-Nbs1
Ni-NTA	Nickel-nitrilotriacetic acid
nm	Nanometer
OD	Optical density
ORF	Open reading frame
PAGE	Polyacrylamide gel electrophoresis
PBS	Phosphate buffered saline
PCR	Polymerase chain reaction
PEI	Polyethylenimine
PFA	Paraformaldehyde
PML	Promyelocytic leukemia protein
PML-NB	PML nuclear body
PMSF	Phenylmethylsulfonyl fluoride
PTM	Posttranslational modification
rev	Reverse
RGD	Arg-Gly-Asp
RING	Really interesting new gene
RIPA	Radioimmunoprecipitation assay
RNA	Ribonucleic acid
rpm	Revolutions per minute

RT	Room temperature
SDS	Sodium dodecyl sulfate
SDS-PAGE	SDS-polyacrylamide gel electrophoresis
shRNA	Small hairpin RNA
SIM	SUMO interacting motif
ss	Single-stranded
STUbL	SUMO-targeted ubiquitin ligases
SUMO	Small ubiquitin-related modifier
TBE	Tris/Borate/EDTA buffer
TBS-BG	Tris-buffered saline with BSA and glycine
TGS	Tris, glycine, SDS running buffer
TP	Terminal protein
UV	Ultraviolet
V	Volt
v/v	Volume per volume
w/v	Weight per volume
wt	Wild type

Abstract

Human adenoviruses (HAdV) are causing a wide range of illnesses such as respiratory infections, gastroenteritis and keratoconjunctivitis. For immunosuppressed individuals, HAdV often promotes severe or lethal outcomes. Oxygen plays a crucial role for various human pathogenic viruses. HIF-1 oxygen responsive subunit HIF-1α (hypoxia-inducible factor 1 alpha) is the key transcription factor. Here we observed that HIF-1α represents a novel restriction factor during HAdV replication under hypoxic conditions. Furthermore, our data indicate that HIF-1α is targeted during HAdV infection and is subsequently sequestered into the cellular proteasomal degradation pathway. We have evidence that HIF-1α binds the early viral E4orf3 protein prior to recruitment into HAdV mediated PML tracks, being sufficient for reduction of HIF-1α protein levels. In conclusion, we propose a novel model of how HAdV regulates productive virus infection under different oxygen levels being a prerequisite for tissue specificity of different HAdV serotypes in various human organs.

Zusammenfassung

Humane Adenoviren (HAdV) führen zu diversen Erkrankungen, wie Infektionen in der Lunge, Gastroenteritis oder Keratoconjunctivitis. Bei immunsupprimierten Patienten können Infektionen tödlich verlaufen. Für eine Vielzahl von Viren spielt Sauerstoff eine wichtige Rolle. Während einer Hypoxie passen sich Zellen dem Sauerstoffmangel an. Ein entscheidender Faktor für die Regulierung dieser Signalwege, ist HIF-1α (hypoxia-inducible factor 1 alpha). Die Ergebnisse der vorliegenden Arbeit zeigen, dass HIF-1α ein neuer negativer Faktor für die HAdV Replikation ist und während der Infektion proteasomal abgebaut wird. Wir konnten zeigen, dass hier nicht wie zunächst vermutet die virale E1B-55K/E4orf6 abhängige E3-Ubiquitin Ligase verantwortlich ist, sondern das frühe virale Protein E4orf3. Basierend auf den erhobenen Befunden nehmen wir an, dass HAdV eine hocheffiziente Virusreplikation in Abhängigkeit der Sauerstoffkonzentrationen im jeweiligen Gewebe steuern kann.

Chapter 1

Introduction

1.1 Adenoviruses

1.1.1 Classification and Pathogenesis

In the early 1950s, Rowe and colleagues were investigating the cause of the common cold. They isolated and discovered adenoviruses (Ads) from adenoid tissues [1]; [2]. Subsequent investigations revealed that they generally result in infections of the respiratory tract [3]; [4], keratoconjunctivitis [5] or the gastrointestinal tract [6], causing diseases called acute respiratory disease (ARD), adenoid-pharyngeal-conjunctival (APC), respiratory illness (RI) or adenoid degeneration (AD). By the age of five, 80 % of children are infected with adenoviruses, mainly causing diarrhea [7]. Depending on their host, adenoviruses are divided into five groups: *Mastadenovirus* (infecting mammalian hosts), *Aviadenovirus* (infecting avian hosts), *Atadenovirus* (infecting reptilian and ruminant hosts), *Siadenovirus* (infecting amphibian hosts) and *Ichtadenovirus* (infecting fish hosts) [8]; [9]; [10]. So far, more than 130 serologically different types are classified in those five groups (Figure 1.1). An adenoviral infection is self-limiting and proceeds mildly. However, the course of infection can be fatal, leading to the development of pneumonia [11]; [12]; [13], meningoencephalitis [14], myocarditis [15]; [16]; [17] or hepatitis [18]. Newborns, immunocompromised patients, patients suffering from AIDS or recipients of an organ transplant are affected most by such complications [19]; [20]; [21]; [22], [23]. Until today adenoviral infections can not be treated. During severe infections only the symptoms can be treated and not unusually results in the death of a patient [24]; [25]; [15]; [17]. Recently, adenoviral infections have been linked to obesity [26]; [27].

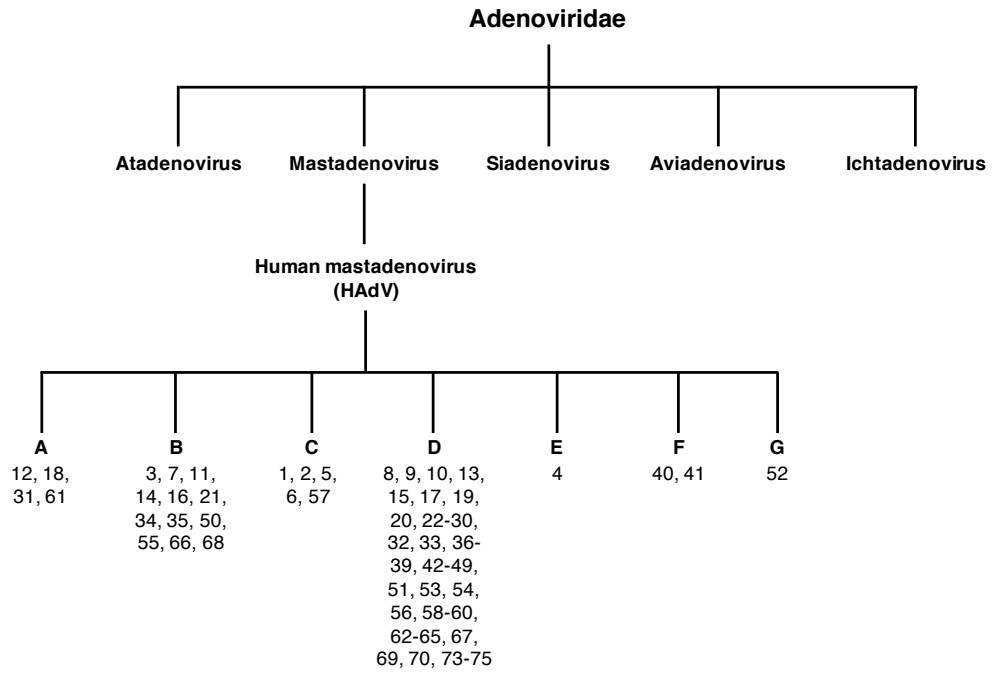

Figure 1.1: Classification of the family of *Adenoviridae*
Illustration of the family *Adenoviridae* taxonomy. HAdV types are classified according to [10] and the International Committee of the Taxonomy of Viruses (ICTV).

To date more than 85 Human adenoviruses (HAdVs) of the genera Mastadenovirus are known [10]. Furthermore, they are the most extensively studied genera and comprise bat, bovine, canine, equine, human, murine, ovine, porcine, simian and three shrew adenoviruses and are subgrouped into seven species (A-G) according to their sequence homology, hemagglutination and oncogenicity in immunosuppressed rodents. Peculiarly the prototypical species C human mastadenovirus types 2 and 5 (HAdV-C2 and HAdV-C5) are the most intensively investigated types due to their non-oncogenic properties (1.2) [28]. The first virus that has been shown to induce malignant tumors in rodents was the human mastadenovirus type 12 [29]. This initial finding led to a vast amount of research in adenovirus mediated transformation and classification of HAdV as a DNA tumor virus resulting in concordant groups, depicted in figure 1.2.

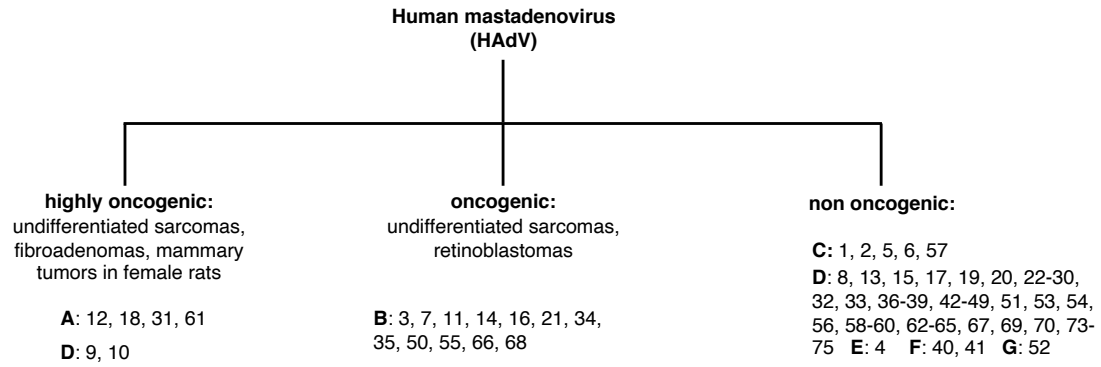

Figure 1.2: Oncogenicity of HAdV
Overview of the oncogenicity of different HAdV subtypes and the kind of tumors they induce. Recently, discovered types are not classified so far.

1.1.2 Structure and genome organization

HAdVs are non-enveloped viruses with an icosahedral capsid of about 910 Å [30]; [31]; [32]. The capsid is composed out of three major proteins: 240 hexon (II) trimers form the 12 triangular facets. The 12 vertexes are built by penton bases (III) pentameters, each form a complex with one of the 12 fiber (IV) trimers [33]. Therefore, the adenoviral capsid corresponds to a pseudo-T = 25 symmetry [34] (Figure 1.3). The C-terminal part of the fiber-knob mediates tropism of HAdVs by high affinity interaction with either the Coxsackie/Adenovirus Receptor (CAR), or CD46 [35]; [36]. Secondary interactions by the penton base with host integrins support efficient uptake of viruses [37]. The minor capsid proteins IIIa, VI, VIII and IX are also present in the protein envelope. Termed capsid „cement “or „glue “they were thought to have stabilizing functions [38]; [32];[39]; [34]. Recently functions in the initial phases of viral entry and transcription were proposed for those proteins [40]; [41]. The adenoviral core contains a double-stranded (ds) linear DNA genome with a size of 26-45 kbp depending on the type and species, HAdV-C5 DNA has a size of 36 kbp. The genome is condensed in a nucleosome-like state through the association with the basic core proteins VII, V and μ [42]; [43];[44]; [45]; [46]. Both ends are comprised of inverted terminal repeats (ITR), which serve as origins of replication (ori) and are covalently linked to the terminal protein (TP), serving as primers for viral DNA synthesis [10].

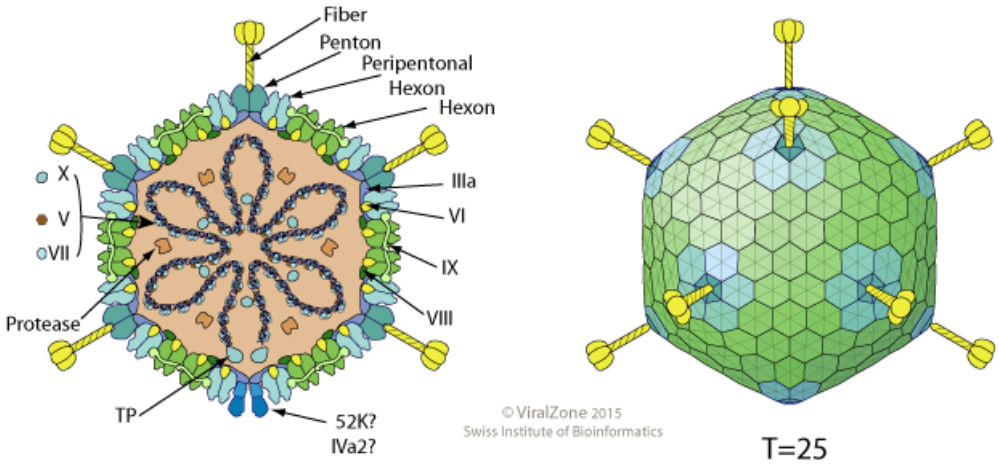

Figure 1.3: Overview of the adenoviral virion
Schematic representation of the HAdV-C5 capsid and packaged dsDNA (Swiss institute of bioinformatics 06/2015). On the left is a schematic cross section of an HAdV particle, in dark blue is the dsDNA within the capsid [47]. On the right is a schematic overview of the non-enveloped capsid with a pseudo T=25 icosahedral symmetry [48].

The HAdV genome contains nine transcription units, which encode for 40 regulatory and structural proteins as well as two virus associated RNAs (VA RNAs). They are divided in five early (E1A, E1B, E2, E3 and E4), three intermediate early (IX, IVa2 and E2 late) and one major late transcription unit (MLTU). During the course of infection the MLTU primary transcript is further processed into five late mRNAs families (L1-L5) [49]; [30]. Transcription is executed by the cellular RNA polymerase II, with the exception of the VA RNAs, which are transcribed by the RNA polymerase III [50]. Sequences of other serotypes show that all HAdVs have a similar genome organization and express a conserved set of gene products [10]; [28]. Early proteins are involved in prevention of the host antiviral response, transcriptional regulation, mRNA export, viral DNA replication and cell cycle control, while late transcribed regions encode for regulatory proteins, that also have functions in initial phases of attachment to host cells and infection [51].

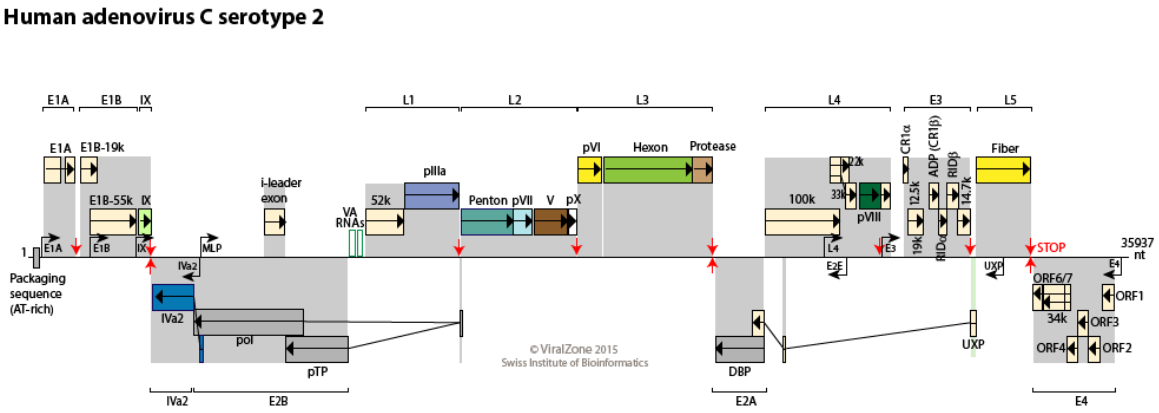

Figure 1.4: Overview of the adenoviral genome
As a representative of HAdV C-types the genome of HAdV-C2 is presented from the 5' end of the + strand. Black arrows illustrate the direction of early (E1, E2A, E2B, E3, E4), delayed (IX, IVa2) and the major late transcription unit (MLTU) on both DNA strands. The MLTU, under the control of the major late promoter (MLP) generates five mRNA families L1-L5. The whole adenoviral genome is transcribed by RNA polymerase II, except for the two virus-associated RNAs (VA RNA), which are transcribed by RNA polymerase III. (ViralZone 2015, Swiss Institute of Bioinformatics)

1.2 Productive infection cycle

The replication cycle of HAdV-C5 can be divided into two phases. The early phase starts with the clathrin-mediated endocytosis of the virus. The partially disassembled virus particle is transported to the nucleus where the viral DNA is imported into the nucleus through the nuclear pore complex (NPC). Expression of the immediate early protein E1A activates transcription of other viral genes from the E1- and E4-region, which are subsequently spliced in order to produce viral early regulatory proteins. These early regulatory proteins are responsible for creating an optimal environment for efficient virus replication [28]. Upon these initial steps, the viral DNA binding protein E2A/DBP, the viral DNA polymerase (E2B) and the precursor terminal protein (pTP) are expressed [28]. The late phase of the infection is induced by the onset of viral DNA synthesis. Transcription of the MLTU is initiated by activation of the major late promoter (MLP) and leads to differential splicing of the 29 kb major late precursoer mRNA resulting in the viral late mRNAs families L1-5 [52]. To ensure an efficient expression of viral mRNA, the host cell mRNA transport is shut off [53]. Adenoviral capsid assembly is still not completely understood. The multimerization of hexon as well as penton monomers seems to occur already in the cytoplasm, whereas the assembly of viral particles is performed in the host nucleus [54]; [55]. One possible mechanism of capsid assembly and genome packaging is related to the encapsidation of large bacteriophage [56]. The empty capsid is assembled

first, followed by the encapsidation of the viral genome to result in premature "virions" and finally their maturation. The encapsidation of the adenoviral genome utilizes a coordinated interplay between the late proteins IVa2, L1-52/55K, L4-22K, L4-33K and IIIa as well as the packaging sequence ψ of the viral DNA [57]; [58]; [59]; [60]; [61]; [62]; [63]; [64]; [65]; [66]; [67], [68]. Infectious particles only emerge, if the contained precursor proteins of IIIa, VI, VII, VIII, μ and TP are processed by cleavage of the adenoviral protease (AVP) ([69]; [70]; [71]. Until today, it is not clear whether empty particles are truly intermediates of viral assembly or rather defective products. If one of the factors involved in genome encapsidation is defective or missing, particle assembly does not occur. Although this process is supposed to follow capsid assembly [72]; [73]; [74]; [75]; [68]. After completion of the viral replication cycle (24-36 h), up to 1 x 10^4 progeny virions per cell are released [28]; [30]; (1.5).

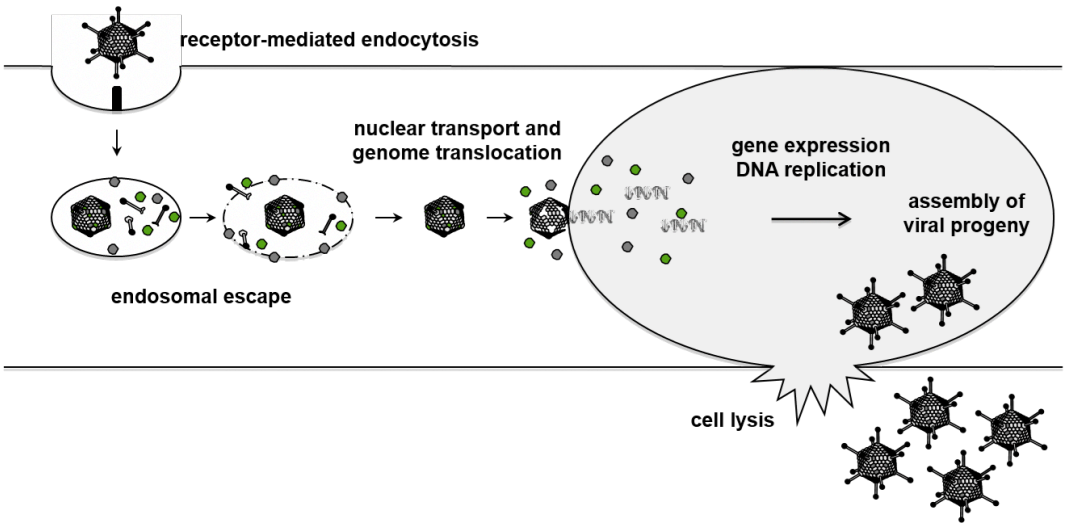

Figure 1.5: Life cycle of HAdV
The adenoviral life cycle starts with the receptor-mediated uptake of the virus into clathrin-coated, early endosomes. Endocytosis is accompanied by partial uncoating of the virions, which enables the endosomal escape through release of the membrane lytic capsid protein VI. Upon arrival in the cytosol, adenoviral virions are transported to the nucleus via microtubules. At the nuclear pore complex, the virions finally disassemble and the viral genome is translocated into the host nucleus. Within the nucleus, the transcription of early viral genes is initiated, followed by replication of the viral genome, the expression of late and structural proteins and finally the assembly of viral progeny. After 24-48 h the infected host cell is lysed. [30], [28]

1.3 Adenovirus early regulatory proteins

1.3.1 Early region 1

1.3.2 E1A

During the immediate early phase of infection, the first transcription unit being transcribed is E1A. The incoming capsid protein pVI is facilitating the expression of E1A [40]. Alternative

splicing of the primary E1A transcript yields in five mRNAs, which in HAdV-C5 are termed 13S, 12S, 11S, 10S and 9S [76]; [77]. They encode for the 289 residues (R), 243R, 217R, 171R and 55R proteins. The protein products 289R (13S) and 243R (12S) from E1A are immediately expressed upon entry of the viral genome into the host cell nucleus. During the course of infection, the splicing preferences switch through changes in splice site usage to the 9S mRNA product, whereas 11S and 10S mRNA species are less abundant [76]; [77]. The protein 13S harbours four conserved regions CR1 - CR4, separated by non-conserved domains. Whereas the 12S protein contains three conserved regions CR1, CR2 and CR4. [78]; [79] (Figure 1.6). 13S is needed for the transcriptional activation of the four early adenoviral transcription units E1- E4. Through recruitment and association with cellular transcription factors, which in turn are binding to the early adenoviral promoters [80]; [81]; [82]; [83]. Moreover, E1A-13S can also bind to the cellular transcriptional coactivators CREB binding proteins (p300/CBP) [84]; [85]; [86]; [87]; [88]; [89] and to MED23 to activate transcription in vitro [90]. Furthermore, both E1A isoforms are able to promote cell cycle entry into S-phase in infected cells [91]; [92]; [93]. E1A interacts with the cellular retinoblastoma protein (pRB) [94]; [95]; [96] and the RB-related proteins, p107 and p130 [97]; [98]; [99]. Taken together, these functions of E1A, together with E1B or activated RAS, are sufficient to transform primary rodent cells [100]; [92]; [101]. Additionally other transcriptional regulators such as PCAF, CtBP, p21Cip1/Waf1, p27Kip1, DYRKs, p400 and TRRAP [102]; [103]; [104] enable E1A to dynamically and temporally modulate all gene promoters [102]; [103]. Another host cell regulatory role of E1A is the impairment of p53 function. On the one hand E1A is able to prevent acetylation of p53 and on the other hand the interaction between the transcription factor SP1 and the p21 promoter is inhibited. This leads to the prevention of the p21 upregulation and thereby is inhibiting the downstream proliferation regulator of p53 [105]. Also E1A interferes with proteasome function, which stabilizes p53 [106]; [107], followed by apoptosis in host cells [108]; [109]; [110]. Additionally E1A triggers apoptosis in a p53-independent mechanism by inducing proteasomal degradation of a B-cell leukemia/lymphoma 2 (BCL-2) family member, the myeloid leukaemia sequence 1 (MCL-1) protein, leading to the release of pro-apoptotic BCL2- Antagonist/Killer (BAK) [111]; [112]. In order to prevent disruption of the viral life cycle, the induction of apoptosis by E1A has to be counteracted. Therefore, several HAdV proteins act to prevent p53 dependent and independent cell death, including products of the E1B transcriptional unit.

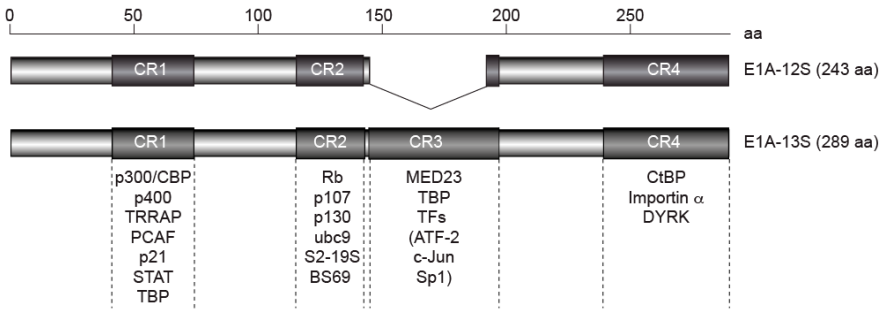

Figure 1.6: Schematic overview of E1A with binding partners
Organization of E1A-12S and E1A-13S domain structure with conserved regions [113]. Proteins interacting within the CRs are listed below. CR: conserved region.

1.3.3 E1B-55K

The major gene products of the E1B region are the E1B-19K and E1B-55K proteins. Both proteins suppress p53-dependent and -independent cell cycle arrest, and apoptosis induced by E1A [108]. E1B-19K is able to bind pro-apoptotic cellular proteins like BAK and BAX and thus inhibits the apoptotic cascade [111]; [112]. E1B-55K is able to relocalize p53 in subcellular structures called perinuclear bodies or aggresomes [114]; [115]; [116], which are formed at the MTOC in response to misfolded proteins [117]; [118]. In the nucleus, E1B-55K is able to prevent p53 mediated transcriptional activation by direct interaction with p53 [119]; [120]; [121]; [122]. Besides, E1B-55K acts as an E3 small ubiquitin-like modifier 1 (SUMO1) ligase of p53, which leads to SUMOylation, followed by sequestration of p53 in nuclear promyelocytic leukemia protein nuclear bodies (PML-NBs) supporting p53 nuclear export [123]. Furthermore, E1B-55K is able to counteract the host cell DNA damage response together with E4 open reading frame 6 (E4orf6) protein. Together with the cellular proteins elongin B and C, cullin 5 and Rbx-1, they built a viral E3 ubiquitin ligase [124] [125]. E4orf6 binds elongin C, while E1B-55K serves as the substrate recognition domain [126] (Figure 1.7A) . This viral E3 ubiquitin ligase promotes ubiquitination and proteasomal degradation of proteins that are part of the DNA damage response, including p53 [127]; [128] and HIV-Tat interacting protein (Tip60) [129], the MRN complex [130] [131]; [132]; [133]; [134], DNA ligases IV [135], ATRX [136] and SPOC1 (Survival-Time Associated PHD Protein In Ovarian Cancer 1) [137] (Figure 1.7B).

A)

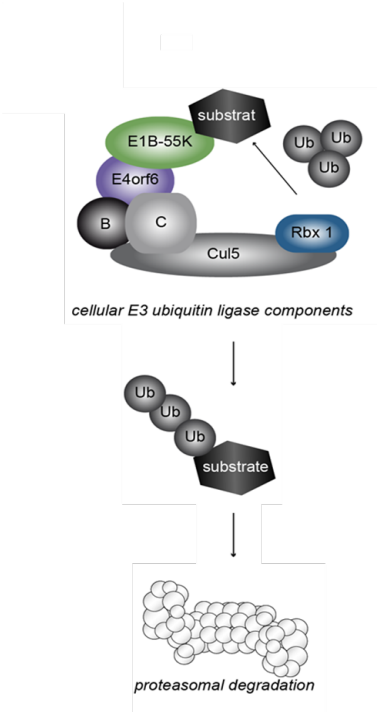

B)

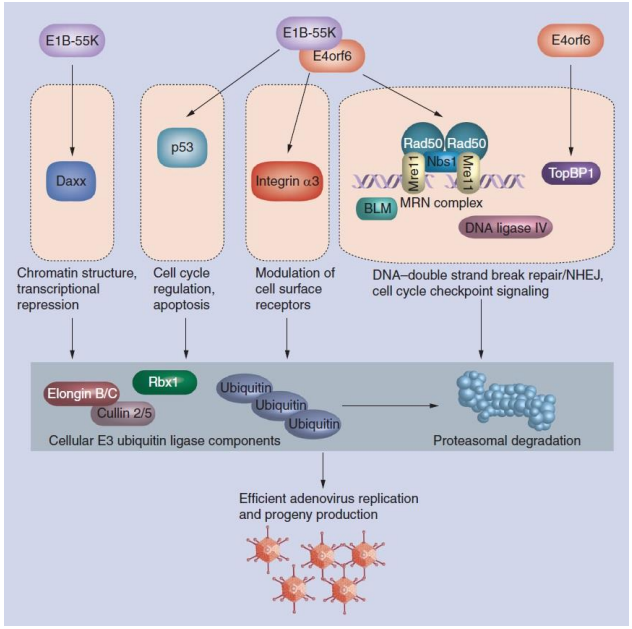

Figure 1.7: Organization of the viral E3 Ubiquitin ligase and target proteins
A) E1B-55K and E4orf6 together with cellular elongin B and C, cullin 5 and Rbx-1 built the viral E3 ubiquitin ligase to counteract the host DDR [124], [125], [126]. B) Schematic overview of the viral E3 ubiquitin ligase with cellular targets. The HAdV counteracts the antiviral host response upon infection. Cellular proteins, i.e. DDR proteins, are degraded by the E3 ubiquitin ligase complex established by the early proteins E1B-55K and E4orf6 (modified from [138]).

1.3.4 Early region 4

The early region 4 (E4) encodes for several multifunctional regulatory proteins. Based on the open reading frames, they are named E4orf1 to E4orf6/7. The functions of E4orf6 have been intensively investigated. It has functions, which are important for efficient viral replication [139], viral late protein synthesis, shut off of host protein synthesis, late viral mRNA transport [140]; [141] and progeny virus production [142]. E4orf6 contains an amphipathic α-helix with a nuclear localization signal (NLS) and a nuclear export signal (NES) that allows it to shuttle between nucleus and cytoplasm [143]; [144]. The protein can interact with p53 and thereby inhibits its function [145]. Together with E1B-55K, E4orf6 enhances HAdV mRNA transport, leading to cytoplasmic accumulation of viral mRNAs and increase in viral late protein production [146]. This complex also regulates the degradation of other cellular proteins, such as Mre11, DNA ligase IV, Bloom Helicase, Tip60, integrinα3, ATRX and SPOC1 in order to change the cellular environment for viral propagation [135]; [126]; [147]; [129]; [127]; [136]; [137].

1.3.5 E4orf3

The early viral protein E4orf3 is essential for the successful replication of the HAdV. It functions in the disruption of cellular antiviral defenses, including the DNA damage response pathway and activation of antiviral genes [148]. Moreover, it inhibits MRN complex function independent of the E1B-55K/E4orf6 ubiquitin ligase activity [149]; [150]. Transfected E4orf3 is sufficient to reorganize PML-NBs into so called track-like structures. PML-NBs are nuclear protein aggregates with antiviral and anti-tumor functions [151]; [152]; [153]. The inhibition of the PML-NBs is conserved among various species of HAdVs [154], indicating that counteraction of this cellular antiviral mechanism is important for an accurate HAdV infection [152]; [155]; [156]. It was shown that the interaction with PML II is essential for the reorganization of the PML-NBs ([154]). In recent studies a specific interaction of PML II with E1A-13S was investigated, which enhances E1A mediated transcriptional activation of viral gene expression. Hence, PML-NBs possess not only antiviral defenses, but promote HAdV-C5 infection and replication cycle ([157]). Recently it has been shown, that E4orf3 interacts directly with E1A to regulate the expression of viral genes [148]. Besides PML, several other proteins are recruited into the track like structures induced by E4orf3 to either inhibit their antiviral function (Daxx) [158] or their regulatory function in transcription (TIF1γ, [159], transcription factor TFII-I [160]). Up to 400 genes have been identified to be regulated by the presence of E4orf3 [161]. For the activity of the E4orf3 proteins, presumably high-order homologous multimerization is required [162] (Figure 1.8). If the asparagin at position 82 is mutated (N82A), E4orf3 is not able to relocalize PML-NBs into track-like structures [130]. Additionally, if the leucin at position 103 is mutated (l103A), E4orf3 is not able to recruit the MRN complex anymore [163]. These mutations lead to an inefficient viral replication [130]; [163]. Recently it has been shown, that E4orf3 leads to the transformation of rodent cells [164]. The transformation potential of the early genes of E1 and E4 are enhanced by E4orf3 [164]; [165]; [166]; [167]. Interestingly, this cooperation might be the basis for the „hit and run“ mechanism, which is characterized by transformation without integrated E1- and E4 genes into the transformed cells [165]; [168]. Other viral proteins, which have been suggested for the „hit and run“ are SV40, HCMV, IE1 and IE2. Those viral proteins are associated with the PML-NBs [151]; [169]; [170]. Since E4orf3 is reorganizing PML-NBs into track-like structures, it supports the idea that E4orf3 is able to transform cells [164]; [165]; [166]; [167].

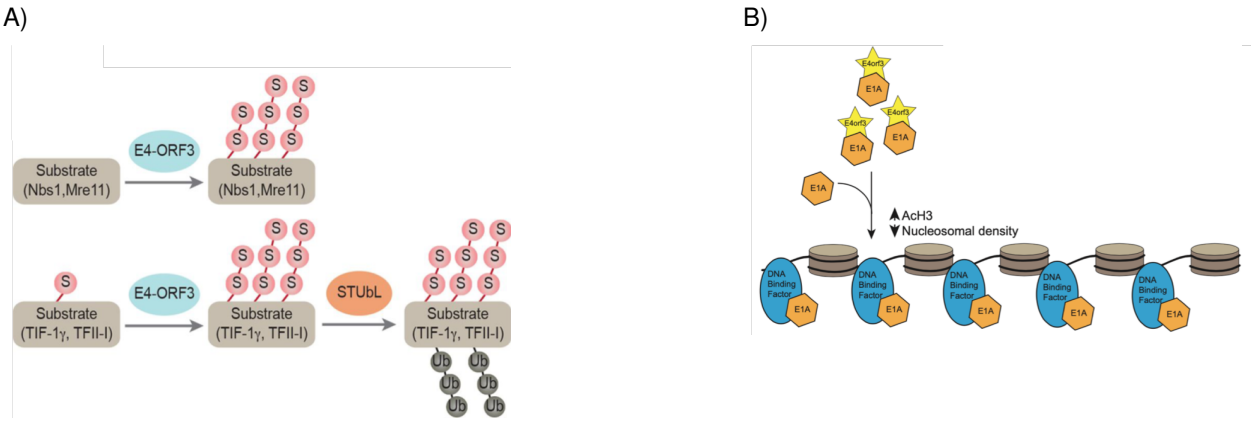

Figure 1.8: Overview of E4orf3 functions
Overview how the early viral protein E4orf3 is counteracting several antiviral host proteins and interacts with E1A to ensure successful viral gene expression. A) E4orf3 functions as an E3 SUMO ligase and triggers SUMOylation of various cellular proteins (modified from [171]) B) Interaction of E1A and E4orf3 leads to less chromatin condensation, thus leading to successful viral gene expression [148].

1.4 PML-bodies

1.4.1 PML - structure, function and regulation by SUMO

Promyelocytic leukemia nuclear bodies (PML-NBs), also stated as PML oncogenic domains (POD) or nuclear domain-10 (ND10) are nuclear, spherical multiprotein complexes, which bind tightly to the nuclear matrix [172]; [173]. Depending on the cell type and cycle phase 5-30 PML-NBs can be found in the nucleus [174]; [172]; [175]; [176]; [177]; [178]; [179]; [180]; [181]; [182]. PML-NBs have a diameter from 0.1-1 μm, where a sphere of proteins surrounds an empty space, which might contain ribonucleoproteins [179], but no nucleic acids. At the proteins periphery, DNA and RNA can be found where PML-NBs make contact with chromatin fibers [183]; [184]. The main scaffolding protein of PML-NBs is the promyelocytic leukemia protein (PML). It was identified in acute promyelocytic leukemia (APL) [185]; [186]; [178]; [187]; [188]; [189]; [182] and subsequently found to be deregulated in various cancer types leading to a classification as a tumor suppressor [181]. Through alternative splicing several isoforms of PML exist. Seven different isoforms (PML I-VII) have been defined. For the formation of high order multi protein complexes all isoforms cointain a conserved motif in their N-terminal multimerization domain, termed RBCC or TRIM (tripartite motif) domain. This motif can be found in many SUMO or ubiquitin E3 ligases [190]; [191]; [192]. It consists of a RING finger domain (R), two cysteine/histidine-rich B-Box domains (B) and an α-helical coiled-coil domain (CC). The PML isoforms are only distinguished in their length of the C-terminal region. PML I is the longest and most abundant isoform wherease PML VII is the shortest isoform [193]; [192].

The different isoforms posses exclusive functions and hint to the formation and maintenance of functionally different PML-NBs [194]; [195]; [196]; [197]. Until today it is not known which role PML-NBs play during hypoxia. Recently it was found that PML-NBs inhibit HIF-1α by repression of mTOR [198].

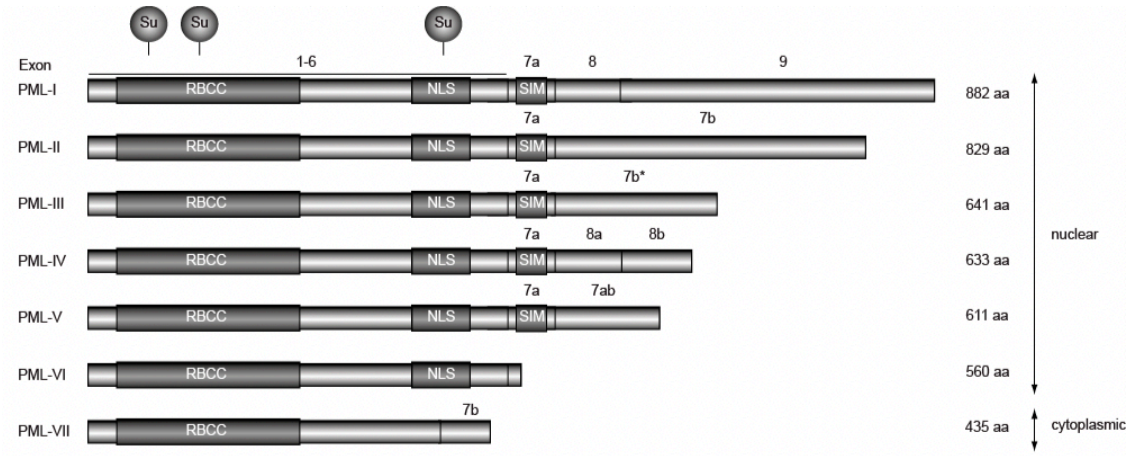

Figure 1.9: Schematic overview of PML isoforms
Representation of the alternatively spliced human PML isoforms according to the nomenclature of Jensen et al. [192]. Indicated by numbers 1-9 are the exon structures and the domain organization of the single PML isoforms. RBCC: RING finger, B-box, coiled-coil domain; NLS: nuclear localization signal; SIM: SUMO interacting motif, Su: SUMO conjugation motif

The post-translational modification by the small ubiquitin-like modifier (SUMO) is needed to establish the PML-NBs structure. Further PML comprises a SUMO interacting motif (SIM). Via this motive PML is able to interact non covalently with SUMO modified proteins, thus enabling to form a PML-NBs network [199]; [200]; [201]; [202]; [203]. It was shown, that PML II and PML V form PML-NBs independently of their N-terminal RBCC domain [204]. The RBCC domain is essential for the establishment of multiprotein complexes [192]; [202]. However, PML isoforms without a SIM motif (PML VI) as well as mutants, which lack their SUMO conjugation sites, are still capable of forming PML-NBs [201]; [202]. Hence, another mechanism how the PML-NB formation emerged. Reactive oxygen species (ROS) leads to the spherical PML framework by the formation of disulfide bonds between cysteine residues of PML proteins. The expansion of PML-NBs relies on SUMO-SIM interactions. Partner proteins that are SUMOylated or contain a SIM motif are recruited to the existing PML-NBs [205]. However, recruitment of proteins to the PML-NBs is not only dependent on SUMOylation. Also phosphorylated and acetylated proteins can interact with PML-NBs [206]; [207]; [208]). Due to the fact that different PTMs influences the structure of PML-NBs, they are highly heterogeneous and dynamic. There is evidence that more than 160 proteins functionally interact with PML-NBs [209]; [210]. These interactions can be either transient or constitutive. For example, the cellular chromatin- re-

modeling factor Daxx (death domain associated protein) and the transcriptional effector Sp100 (speckled protein 100 kDa) are constitutively at the PML-NBs. In conclusion, PML-NBs play a role in a tremdenous amount of cellular pathways such as the DNA Damage Response, tumor suppression, antiviral and antibacterial responses, inflammatory responses, metabolism, ageing, transcriptional regulation or senescence/apoptosis [211]; [184]; [210]; [212];[205].

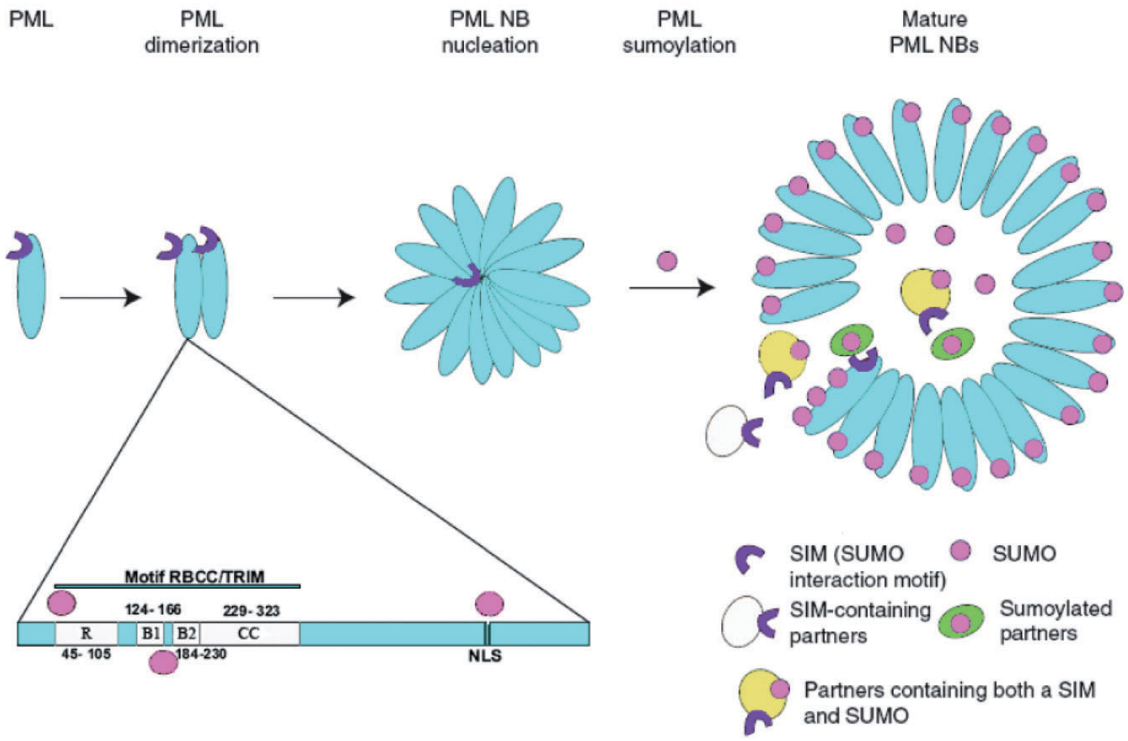

Figure 1.10: Biogenesis of PML-NBs
PML is the main scaffolding protein of the PML-NBs. It belongs to the RBCC/TRIM protein family and is modified by SUMO at the indicated sites. PML proteins dimerize through the RBCC domains followed by multimerization. SUMOylated PML form a spherical body. SUMOylated interaction partners are recruited to the PML-NBs, leading to a variety of functions of the PML-NBs (modified from [172]; [213]; [179]).

1.4.2 Role of PML-NBs in antiviral defense

As an immune response to pathogen permeation, interferons (IFNs) are released by the cell. This leads to an enhanced PML gene transcription [214]. During a virus infection, the number and the size of PML-NBs increases. At the same time the expression of SUMO as well as different PML-NBs associated factors increase [215]; [216]; [217]. PML is also known to promote the expression of IFN-β and is required for the successful transcription of ISGs (interferon induced genes) [218]. PML II seems to be of notably importance. For example, PML II interacts with IRF3 (interferon regulatory factor 3) and STAT1 (signal transducer and activator of transcription 1) which are transcription factors of the type I and type II IFN signaling pathways [219]. Furthermore, there is evidence that PML influences the production of proinflammatory

cytokines. Suggesting a variety role of PML in innate immune signaling [220]. Subsequently, various human viruses evolved unique mechanisms to counteract the defensive functions of PML-NBs (Figure 1.11). Despite the negative effects of the PML-NBs, the replication of many DNA viruses happens in close proximity to the PML-NBs. Indicating that the virus benefits of some components of the PML-NBs, while counteracting others [221]; [156]; [222]; [223]; [224]; [225]. During infection several viral proteins of HAdV-C5 interact with the PML-NBs. The early viral protein E4orf3 oligomerizes to a filamentous network within the nucleus. As a consequence PML-NBs are reorganized into track-like structures [151]; [154]; [163]; [161]. In addition the early viral protein E1A-13S interacts with PML II, which enhances the trans activating capacity of E1A-13S towards adenoviral genes [157]; [151]. Also, the HAdV-C5 targets Daxx and Sp100. The isoforms Sp100B, -C and -HMG are relocalized from the PML-NBs to viral replication centers. Whereas Sp100A is kept at the PML tracks, thus the virus can benefit from the activating capabilities of Sp100A [226]. Negative factos like Daxx are proteasomal degraded by the early viral protein E1B-55K [227].

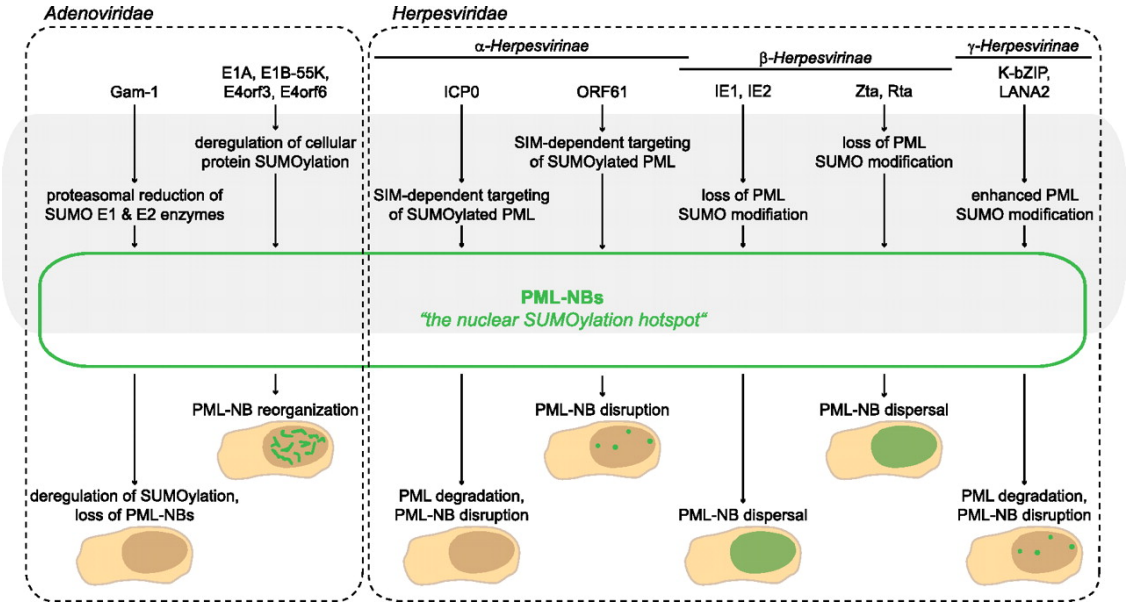

Figure 1.11: PML-NB is the target of several DNA viruses
PML-NBs counteract viral replication via different mechanisms. They are able to induce the transcription of genes, which are part of the innate immune signalling, such as IFN-β, ISGs or certain cytokines. The expression of PML, SUMO and several partner proteins of the PML-NBs like Sp100 are stimulated by type I interferons. Respectively, many viruses developed strategies to counteract these antiviral properties of PML-NBs. Specific PML-NB components are targeted for degradation or relocalization. They are also able to disrupt the whole PML-NB structure (modified from [228];[222]).

1.5 Cellular posttranslational modification - SUMO

As described in 1.4.1 the PTM by SUMO plays a crucial role for the functions of the PML-NBs. SUMO is an abbreviation term for small ubiquitin-like modifier, since it shares around 18 % of sequence similarity with ubiquitin and is covalently bound to its target proteins in a mechanistically comparable manner (Figure 1.12). To date the SUMO protein family comprises five isoforms, although SUMO1-3 constitute the main members. They are often referred to as SUMO 1 and SUMO 2/3, the latter share 95% sequence identity, whereas they match 50% of the SUMO 1 sequence [229]; [230]; [231]. SUMO 4 expression is restricted to kidneys, lymph nodes and spleen and it is not assured, whether it can be conjugated to target proteins in vivo [232]; [233]. SUMO 5 has not been confirmed on protein level and is most likely a pseudogene [234]. SUMO 2/3 contain a conserved acceptor lysine residue within their sequence and are able to form polymeric chains [235]. Whereas SUMO 1 can be detected in mixed SUMO chains, leading to the assumption that it functions as a chain terminator [236]. Recently, an inverted SUMO conjugation motif was found within the sequence of SUMO 1 leading to the formation of SUMO chains, although with lower efficiency than SUMO 2/3 [237]; [238]; [239].

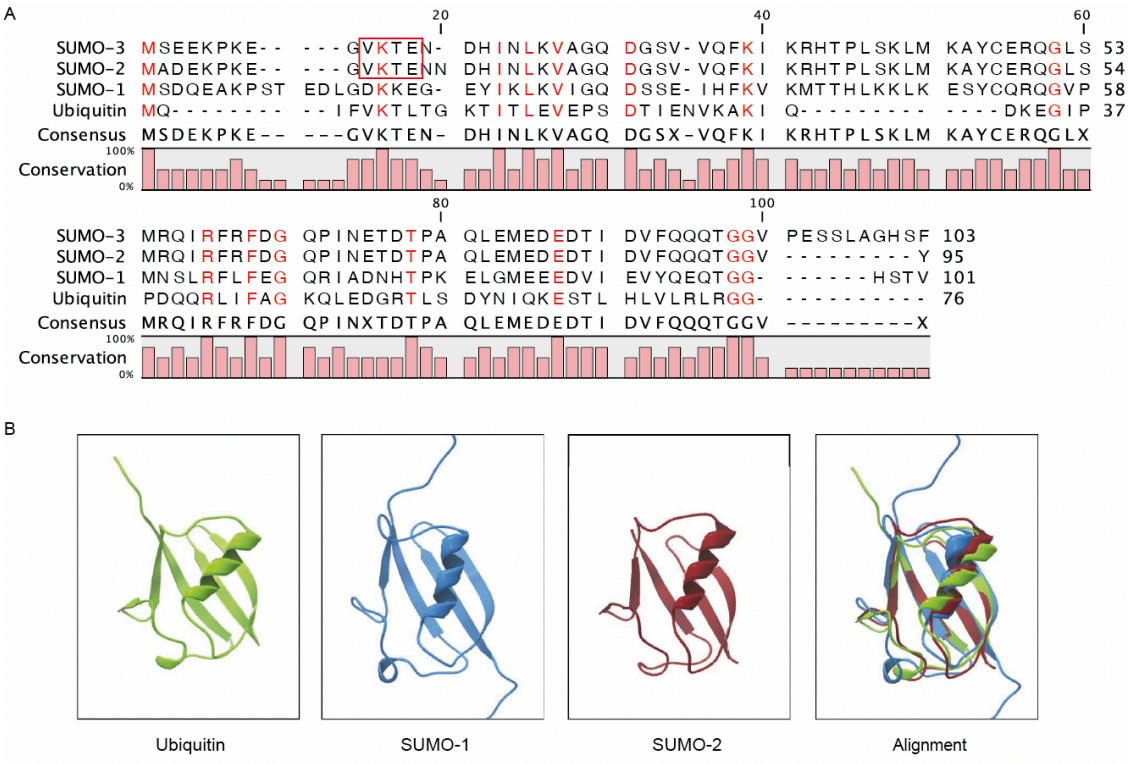

Figure 1.12: SUMO and Ubiquitin protein structures
A) Amino acid sequence alignments of SUMO 1-3 and Ubiquitin. Identities are indicated in red. A SUMO conjugation site (SCS) are marked in red for SUMO 2 and SUMO 3. B) Schematic protein structures with data obtained from the protein data bank (PDB; [235]) highlight the similarities of the three-dimensional structures from Ubiquitin, SUMO 1 and SUMO 2. PBD-IDs: Ubiquitin, green: 1ubq; SUMO 1, blue: 1a5r; SUMO 2, red: 1wm3. [240].

The binding of SUMO proteins to their targets occurs in a three-step enzymatic cascade, which is reversible (Figure 1.13). All isoforms are processed by SUMO specific protease to liberate a diglycine motif at the C-terminus of SUMO [241]; [242]. Through this process the premature SUMO proteins mature and are able to interact with the catalytic domain of the activating enzyme E1. ATP is consumed to establish a thioester bond [243]; [229]; [244]; [245]. E1 is a heterodimer, consisting of the subunits SAE1 and SAE2, whereby the latter contains the catalytically active cysteine. Subsequently, another thioester bond is established and enables E1 to transfer the SUMO proteins to the conjugating enzyme E2, termed Ubc9 [246]; [247]. Within the target protein Ubc9 is able to recognize the SUMO conjugation site and enables the required E3 SUMO ligase to mediate the formation of an isopeptide bond between the C-terminal diglycine residues of SUMO and an ϵ-amino group of a target lysine residue [248]. Even though the presence of an E3 ligase is not required for the transfer of SUMO from Ubc9 to the target, it does stabilize the transition, consequently reducing the energy needed for the transfer [249]; [250]. In contrast to the unique enzymes E1 and E2, several unrelated proteins have been attributed E3 SUMO ligase activity [251]. The process of attaching SUMO to proteins is reversible, SENPs are able to revert the SUMO-conjugation. Six SENP isoforms are known, SENP1-3 and SENP5-7 [252]; [242]. All SENPs localize to the nucleus or to nucleus-associated structures. Furthermore, the isoforms differ in their affinity to different SUMO proteins, regarding either their maturation or their de-conjugation from substrates. For example, SENP2 is localized at the nuclear pore where it de-conjugates both SUMO1 and 2/3 [253]; [254]. However, SENP3 and SENP5 are located to the nucleolus where they target SUMO 2/3 modifications [255]; [252].

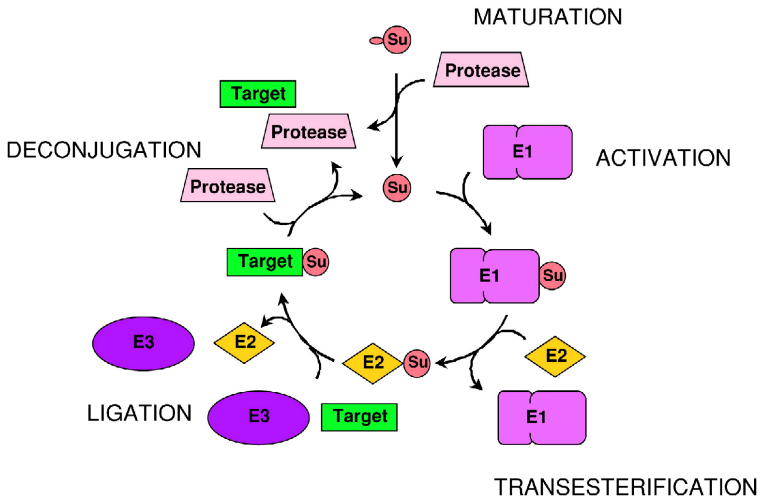

Figure 1.13: Activation and binding of SUMO to target proteins
The premature SUMO is processed by a SUMO specific protease to reveal the C-terminal diglycine that is activated by the E1 enzyme (SAE1/SAE2 in humans). After transesterification onto the E2 SUMO conjugating enzyme (Ubc9), the protein target is selected, and with the help of an E3 ligase, the SUMO is ligated to the substrate. SUMO can be deconjugated from the target protein by the action of SENPs (modified from [229]).

Depending on the SUMOylation of target proteins it can influence their functions in various ways. On the one hand it can promote or inhibit the interaction with other proteins. In addition it can alter their subcellular localization, conformation or stability [256]. SIM motifs contribute to the broad function of SUMO by promoting non covalent interactions with SUMOylated proteins [257]; [258]; [259]. In addition, enzymes, which are part of the SUMOylation process, include SIMs themselves [236]. Therefore, PML-NBs that are enriched with SUMO proteins might capture SIM-containing proteins and in turn promote the SUMOylation of surrounding target proteins [260]; [261]; [205]. In addition, it appears to play a role in the cross-regulation of other PTMs. Human proteomic studies revealed that the majority of the identified SUMO target proteins are nuclear. They are usually enriched within nuclear bodies and at the chromatin, particularly at PML-NBs [262]; [263]; [264]; [265]; [209]; [207]. The classical consensus motif for SUMOylation is ΨKxE, with Ψ representing a hydrophobic amino acid and x any amino acid residue, however, only 44% identified sites of SUMOylation contain this motif [248]; [266]. Target SUMOylation becomes less stringent under different cellular stresses, the consensus motif was only found up to 23 %. During cellular stress an upregulation of cell cycle- and DDR-factor-SUMOylation can be observed. Recent studies revealed a major participation in pre-mRNA splicing, ribosome biogenesis, chromatin remodeling, the DDR, transcriptional regulation (also of viruses), DNA-replication, SUMO-ligase activity, nuclear body organization, pathways involved in the development of cancer and to a lesser extent cell cycle regulation [256].

1.5.1 Role of SUMOylation during productive HAdV infection

Besides cellular proteins also viruses are known to be exposed to PTMs during infection. Additionally, they can manipulate PTMs for their own benefit [267]. For example the infection cycle of HAdV is supported by several PTMs. CAR or integrins have been shown to depend on ubiquitination, thereby affecting viral entry [268]; [269]. In order to additionally benefit the virus, the adenoviral proteinase deubiquitinylates a variety of cellular proteins, which emphasizes the importance of the ubiquitin pathway for adenoviral infection [270]. Also the SUMOylation pathway is critically involved in HAdV infections. To ensure efficient viral replication, early viral proteins extensively use SUMO modifications [171]. The early viral protein E1A binds Ubc9, thereby interfering with polySUMOylation [271]. Furthermore, E1A inhibits the pRB SUMOylation, which enhances E2F-dependent transcriptional activation [272] (Figure 1.6). A known adenoviral SUMO substrate is the early viral protein E1B-55K, which can be covalently modified by SUMO 1, -2 and -3 at its lysine residue 104 within the SUMOylation consensus motif (ΨKxE) [273]; [274]. For example, E1B-55K has an influence on the SUMO status of the cellular KAP1 protein, which was identified as a host restriction factor for HAdV. By a so far unknown mechanism it is deSUMOylated during viral infection, thereby decreasing epigenetic gene silencing and increasing E1B-55K SUMO conjugation [275]. Additionally, E1B-55K functions as a SUMO E3 ligase and inhibits several antiviral host proteins during infection. For instance it SUMOylates p53 at PML-NBs, which contributes to the inhibition of p53 followed by its nuclear export to cytoplasmic aggresome complexes (1.3.2). Another cellular target is Daxx. It has been shown, that the cellular SUMO-targeted ubiquitin ligase (STUbL) RNF4 plays an important role in the degradation of Daxx. E1B-55K recruits RNF4 into the insoluble matrix fraction, which leads to the SUMO conjugation of Daxx and thereby inhibits its antiviral functions [276]. Another early viral protein known to influence several antiviral host proteins is E4orf3. It SUMOylates Mre11 and Nbs1 of the Mre11-Rad50-Nbs1 (MRN) complex (Figure 1.8), which leads to the relocalization of Mre11 and Nbs1 into E4orf3 nuclear tracks and negatively modulates the cellular DNA damage response [277]. Besides an E3 SUMO ligase function, E4orf3 also has an E4 SUMO elongase activity, leading to increasing poly-SUMO chain formation [278]. Recently it was shown, that the cellular transcription factors TIF1γ as well as TFII-I are SUMOylated by the viral E4orf3, which targets them for direct proteasomal degradation, without involving E1B-55K and E4orf6 [279]; [160]; [278]. Taken together this emphasizes the importance of the SUMO pathway for HAdV infections.

1.6 Hypoxia and Hypoxia inducible factor 1 α

For living organisms oxygen plays a crucial role. The oxygen concentration in tissues decides the fate of the cell. Depending on the oxygen concentration the cell can proliferate, differentiate or induce apoptosis [280]. Organisms developed and refined a complex mechanism for adaptation of less to no oxygen concentrations, also termed hypoxia. During oxygen deprivation the hypoxia inducible factors (HIF) are stabilized. HIF is a heterodimeric transcription factor which regulates cellular responses to maintain oxygen homeostasis and adapt to low oxygen levels [281]. The HIF heterodimer consists of an oxygen-dependent α-subunit (HIF-1α) and a constitutively expressed β-subunit, both are basic helix-loop-helix (bHLH) transcription factors. During studies of the hematopoietic growth hormone erythropoietin (EPO), the transcription factor was first identified. In anemia, the blood oxygen content is decreased, however, the EPO production is swiftly turned on followed by an increase in blood oxygen transport. DNA-protein interaction studies revealed a protein complex that bound to the 3' enhancer of the EPO gene and was termed HIF-1α [282]. Besides HIF-1α, a structurally and functionally similar protein named HIF-2α exists. It is a product of the EPAS1 gene and also able to heterodimerize with HIF-1β [283]. HIF-2α is not expressed in all cell types and it can be inactivated by cytoplasmic sequestration [284]. Even though HIF-1α and HIF-2α share a similar structure, target genes are distinctively different [285]. Additionally, HIF-3α was identified, but its role is unknown [286]. This frail balance is disrupted in heart disease, cerebrovascular disease, chronic obstructive pulmonary disease and cancer, which is the second leading cause of death word wide in 2018 [282]; [287].

1.6.1 Structure and regulation of HIF-1α

HIF-1α contains 826 amino acids [288]. The N-terminus of the protein consists of a basic helix-loop-helix domain (bHLH), which mediates the dimerization with the HIF-1β. It is followed by a DNA-binding domain [289]. The C-terminus contains domains for degradation and transactivation. The transactivation domains (TADs) determine the transcriptional activity of HIF-1α [290]; [291]. Deletions of amino acids 576-785 in this region showed increased HIF-1α transcriptional activity [291], revealing that this region contains an inhibitory domain (ID). The C-terminal TAD interacts with the coactivator p300/CBP. This interaction is independent of protein stability, but is required for HIF activity [292]. HIF-1α also contains an oxygen-dependent degradation domain (ODD). At this domain the most post-translational modifications occur,

which play a crucial role in the stabilization of HIF-1α [293]. Those modifications can be phosphorylation, SUMOylation, hydroxylation, acetylation, ubiquitination and S-nitrosylation [294]. Furthermore, HIF-1α contains two nuclear localization sequences in the N-and C-terminus, which are responsible for the translocation of the accumulated HIF-1α to the nucleus under hypoxic conditions [295] (Figure 1.14).

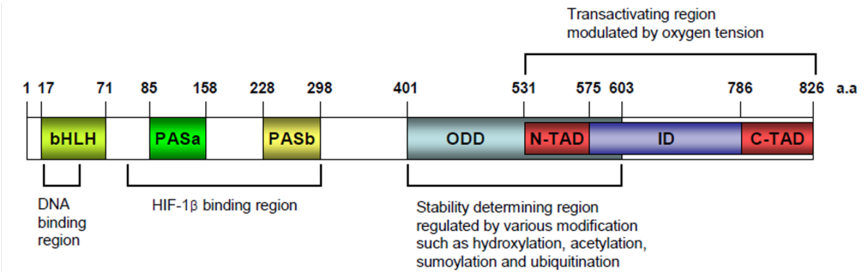

Figure 1.14: Schematic overview of HIF-1α domains
HIF-1α contains the basic helix-loop-helix (bHLH) and PER-ARNT-SIM (PAS) domains, which are involved in the dimerization of HIF-1α with HIF-β and DNA binding. The C-terminus contains two TAD (transacting domain) and an ID (inhibitory domain). The ODD (oxygen dependent degradation) regulates the stability of HIF-1α. The von Hippel Lindau (pVHL) E3 ubiquitin ligase recognizes hydroxylated HIF-1α (modified from [296]).

As described above HIF-1α is oxygen dependently regulated. During normal oxygen levels, prolyl hydroxylases (PHD 1-3) utilize oxygen to hydroxylate HIF-1α [297]; [298]. The VCB-Cul2 ubiquitin-ligase von Hippel-Lindau (VHL) protein recognizes the hydroxylated HIF-1α, leading to its ubiquitination and subsequently degradation of HIF-1α by the proteasome [299]; [300]. Under hypoxic conditions PHD are inactive, leading to the stabilization, relocalization and accumulation of HIF-1α in the nucleus, where it is able to bind HIF-1β followed by the formation of a heterodimeric transcription factor. Consequently, the complex binds to hypoxia response elements (HRE), which promotes the expression of several target genes [301].

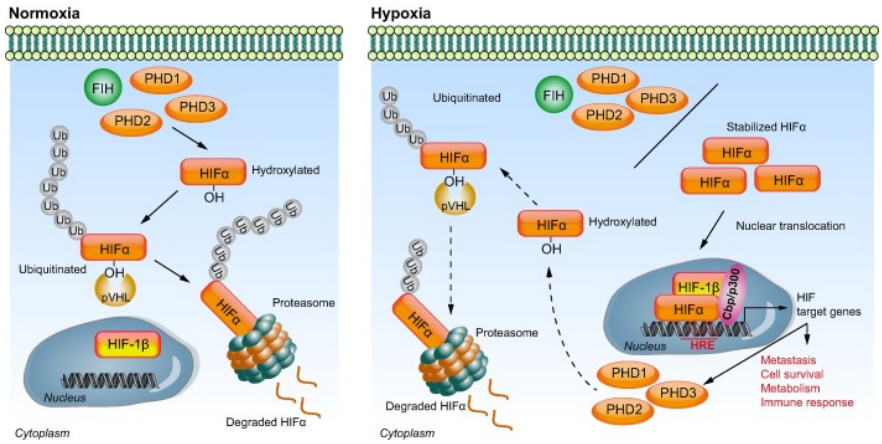

Figure 1.15: Overview of HIF-1α stability during normoxia and hypoxia
Oxygen dependent HIF signalling. Under normoxia PHD1–3 and factor inhibiting HIF (FIH) hydroxylate specific residues of HIF-1α, which is recognized by the von Hippel-Lindau (pVHL) E3 ubiquitin ligase that polyubiquitinates HIF-1α resulting in proteasomal degradation. Under hypoxia PHD and FIH activity is inhibited, resulting in stable HIF-1α expression and nuclear translocation, where it dimerizes with HIF-1β. With the help of co-activators, including CBP/p300, the HIF complex acts as transcription factor by binding to specific DNA sequences defined as hypoxia responsive elements (HREs), activating the transcription of genes involved in an array of signalling events including tumour metastasis, cell survival, metabolism and immune functions. Nuclear HIF-1α promotes PHD expression resulting in a negative feedback loop that ensures the pathway is not constitutively active (modified from [302].

1.6.2 Role of SUMO on HIF-1α protein

As described in 1.5, SUMOylation belongs to PTMs such as ubiquitination, phosphorylation or acetylation. These PTMs can influence signaling pathways and play a part in gene regulation or protein stability. Until today, modifications of HIF-1α by SUMO are conflicting. On the one hand it was shown that HIF-1α can be SUMOylated by SUMO 1, -2 and -3 in vitro, whereas SUMOylation occurs in proximity to the ODD domain and SUMO 1 leads to a stabilization of HIF-1α [303]; [304]. On the other hand it was shown that in vivo SUMOylation does not change HIF-1α stability, but decreases its transcriptional activity. Recent studies observed that the SUMOylation of HIF-1α promoted its binding to VHL, leading to HIF-1α ubiquitination and degradation through a proline hydroxylation-independent mechanism [305], [306].

1.6.3 HIF-1α expression during viral infections

Recently, activation of hypoxia and thus HIF-1α has been in the focus of research. HIF-1α supports the host defense program to reduce cell damage caused by viral infection. For example, the vesicular stomatitis virus (VSV) induces an acute cytolytic effect on host cells. Under hypoxic conditions the virus showed reduced replication and cytopathogenicity, but the interferon α and γ levels in the cells were increased [307]. Inhibition of HIF-1α showed that the cytotoxic effect and replication of the VSV was enhanced, however, this effect was reversed again by the

usage of cobald(II) chloride ($CoCl_2$), which stabilizes HIF-1α by inhibition of the PHDs [308]. During persistent viral infections, induction of HIF-1α is not sufficient to eradicate the virus, but the activated proangiogenic mechanism can lead to oncogenicity. For example, Chronic Hepatitis B infection is associated with the development of cancer, termed hepatocellular carcinoma (HCC). The tumor is highly vascularized and the X protein of HBV (HBx) is linked with angiogenesis and metastasis of HCC. In cultured liver cells, expressing HBx, HIF-1α levels are increased and the protein is translocated into the nucleus. In livers of HBx transgenic mice it was shown that HIF-1α activates target genes including VEGF, which promotes the vascularization of the tumor [309]; [302]. Another virus, where HIF-1α activation supports tumour development is the human papillomavirus-16 (HPV-16). Advanced cervical tumours are mainly hypoxic, and show increased levels of HIF-1α, which correlates with a poor prognosis [310]; [311]. Furthermore, studies have shown that the transfection of HPV-16 oncoproteins E6 and E7 in human cervical cancer cell line induce VEGF expression, while this effect is abrogated, if the cells are cotransfected with siRNA targeting HIF-1α [312]. In the case of the Epstein Barr virus (EBV), the oncoprotein latent membrane protein 1 (LMP1) increases HIF-1α expression levels [313]. It has been shown that LMP1 enhances an E3 ubiquitin ligase Siah1 that induces proteasomal degradation for PHDs, that normally hydroxylate HIF-1α, subsequently inhibiting the interaction of pVHL and HIF-1α [314]. These examples underline the importance of the connection between HIF-1α expression, viral replication and viral oncogenicity.

1.7 Aim of thesis

As described in 1.6.3 HIF-1α plays a crucial role in the successful replication and oncogenesis of several DNA viruses. However, until today it was not investigated, if HIF-1α plays a role during HAdV infection. Our initial hypothesis proposed a supportive role of HIF-1α on HAdV infection, as HIF-1α is a known repressor of PML function [315]. This thesis aims to elucidate the role of HIF-1α during the HAdV infection. Therefore, it was investigated how hypoxia influences the HAdV replication. To validate the results of the hypoxia experiments overexpression of HIF-1α and a mutant of HIF-1α, which can't be recognized by the pVHL, were performed. It was of special interest, if HAdV stabilzes HIF-1α during infection under normoxic environment. Additionally, several mutants of HAdV, lacking early viral proteins, were used to further investigate the adenoviral influence on HIF-1α. The majority of investigated viruses stabilize HIF-1α during infection, and PTMs play a crucial role in the function of several proteins and during viral replication (1.5; 1.5.1). Since it is known that SUMOylation plays a crucial role for the HAdV

replication cylce (1.5.1), it was of interest how and if HAdV affects PTMs of HIF-α. Hereby, it was hypothesized that HAdV infection has an impact on HIF-1α, which might be another mechanism to ensure successful HAdV replication. Consequently, it was of interest to see how different serotypes of HAdV influence HIF-1α stability and function. Taken together, this work aimed to further elucidate HAdV host interplay, which could improve its vector application in the fields of gene therapy, vaccination and cancer treatment.

Chapter 2

Material

2.1 Bacteria & cells

2.1.1 Bacterial strain

For this work following bacteria were used. The first row shows the bacterial strain. The second row the phenotype of the bacterial strain.

Table 2.1: Bacterial strain with phenotype and reference

Bacterial strain	Phenotype	Reference
DH5α	*fhuA2 lac(del)U169 phoA glnV44 ϕ80' lacZ(del)M15 gyrA96 recA1 relA1 endA1 thi-1 hsdR17*	[316]

2.1.2 Mammalian Cells

During this work the listed mammalian cellines were used. Numbers are according to the internal *FileMaker Pro* database.

Table 2.2: Mammalian Cells

#	Cell line	Properties	Reference
1	HepaRG	Pseudo primary hepatocyte	[317]
15	H1299	Human lung carcinoma cells, derived from metastatic lymph node, lack of p53 expression	[318]
38	H1299 CTR	Control cell line for the H1299 stably depleted for PML	Group database
37	H1299 shPML	Human lung carcinoma cellline stably expressing shRNA against PML	Group database
4	Hela	Human cervix carcinoma cells with HPV-18 genome integration	[319]
7	Hela-SUMO2-His	Human cervix carcinoma cells with HPV-18 genome integration, cells stably express 6xHis tagged SUMO2	[320]
16	HEK293	Human embryonic kidney cell line transformed by HAdV-C5 and stably expressing the HAdV-C5 E1 region	[321]
8	HEK293T	HEK-293 derived cell line expressing the SV40 large T-Ag	[322]

2.2 Adenoviruses

The following human adenoviruses (HAdV) were used for infection assays during this work. Numbers are according to the internal *FileMaker Pro* database.

Table 2.3: Used HAdV

#	HAdV	Phenotype	Reference
4	HAdV-wt	Wt Ad5 containing an 1863 bp deletion (nt 28602-30465) in the E3 region	[323]
3	HAdV-$\triangle$E1B-55K	Ad5 E1B-55K null mutant containing four stop codons at the aa positions 3, 8, 86 and 88 of the E1B-55K sequence	[323]
2	HAdV-$\triangle$E4orf6	Ad5 E4orf6 null mutant containing a stop codon at aa 66 within the E4orf6 sequence	[324]
16	HAdV-$\triangle$E4orf3	Ad5 E4orf3 nul lmutante containing a frame shift mutation after codon 37 by insertion of a thymidine at position nt 34592 (first stop at codon 38)	[325]

2.3 Nucleic acid

2.3.1 Oligonucleotides

The following oligonucleotides were used for sequencing, PCR, RT-PCR and site directed mutagenesis. All oligonucleotides were ordered from Metabion (Planegg) and numbered according to the internal *FileMaker Pro* database.

Table 2.4: Oligonucleotides

#	Name	Sequence	Purpose
71	366CMV fwd	5'-CCCACTGCTTACTGGC-3'	sequencing
92	pcDNA3 fwd	5'-TAATACGACTCACTATAGGG-3'	sequencing
134	E4orf6 fwd	5'-GGAGGATCATCCGCTGCTG-3'	viral DNA analysis
135	E4orf6 rev	5'-GCACAACACAGGCACACG-3'	viral DNA analysis
181	E1A fwd	5'-GTGCCCCATTAACCAGTTG-3'	viral mRNA analysis
182	E1A rev	5'-GGCGTTTACAGCTCAAGTCC-3'	viral mRNA analysis
187	18S fwd	5'-CGGCTACCACATCCAAGGAA-3'	viral mRNA/ DNA analysis
188	18S rev	5'-GCTGGAATTACCGCGGCT-3'	viral mRNA/ DNA analysis
189	Hexon fwd	5'-CGCTGGACATGACTTTTGAG-3'	viral mRNA analysis
190	Hexon rev	5'-GAACGGTGTGCGCAGGTA-3'	viral mRNA analysis
193	E4orf6 fwd	5'-CCCTCATAAACACGCTGGAC-3'	viral mRNA analysis
194	E4orf6 rev	5'-GCTGGTTTAGGATGGTGGTG-3'	viral mRNA analysis
321	HIF-1α rev (EcoRV)	5'-TATGATATCTCAGTTAACTTGATC CAAAGCTC-3'	cloning of HIF-1α into pcDNA3-HA vector
322	HIF-1α rev (NheI)	5'TATGCTAGCTCAGTTAACTTGA TCCAAAGCTC-3'	cloning of HIF-1α into pCMBX3B vector
323	E1B-55K fwd	5'-ATGAGCGACGAAGAAACCCATC TGAGC-3'	viral DNA analysis
324	E1B-55K rev	5'-CGGTGTCTGGTCATTAAGCT-3'	viral DNA analysis
356	HIF-1α fwd (BamHI)	5'-ATAGGATCCGAGGGCGCCGG CGGCG-3'	cloning of HIF-1α into pcDNA3-HA and pCMBX3B vector
429	HIF-1α fwd	5'-GCCAGACGATCATGCAGC-3'	qPCR primer
430	HIF-1α rev	5'-TGCTGGGGCAATCAATGGAT-3'	qPCR primer

2.3.2 Recombinant plasmids

The following plasmids were used for cloning and transfection experiments. All plasmids are numbered according to the internal *FileMaker Pro* database.

Table 2.5: Recombinant plasmids

#	Name	Purpose	Reference
12	pcDNA3	empty pcDNA3 vector	Invitrogen
18	pcDNA3-HA	empty pcDNA3 vector with CMV promoter and N-terminal HA tag	Group database
26	pcDNA3-E4orf6-HA	pcDNA3 vector encoding HAdV E4orf6 with CMV promoter and N-terminal HA tag	Group database
61	pcDNA3-E1B-55K	pcDNA3 vector encoding HAdV E1B-55K with CMV promoter and N-terminal HA tag	Group database
384	pCMV-VSV-G	Envelope protein for producing lentiviral and MuLV retroviral particles	[326]
385	pMDLg/pRRE	3rd generation lentiviral packaging plasmid; contains Gag and Pol	[327]
83	pRenilla-TK	Renilla-Luciferase-Assay	Promega
383	pRSV-Rev	3rd generation lentiviral packaging plasmid; contains Rev	[327]
91	pGLbasic3 E1A promoter	HAdV-C5 E1A promoter reporter gene construct	[137]
94	pGLbasic3 E2E promoter	HAdV-C5 E2E promoter reporter gene construct	[137]
100	pGLbasic3 empty	Firefly-Luciferase-Assay	Promega
224	pcDNA3 HIF-1α	pcDNA3 vector encoding HIF-1α	kindly provided by Jane McKeating
587	pcDNA3 HIF-1α -P405A/G531P	pcDNA3 vector encoding HIF-1α with mutations at position 405 and 531	kindly provided by Jane McKeating
510	HIF-1α HA	pcDNA3-HA vector encoding HIF-1α	this work
511	HIF-1α pcMX3B	pcMX3B-Flag vector encoding HIF-1α	this work

2.4 Antibodies

2.4.1 Primary antibodies

The following Antibodies were used for Western Blot or Immunofluorescence experiments. Numbers are according to the internal *FileMaker Pro* database.

Table 2.6: Primary antibodies

#	Name	Properties	Reference
62	2A6	Monoclonal mouse Ab; against N-terminus of HAdV-C5 E1B-55K	[115]
21	3F10	Monoclonal rat Ab; against the HA-tag	Roche
94	4E8	Monoclonal rat Ab; against the central region of HAdV-C5 E1B-55K	Group database [323]
45	M73	Polyclonal rabbit Ab; against HAdV-C5 E1A protein	kindly provided by R. Grand University of Birmingham
105	6A11	Monoclonal rat Ab; against HAdV-C5 E4orf3 protein	[164]
41	6xHis	Monoclonal mouse Ab; against 6xHis-tag	Clontech
61	β – actin (AC-15)	Monoclonal mouse Ab; against β-actin	Sigma Aldrich
49	B6-8	Monoclonal mouse Ab; against HAdV-C5 E2A protein	Group database [328]
1	DO-I	Monoclonal mouse Ab; against the N-terminal aa 11-25 of human p53	Santa Cruz
38	Hexon	Monoclonal mouse Ab; against Adenoviral hexon antigen	Abcam
24	HIF-1α	Monoclonal mouse Ab; against C-terminal aa 329-530	Santa Cruz
66	HIF-1α	Monoclonal mouse Ab; against C-terminal aa 610-727	BD Science
43	L133	Polyclonal rabbit serum; against HAdV-C5 capsid	Group databse [323]
2	MDM2	Monoclonal mouse Ab, against human MDM2	Santa Cruz
12	Mre11	Polyclonal rabbit Ab; against human Mre11	Abcam/Novus
16	PML (NB100-59787)	Polyclonal rabbit Ab; against human PML	Novus
34	RSA3	Monoclonal mouse Ab; against the N-terminus of HAdV-C5 E4orf6 and E4orf6/7	[329]

2.4.2 Secondary antibodies

The following secondary antibodies were used for Western Blot experiments.

Table 2.7: Secondary antibodies western blot

Antibody	Properties	Company
HRP-Anti-Mouse IgG	HRP (horseradish peroxidase)-coupled; raised in sheep	Dianova
HRP-Anti-Rabbit IgG	HRP (horseradish peroxidase)-coupled; raised in sheep	Dianova
HRP-Anti-Rat IgG	HRP (horseradish peroxidase)-coupled; raised in sheep	Dianova

The following secondary antibodies were used for Fluorescence experiments.

Table 2.8: Secondary antibodies fluorescence

Antibody	Properties	Company
Alexa 488 Anti-Mouse IgG	Alexa 488 antibody raised in goat (H + L; F(ab')2 Fragment)	Invitrogen
Alexa 488 Anti-Rabbit IgG	Alexa 488 antibody raised in goat (H + L; F(ab')2 Fragment)	Invitrogen
Alexa 488 Anti-Rat IgG	Alexa 488 antibody raised in goat (H + L; F(ab')2 Fragment)	Invitrogen
Alexa 647 Anti-Mouse IgG	Alexa-647 antibody raised in goat (H + L; F(ab')2 Fragment)	Dianova
Alexa 647 Anti-Rabbit IgG	Alexa-647 antibody raised in goat (H + L; F(ab')2 Fragment)	Dianova
Alexa 647 Anti-Rat IgG	Alexa-647 antibody raised in goat (H + L; F(ab')2 Fragment)	Dianova
Alexa 568 Anti-Rabbit IgG	Alexa 568 antibody raised in goat (H + L; F(ab')2 Fragment)	Dianova

2.5 Standards & Markers

To determine the molecular weight of proteins on SDS-polyacrylamid gels the protein ladder *PageRuler*^{TM} *Prestained Protein Ladder Plus* (Fermentas) was used. This ladder covers a range of 10 kDa – 250 kDa. Size determination of DNA fragments on agarose gels was based on a 1 kp and 100 bp DNA ladder (New England Biolabs).

2.6 Commercial Systems

The following commercial avaible systems were used.

Table 2.9: Commercial systems

Product	Company
Dual-Luciferase® Reporter Assay System	Promega
Protein Assay	BioRad
Quiagen Plasmid Mini, Midi and Maxi Kit	Qiagen
QIAquick Gel Extraction Kit	Qiagen
QuikChangeTM Site-Directed Mutagenesis Kit	Agilent

2.7 Chemicals & Reagents

The following chemicals and reagents were used.

Table 2.10: Chemicals & Reagents used

Substance	Company
10x Antarctic phosphatase reaction buffer	New England BioLabs, Frankfurt a.M.Germany
2-Propanol	Carl Roth, Karlsruhe, Germany
30% acrylamide/bisacrylamide mixture	Carl Roth, Karlsruhe, Germany
6x DNA loading dye	New England BioLabs, Frankfurt a.M., Germany
Agarose	Biozym, Hessisch Oldendorf, Germany
Ampicillin	Sigma-Aldrich, Darmstadt, Germany
Aprotinin	Sigma-Aldrich, Darmstadt, Germany
APS	Carl Roth, Karlsruhe, Germany
Boric acid, > 99,8%	Sigma-Aldrich, Darmstadt, Germany

(continuation...)

(continuation Chemicals & Reagents)

Substance	**Company**
Bovine serum albumin (BSA)	Thermo Scientific, Dreieich, Germany
Bradford reagent	Bio-Rad, München, Germany
Bromphenol blue	Carl Roth, Karlsruhe, Germany
Chloroform	Carl Roth, Karlsruhe, Germany
Cobald Chloride (Co_2Cl) 0.1 M	Sigma-Aldrich, Darmstadt, Germany
DAPI	Sigma-Aldrich, Darmstadt, Germany
Developing solution	Tetenal, Norderstedt, Germany
Dimethyl sulfoxide (DMSO) $\geq$ 99.5%	Carl Roth, Karlsruhe, Germany
DNase I	Carl Roth, Karlsruhe, Germany
dNTP mix (100mM)	New England BioLabs, Frankfurt a.M., Germany
Dulbecco's modified eagle's medium (DMEM)	Sigma-Aldrich, Darmstadt, Germany
Paraformaldehyd	Sigma-Aldrich, Darmstadt, Germany
Luminol sodium salt	Sigma-Aldrich, Darmstadt, Germany
p-Coumaric Acid	Sigma-Aldrich, Darmstadt, Germany
EDTA	Carl Roth, Karlsruhe, Germany
Ethanol	Carl Roth, Karlsruhe, Germany
Ethidium bromide	Sigma-Aldrich, Darmstadt, Germany
Fetal Bovine Serum (FBS)	Thermo Fisher Scientific, Dreieich, Germany
Fixation solution	Tetenal, Norderstedt, Germany
Glycerol	AppliChem, Darmstadt, Germany
Glycine	AppliChem, Darmstadt, Germany

(continuation...)

(continuation Chemicals & Reagents)

Substance	**Company**
Guanidine hydrochloride	AppliChem, Darmstadt, Germany
H_2O_2	Sigma-Aldrich, Darmstadt, Germany
HCl	Carl Roth, Karlsruhe, Germany
Hydrocortisone	Sigma-Aldrich, Darmstadt, Germany
Insulin	Sigma-Aldrich, Darmstadt, Germany
Imidazole	AppliChem, Darmstadt, Germany
Iodacetamide	Sigma-Aldrich, Darmstadt, Germany
KCl	Carl Roth, Karlsruhe, Germany
Leupeptin	Sigma-Aldrich, Darmstadt, Germany
Methanol	Carl Roth, Karlsruhe, Germany
MgCl2	Carl Roth, Karlsruhe, Germany
MG132	Sigma-Aldrich, Darmstadt, Germany
Mowiol 4-88	Carl Roth, Karlsruhe, Germany
Na2HPO4	AppliChem, Darmstadt, Germany
NaCl	Carl Roth, Karlsruhe, Germany
NaH2PO4	AppliChem, Darmstadt, Germany
N-ethylmaleimide	Sigma-Aldrich, Darmstadt, Germany
Ni-NTA resin	Thermo Scientific,Dreieich, Germany
Nonidet-P40	Carl Roth, Karlsruhe, Germany
Pansorbin	Calbiochem, Bad Soden, Germany

(continuation...)

(continuation Chemicals & Reagents)

Substance	Company
Penicillin/Streptomycin	Sigma-Aldrich, Darmstadt, Germany
Pepstatin	Sigma-Aldrich, Darmstadt, Germany
Phenol/chloroform/ isoamyl alcohol (25:24:1)	Sigma-Aldrich, Darmstadt, Germany
Phenylmethylsolfonyl fluoride (PMSF)	Sigma-Aldrich, Darmstadt, Germany
Phosphate buffered saline (PBS)	Biochrom, Berlin, Germany
Polyethyleneimine (PEI)	Sigma-Aldrich, Darmstadt, Germany
Proteinase K	Carl Roth, Karlsruhe, Germany
QIAGEN Plasmid DNA Purification Kit	QIAGEN, Hilden, Germany
RNase A	Carl Roth, Karlsruhe, Germany
Sepharose A beads	Sigma-Aldrich, Darmstadt, Germany
Skim milk powder	Sigma-Aldrich, Darmstadt, Germany
Sodium acetate	Carl Roth, Karlsruhe, Germany
Sodium azide	AppliChem, Darmstadt, Germany
Sodium dodecylsulfate (SDS)	Carl Roth, Karlsruhe, Germany
Sodiumacetate	Sigma-Aldrich, Darmstadt, Germany
T4 DNA ligase	Roche, Basel, Switzerland
T4 DNA Ligation buffer, 2 x conc.	Roche, Basel, Switzerland
TEMED	AppliChem, Darmstadt, Germany
Tris(hydroxymethyl)aminomethane (Tris)	Carl Roth, Karlsruhe, Germany
Triton X-100	AppliChem, Darmstadt, Germany
Trizol	Thermo Scientific, Dreieich, Germany

(continuation...)

(continuation Chemicals & Reagents)

Substance	Company
Trypsin/EDTA	Sigma-Aldrich, Darmstadt, Germany
Tween-20	AppliChem, Darmstadt, Germany
Urea	AppliChem, Darmstadt, Germany
β-mercaptoethanol	AppliChem, Darmstadt, Germany

2.8 Laboratory equipment

The following equipment were used.

Table 2.11: Laboratory equipment

Device	Company
Agfa Curix 60	AGFA, Mortsel, Belgium
Avanti Je centrifuge	Beckman Coulter, Munich, Germany
Axiovert 200 M microscope	Zeiss, Oberkochen, Germany
BakerInvivO2 l 400 Hypoxia workstation	Baker, Sanford, Main, USA
BRAND® accu-jet® pro pipette controller	Sigma-Aldrich, Darmstadt, Germany
Branson Ultrasonics Sonifier^{TM} S-450 Digital Ultrasonic Cell Disruptor/Homogenizer	Thermo Fisher Scientific, Dreieich, Germany
Eppendorf® Mastercycler Gradient	Eppendorf, Hamburg, Germany
Bio-Rad PowerPac 3000 electrophoresis power supply	Bio-Rad, München
ELMI Shaker S4	ELMI, Riga, Lettland
Eppendorf® Multipipette Plus	Eppendorf, Hamburg, Germany
Eppendorf® Research® plus pipette, 0.1-2.5 μl	Eppendorf, Hamburg, Germany

(continuation...)

(continuation Laboratory equipment)

Device	**Company**
Eppendorf® Research® plus pipette, 0.5-10 μl	Eppendorf, Hamburg, Germany
Eppendorf® Research® plus pipette, 2-20 μl	Eppendorf, Hamburg, Germany
Eppendorf® Research® plus pipette, 10-100 μl	Eppendorf, Hamburg, Germany
Eppendorf® Research® plus pipette, 20-200 μl	Eppendorf, Hamburg, Germany
Eppendorf® Research® plus pipette, 100-1000 μl	Eppendorf, Hamburg, Germany
Eppendorf® Thermomixer Comfort 5355	Eppendorf, Hamburg, Germany
Eppendorf® Thermomixer Compact	Eppendorf, Hamburg, Germany
Freezer, -20 °C	Liebherr-International Deutschland GmbH, Biberach an der Riß, Germany
Gel Doc^{TM} XR+ Gel Documentation System	Bio-Rad, Munich, Germany
Glass Micro Pipette	Hamilton Company, Reno, US
GlowMax Multi Jr	Promega, Madison, Wiscons, USA
Heraeus® BB16 Function Line CO_2 incubator	Heraeus Instruments GmbH, Hanaua, Germany
Heraeus^{TM} Biofuge Pico^{TM}	Thermo Fisher Scientific, Dreieich, Germany
Heraeus^{TM} Fresco^{TM}17 Microcentrifuge	Thermo Fisher Scientific, Dreieich, Germany
Heraeus^{TM} Fresco^{TM} 21 Microcentrifuge	Thermo Fisher Scientific, Dreieich, Germany
Heraeus^{TM} Herafreeze HFU 586 Basic, -80 ℃	Thermo Fisher Scientific, Dreieich, Germany
Heraeus^{TM} Laminair HLB 2448 GS	Thermo Fisher Scientific, Dreieich, Germany
Heraeus^{TM} Megafuge^{TM} 40 centrifuge	Thermo Fisher Scientific, Dreieich, Germany

(continuation...)

(continuation Laboratory equipment)

Device	**Company**
Heracell^{TM} 150i CO_2 incubator	Thermo Fisher Scientific, Dreieich, Germany
Memmert incubator model 200, D 06058	Memmert, Büchenbach, Germany
Microwave 9029GD	Privileg, Stuttgart, Germany
ML-DNY-43 NewClassic	Mettler Toledo, Greifensee, Switzerland
MS 3 basic vortexer	IKA® -Werke GmbH & Co. KG, Staufen, Germany
Multigel electrophoresis chamber	Biometra, Jena, Germany
Multitron incubation shaker	Infors HT, Bottmingen, Switzerland
Nalgene Mr. Frosty^{TM} Cryo 1 ℃ freeze container	Thermo Fisher Scientific, Dreieich, Germany
NanoDrop 2000c UV-Vis Spectrophotometer	Thermo Fisher Scientific, Dreieich, Germany
Neubauer counting chamber (improved)	LO Laboroptik
No frost refrigerator and freezer CUN3523	Liebherr, Biberach an der Riß, Germany
Pipetboy acu	Integra Biosciences GmbH, Biebertal, Germany
Pipetboy acu 2	Integra Biosciences GmbH, Biebertal, Germany
PowerPac^{TM} Basic Power Supply	Bio-Rad, Munich, Germany
PowerPac^{TM} Universal Power Supply	Bio-Rad, Munich, Germany
Primovert light microscope	Zeiss, Oberkochen, Germany
Reciprocating Shaker 3016	GFL Gesellschaft für Labortechnik GmbH, Burgwedel, Germany
Rotina 420R centrifuge	Hettich Zentrifugen, Tuttlingen, Germany
Rotixa 50 RS centrifuge	Hettich Zentrifugen, Tuttlingen, Germany
Sartorius portable	Sartorius AG, Göttingen, Germany

(continuation...)

(continuation Laboratory equipment)

Device	Company
SmartSpecTM Plus Spectrophotometer	Bio-Rad, Munich, Germany
Sprout® Mini Centrifuge	Heathrow Scientific
Test Tube Rotating Shaker 3025	GFL, Burgwedel, Germany
Thermocycler peqSTAR 96x universal gradient	VWR International GmbH, Darmstadt, Germany
Trans-Blot® Cell	Bio-Rad, Munich, Germany
Unitwist RT	UniEquip Laborgeraätebau- und Vertriebs GmbH, Planegg, Germany
Vacusafe vacuum pump	Integra, Biosciences GmbH, Biebertal, Germany
Vortex-Genie 2	Scientific Industries, Inc., Bohemia, US
PTC-100 Peltier Thermal Cycler	MJ Research, Reno, Nevada, USA
Schüttelinkubator GFL 3031	GFL, Großburgwedel
Werkbank, Heraeus HB 2448	Heraus, Hanau
Zentrifuge, Beckmann J2-21M/E	Beckmann, Krefeld
Zentrifuge, Sigma 2K 15 Sigma	Osterode am Harz

2.9 Disposable equipment

Table 2.12: Disposable laboratory equipment

Device	Company
Blotting paper 460x570 mm, 195 g/m^2	A. Hartenstein GmbH, Würzburg, Germany
Cell scraper	Sarstedt, Nürnbrecht, Germany
CryoPure Tube 72.379, 1,8 ml white	Sarstedt, Nürnbrecht, Germany
Eppendorf® Combitips advanced® pipette tips	Eppendorf, Hamburg, Germany
Falcon® 2059 polypropylene round-bottom tube	Fisher Scientific Company LLC, Pittsburgh, US

(continuation...)

(continuation Disposable equipment)

Device	**Company**
Greiner CELLSTAR® serological pipette, 2 ml	Sigma-Aldrich, Darmstadt, Germany
Greiner CELLSTAR® serological pipette, 5 ml	Sigma-Aldrich, Darmstadt, Germany
Greiner CELLSTAR® serological pipette, 10 ml	Sigma-Aldrich, Darmstadt, Germany
Greiner CELLSTAR® serological pipette, 25 ml	Sigma-Aldrich, Darmstadt, Germany
Kimtech Science* Purple Nitrile*gloves, small	Kimberly-Clark Worldwide, Inc., Koblenz, Germany
Kimtech Science* Purple Nitrile*gloves, medium	Kimberly-Clark Worldwide, Inc., Koblenz, Germany
Kimtech Science* Purple Nitrile*gloves, large	Kimberly-Clark Worldwide, Inc., Koblenz, Germany
Micro tube 1.5 ml	Sarstedt, Nürnbrecht, Germany
Multiply®Pro tube0.2 ml	Sarstedt, Nürnbrecht, Germany
Nitril® NextGen® gloves, small	Meditrade GmbH, Kiefersfelden, Germany
Nitril® NextGen® gloves, medium	Meditrade GmbH, Kiefersfelden, Germany
Nitrocellulose membrane 0.45 μm NC, Amersham^{TM} Protran^{TM}	GE Healthcare, Solingen, Germany
Parafilm® M All-Purpose Laboratory Film	Bemis Company, Inc., Oshkosh, US
PFA membrane 0.2 μm	GE Healthcare, Solingen, Germany
Semi-micro cuvette, acrylic	Sarstedt, Nürnbrecht, Germany
TC dish 100, standard 83.3902	Sarstedt, Nürnbrecht, Germany
TC dish 150, standard 83.3903	Sarstedt, Nürnbrecht, Germany
TC plate 6 well, standard F 83.3920	Sarstedt, Nürnbrecht, Germany
TC plate 12 well, standard F 83.3921	Sarstedt, Nürnbrecht, Germany
Tube 50 ml, 114x23, PP, 62.547.254	Sarstedt, Nürnbrecht, Germany

(continuation...)

(continuation Disposable equipment)

Device	Company
Tube 15 ml, 120x17, PP, 62.554.502	Sarstedt, Nürnbrecht, Germany
X-ray films	Consumer Electronics Association (CEA), Arlington, US

2.10 Software

The following software was used for this work.

Table 2.13: Software

Software	Purpose	Company
Adobe Reader XI	PDF data processing	Adobe
BioEdit	sequence alignment editor	Ibis
BLAST	local alignment tool	NCBI
CLC Sequence Viewer 6	Genome and Sequencing analyses	CLC bio
Endnote X8	Reference organization	Thomson Reuters
Excel 2010	Data and table processing	Microsoft
Filemaker Pro 14	Database management	Filemaker, Inc.
GPS-SUMO	Prediction of potential SUMOylation and SUMO interacting motifs	The CUCKOO Workgroup
GraphPad Prism 5	Figure processing and statistical analyses	GraphPad Software
ImageJ	Signal intensity calculations	NIH
LaTeX	Text processing	The LaTeX project
Papers 3.4.20	Reference management	Readcube
PowerPoint 2010	Presentation and image processing	Microsoft
PubMed	literature database	Open Software sequence analysis software

(continuation...)

(continuation Software)

Software	**Purpose**	**Company**
Serial Cloner	Software to visualize and manipulate DNA sequences	Serial Basics
Volocity	Microscopic image processing	PerkinElmer Inc.
Word 2010	Text processing	Microsoft

Chapter 3

Methods

3.1 Bacteria

3.1.1 Culture & Storage

Solid Plate culture

Transformed bacteria or bacteria from glycerin culture were plated on solid LB medium containing 15 g/l agar with the appropriate antibiotics (100 μg/ml ampicillin; 50 μg/ml kanamycin) and incubated at 30 °C or 37 °C.

Liquid culture

Sterile LB medium containing the appropriate antibiotic (100 μg/ml ampicillin; 50 μg/ml kanamycin) was inoculated with a single bacteria colony to establish liquid E. coli culture. Therefore, cultures were incubated at 30 °C or 37 °C at 150 rpm in an Multitron Incubator overnight.

Storage

5 ml of liquid culture from a single colony bacteria was centrifuged briefly at 4000 rpm for 10 min (Heraeus^{TM}) at RT. After discarding the supernatant, the bacteria pellet was resuspended in 1 ml LB medium containing 50 % sterile glycerol (87 %) and transferred into CryoTubes^{TM} (Nunc). Resulting glycerol cultures were stored at -80 °C.

1xLB-Medium	10 g Bacto-Tryptone 5 g Bacto-Yeast 10 g NaCl ad 1 L

3.1.2 Chemical transformation of *E. coli*

In order to make chemical competent bacteria (*E. coli* DH5α), 50 μl of bacteria were plated on a LB plate without antibiotics and incubated at 37 °C overnight (Memmert). Afterwards a single colony was inoculated in 10 ml LB medium without antibiotics and incubated overnight at 37 °C at 150 rpm. 2 ml of the overnight culture were added to 200 ml LB medium without antibiotics and incubated at 37 °C at 150 rpm until the optical density (OD_{600}) of 0.3 - 0.5 was reached. The *E. coli* were cooled down for 20 min on ice water and transferred to a 50 ml falcon. After centrifugation at 3000 rpm at 4 °C for 5 min (Rotina 420R).The pellet was resuspended in 5 ml of TfB-1 buffer. The suspension was centrifuged as described before and resuspended in 4 ml of TfB-2 buffer. Afterwards 100 μl aliquots were prepared and frozen in liquid nitrogen. The chemically competent bacteria were stored at -80 °C.

TfB-1	0.03 M K-Acetat 0.05 M $MnCl_2$ 0.1 M RbCl 0.01 M $CaCl_2$ 15 % Glycerin pH 5.8
TfB-2	0.01 M Na-MOPS pH 7.0 0.075 M $CaCl_2$ 0.01 M RbCl 15 % Glycerin

3.1.3 Transformation of *E. coli*

Chemical transformed *E. coli* were used to insert and manifold vectors of interest. For the transformation the bacteria as described at 3.1.2 were thawed on ice and 100 μl were added to 1 μg of DNA in a 15 ml falcon® 2059. Incubation on ice for 30 min followed by a heat shock at 42 °C for 30 s. The cells were immediately cooled down on ice. Afterwards, 1 ml of LB medium without antibiotics was added and the mixture was incubated for 1 h at 30 °C/ 37 °C at 150 rpm. The bacteria were centrifuged at 4000 rpm for 3 min and resuspended in 100 μl of LB medium and plated on LB plates containing the appropriate antibiotics, followed by overnight incubation at 30 °C or 37 °C.

3.2 Tissue culture techniques

3.2.1 Maintenance and passage of cells

All tissue culture techniques were performed in specialized flow hoods under sterile conditions. Adherent mammalian cells were cultured as monolayers in polystrene cell culture dishes (Sarstedt) with Dulbecco's modified Eagles Medium (DMEM; Sigma) containing 0.11 g/l sodium pyruvate 5 % FBS and 1 % of penicillin/streptomycin solution (1000 U/ml penicillin and 10 mg/ml streptomycin in 0.9% NaCl). To split confluent cells the media was removed and washed once with PBS, followed by addition of the appropriate amount of trypsin (Sigma) for 3-5 min at 37 °C. Trypsin activity was inhibited by addition of standard culture medium. Detached cells were transferred to a 50 ml falcon tube and centrifuged for 3 min at 2000 rpm. The supernatant was removed and the pellet was resuspended in the appropriate volume of standard culture medium. Depending on the experimental procedure cells were further cultivated in the appropriate amount (1:5 or 1:10) or counted as described in 3.2.3.

3.2.2 Storage of mammalian cell line

For long time storage subconfluent mammalian cell lines were trypsinized and pelleted as described in 3.2.1. The cell pellets were resuspended in pure FBS with 10 % DMSO (Sigma) and transferred to Cryotubes^{TM}. The samples were frozen slowly using "Mr. Frosty" (Nalgene). To re-cultivate, cells were rapidly thawed at 37 °C and centrifuged to remove the DMSO. Afterwards, the pellet were resuspended in the appropriate volume of culture medium and seeded in an appropriate cell culture dish followed by incubation as described in 3.2.1.

3.2.3 Determination of cell number

In order to determine the total number of viable cells a Neubauer counter was used. As described in 3.2.1 cells were trypsinized, centrifuged and resuspended in an appropriate volume of culture medium. 10 μl were mixed with 10 μl of trypan blue solution. A small volume of the mixture was added to a Neubauer counter. To obtain the cell number/ ml the mean value of two manual counts (16 squares) was multiplied by the dilution factor and the factor 10^4.

$$\text{cells/ml} = \text{counted cell x 2 (dilution factor) x } 10^4$$

trypan blue solution	0.15 % (w/v) trypan blue 0.85 % (w/v) NaCl

3.2.4 Induction of HIF-1α

Cells were treated as mentioned in 3.2.1 and 3.2.3. For physiological normoxia experiments cells were cultured at 37 °C with 5% of CO_2 (Heraeus®). For hypoxia experiments cells were cultured at 37 °C with either 0.1% of O_2 or 1% of O_2 in an Invivo$_2$ (Baker Ruskinn). To induce HIF-1α under physiological normoxia, cells were treated with 100 μM $CoCl_2$ 16 h prior the experimental procedure.

3.2.5 Transfection with Polyethylenimine

For transfection of mammalian cells linear 25 kDa polyethylenimine (PEI) was used. PEI was dissolved in ddH_2O at a concentration of 1 mg/ml. Using 0.1 M HCl the pH was adapted to 7.2, sterile filtered, aliquoted and stored at -80 °C. Due to the electrostatic interactions PEI is able to build complexes with the DNA and therefore is able to penetrate the membrane and deliver the DNA into the cell. Prior to transfection, cells were seeded at the appropriate concentration. For transfection, DNA and PEI in a ratio 1:5 or 1:10 were added in a 2 ml tube and mixed with 1.8 ml pre warmed DMEM without supplements. The samples were vortexed and incubated for 10-20 min at RT. Before adding the transfection solution, the medium of the cells was removed and DMEM without supplements was added in an appropriate volume. After 4-6 h the medium was exchanged to standard culture medium. Transfected cells were harvested 24-48 h after transfection.

3.2.6 Harvest of mammalian cells

Transfected or infected mammalian cells were harvested by using cell scrapers (Sarstedt) and were collected into 15 or 50 ml falcons which were then centrifuged at 2000 rpm for 3 min at RT (Multifuge 3S-R; Heraeus). After discarding the supernatant, the pellet was washed once with PBS and stored at -20 °C for following experiments.

3.3 Generation of stable knock down cell lines

3.3.1 Generation of recombinant lentiviral particles

To generate recombinant lentiviral particles, HEK293T cells were used. The cells were co-transfected with a plasmid encoding for either scrambled shRNA or shRNA specific for the pro-

tein of interest, as well as the envelope and packaging plasmids pCMV-VSV-G, pMDLg/pRRE and pRSV-Rev. Transfection was peformed as described in 3.2.5. Approximately 48-72 h after transfection cells were harvested and centrifuged for 10 min at 2000 rpm. The supernatant was sterile filtered (0.45 μl) into 2 ml tubes and frozen in liquid nitrogen. Long term storage was at -80 °C.

3.3.2 Infection of mammalian cell line with lentiviral particles

Chosen cell lines for transduction with lentiviral particles were grown to a confluence of 70 to 80% in 12-well culture plates. Prior to infection, media was replaced by DMEM without supplements and 100 μl lentiviral particles were added drop wise. Approximately 2 h post transduction, standard culture media was added. For selection of transduced cells, puromycin (1.5-2 μg/ml) was added to the cells. Cells were cultured and propagated under these conditions. Determining knockdown efficiency was performed via western blot and RNA analysis.

3.4 Adenovirus

3.4.1 Infection of mammalian cell line with HAdV

Prior to infection chosen cell lines were seeded out in the appropriate density (approximately 60-80%). Before adding DMEM without supplements, cells were washed once with PBS. The amount of volume of the virus stock solution, which is needed for infection, was calculated with the following formula:

$$\textit{volume virus stock solution } (\mu l) = \frac{\textit{multiplicity of infection (MOI) x total cell number}}{\textit{virus titer (focus forming units (ffu)/}\mu l)}$$

3.4.2 Propagation and storage of high titer virus stocks

To produce high titer virus stocks several 150 mm cell culture dishes with approximately 80% confluent HEK293 cells were infected as described in 3.4.1. Here a MOI of 20 ffu/cell was used. After 3-5 days post infection, cells were harvested and centrifuged |2000 rpm for 3 min (Rotina 420R). The supernatant was removed and the pellet resuspended in the appropriate volume of DMEM without supplements (approximately 1 ml per dish). Viral particles were released by three subsequent freeze and thaw cycles in liquid nitrogen and at 37 °C. In order to pellet cell debris the samples were centrifuged at 3000 rpm for 10 min. The virus containing supernatant was mixed with 10 % glycerol (97 %) for preservation at -80 °C.

3.4.3 Titration of virus stocks

To determine the titer of virus stocks, immunofluorescence was performed. Infected cells were stained for the adenoviral E2A-72K DNA binding protein (DBP) [328]. In six-well dishes 4x10^5 of HEK293 cells were seeded and infected with 1 ml of virus dilution ranging from 10^{-2} - 10^{-6}. 24 h post infection cells were fixed with ice cold methanol for 15 min at -20 °C and air dried. Plates were stored at -20 °C or directly stained. TBS-BG buffer was used to block non specific antibody binding sites. Samples were incubated for 30 min at RT followed by primary antibody (B6-8, 1:10) incubation for 1 h at RT or up to 16 h at 4 °C. After removing the primary antibody plates were washed three times with PBS-T at RT for 5 min followed by incubation of the secondary antibody (Alexa®488 anti mouse, 1:1000) for 1 h at RT or up to 16 h at 4 °C. The secondary antibody solution was replaced by PBS-T and plates were washed three times followed by counting using a fluorescence microscope (Axiovert 200 M). The total number of infectious particles was calculated according to the infected cell number, virus dilutions and microscope magnification. With this titration technique, the fluorescence forming units (ffu) is determined.

TBS-BG	20 mM Tris-HCl pH 7.6 137 mM NaCl 3 mM KCl 1.5 mM $MgCl_2$ 0.05 %(v/v) Tween 20 0.05 %(w/v) Sodium Azid 5 %(w/v) Glycin 5 %(w/v) BSA
PBS-T	0.001 % (v/v) Tween 20 100 ml 10xPBS ad 1 L
10xPBS	1.4 M NaCl 30 mM KCl 40 mM Na_2HPO_4 15 mM KH_2PO_4 pH 7.3, autoclaved ad 1L

3.4.4 Determination of virus yield

The viral progeny production is determined by seeding 4x10^5 cells in a 6-well plate that were infected afterwards with adenoviruses. They were harvested at appropriate time points post infection as described in 3.2.6. Here cells were resuspended in an adequate volume of DMEM. After virus particle breaking the cells by repeating freeze (liquid nitrogen) and thaw cycles (37 °C), the titer of the virus solution was determined as described above 3.4.3. The particle number produced per cell was calculated by dividing the density of cells.

3.5 DNA Methods

3.5.1 Isolation of plasmid DNA from *E. coli*

For a large scale plasmid preparation a single colony was picked and pre-cultured with 5 ml of LB medium with the appropriate antibiotics. Incubation was at either 37 °C or 30 °C (Multitron) for 8 h. The pre culture was added to 500 ml of LB medium supplemented with the appropriate antibiotics and incubated at either 37 °C or 30 °C (Multitron) for 16-24 h. The bacteria were pelleted by centrifugation at 4500 rpm (Rotixa 50 RS) for 20 min and the plasmid DNA was extracted according to the manufacturers instructions using a MaxiKit (Qiagen). For mini preparation 5 ml of inoculated culture were used. DNA was isolated by a modified protocol of Sambrook and Russel [330]. To 1 ml of culture 0.1 volume of NaAc was added and centrifuged at 14800 rpm (Eppendorf) for 10 min. The supernatant was removed and the pellet was resuspended in 300 μl P1 buffer (Quiagen). To lyse the cells 300 μl of P2 (Quiagen) buffer was gently mixed to the suspension and incubated for 5 min at RT. After the incubation time 300 μl of neutralizing P3 buffer (Quiagen) was added. Finally cell debris was removed by centrifugation at 4800 rpm for 5 min and air dried at RT or 42 °C. The DNA was rehydrated in an appropriate volume of 20-50 μl 10 mM Tris (pH 8.0) solution.

P1	50 mM Tris HCl, pH 8.0 10 mM EDTA 100 μg/ml RNase store at 4 °C
P2	200 mM NaOH 1 % SDS
P3	7.5 M Ammoniom Acetat

3.5.2 Viral DNA synthesis

To determine the viral DNA synthesis samples were prepared as described in 3.7.1. 10 μg of the samples were transferred to a new 1.5 ml reaction tube and mixed with 50 % (v/v) Tween-20, 10 % (v/v) Proteinase K (PK) and 20 μl of ddH_2O. This mixture was incubated for 1 h at 55 °C and subsequently inactivated for 10 min at 95 °C. For further PCR analysis 12.5 μl were used and prepared as described in 3.5.5. Following PCR program was used:

pre denaturing	2 min	95 °C
DNA denaturing	30 sec	95 °C
annealing	60 sec	55 °C
elongation	2 min	72 °C
		25 cycles
final elongation	10 min	72 °C
storage	∞	10 °C

3.5.3 Quantitative determination of DNA/RNA concentrations

Concentration of DNA/RNA was measured with a Nanodrop 2000c UV-Vis spectrophotometer at a wavelength of 260 nm. Purity of the DNA/RNA was determined by the ratio of OD_{260}/OD_{280} with a value of 1.8 for highly pure DNA or at 2.0 for highly pure RNA.

3.5.4 Agarose gel electrophoresis

To prepare an analytical or preparative agarose gel Agarose (Biozym) was dissolved in TBE buffer to a final concentration of 0.6-1.0 % (w/v). The solution was heated in a microwave till the agarose dissolved. After the solution cooled down, ethidium bromide was added in a final concentration of 0.5 μg/ml and poured into an appropaite gel tray with fitting combs. The DNA samples were mixed with 6x loading buffer and subjected to the agarose gel. Electrophoresis was carried out at a voltage of 5-10 V/cm gel length. In order to indicate DNA fragment sizes either a 100 bp or a 1 kb ladder (Fermentas) was applied. For the purpose of visualization of DNA fragments a gel documentation system (Gel Doc^{TM} XR+) at 365 nm was used. Aiming to minimize harmful UV irradiation for preparative purposes, agarose gels were supplemented with 1 mM guanosine. DNA was extracted from gel slices by centrifugation at 20,000 rpm for 2 h (Avanti Je, Beckman) precipitated with isopropanol and 3 M NaAc from the obtained supernatant, washed, dried and rehydrated as described in 3.5.1.

6x loading buffer	10 mM EDTA 50 % (v/v) Glycerol 0.25 % (w/v) Bromphenol blue 0.25 % (w/v) Xylene Cyanol

5x TBE	450 mM Tris pH 7.8 450 mM Boric acid 10 mM EDTA

3.5.5 Polymerase chain reaction

For standard amplification of a DNA template, a 50 μl mixture was prepared by adding 25-100 ng DNA template, 125 ng forward and reverse primer, 5 μl 10x PCR reaction buffer, 1 μl of dNTP mixture (dATP, dTTP, dCTP, dGTP) and 1 μl polymerase (Pfu Ultra II Fusion or Taq) and

filled up to 50 μl with ddH_2Owater in a 0.2 ml tube. Following program was used:

pre denaturing	2 min	95 °C
DNA denaturing	1 min	95 °C
annealing	30-60 sec	55-70 °C
elongation	15-270 sec	72 °C
		25-30 cycles
final elongation	10 min	72 °C
storage	∞	10 °C

DNA denaturation, primer annealing and extension were performed for 25-30 cycles. To determine PCR efficiency 5 μl PCR reaction were analyzed by gel electrophoresis as described in 3.5.4.

3.5.6 Site directed mutagenesis

As a means to introduce site directed mutagenesis forward and reverse primers with the desired mutations were designed and ordered by Metabion. With the following PCR program the mutations were introduced:

DNA denaturing	1 min	95 °C
annealing	45 sec	55 °C
elongation	45 sec/kb	68/72 °C
		12-16 cycles
final elongation	10 min	68/72 °C
storage	∞	10 °C

As described in 3.5.4 PCR efficiency was determined with 10 μl of the PCR product. To remove unmethylated DNA the remaining 40 μl were digested with the enzyme Dpn1 for 1-2 h at 37 °C. To precipitate DNA, 1 volume of isopropanol and 0.1 volume of 3 M sodium acetate (NaAc, pH 5.2) were added and centrifuged at 14800 rpm for 10 min (Heraeus^{TM} Fresco^{TM} 21 Microcentrifuge). Followed by a washing step with 75 % ethanol, spun down for 3 min, dried at 42 °C and dissolved in 30 μl sterile ddH_2O.

3.5.7 Cloning of DNA fragments

Enzymatic DNA restriction

Restriction enzymes were used according to the manufacturer's instructions in suggested reaction buffers (New England Biolabs; Roche). 1 μg DNA was used for analytical restriction digest and incubated with 3-10 U of enzyme for 2 h at 37 °C, unless indicated otherwise. Preparative restriction digests were done with 20 μg of DNA which were incubated with 50 U enzyme

for at least 3 h at 37 °C. If necessary, multiple steps of enzymatic restriction were carried out sequentially.

Ligation and transformation

Enzymatically restricted DNA fragments were ligated using 5 U of antarctic phosphatase (New England Biolabs) at 37 °C for 30 min or 13 °C overnight and if required, dephosphorylated with shrimp alkaline phosphatase (SAP; Roche) at 65 °C for 45 min. Before ligation, the DNA fragments were purified by agarose gel electrophoresis (3.5.4) and/or isopropanol/ethanol precipitation. For a standard ligation 20-100 ng of vector DNA was mixed with 3-5 times more insert DNA in a final volume of 20 μl, including 2 μl of 10x ligation buffer and 1 U of T4 DNA ligase (Roche). Subsequently 10 μl of the ligation product was transformed into chemical competent E. coli as described in 3.1.3, single clones were picked, cultured in 5-10 ml LB media (3.1.1) and prepared plasmid DNA (3.5.1) was analysed by restriction digest (3.5.7), agarose gel electrophoresis (3.5.4) and sequencing (3.5.8) before storage (3.1.1).

3.5.8 DNA Sequencing

For DNA sequencing 1.0 μg of DNA and 20 pmol of sequencing primer were mixed with ddH2O to reach a total volume of 7 μl. Sequencing reactions were performed by Eurofins (Planegg).

3.6 RNA Methods

3.6.1 Isolation of total RNA of mammalian cells

Mammalian cell lines were seeded in the appropriate density and culture dishes, transfected and/or infected as described in 3.2.5 and 3.4.1 followed by harvesting at the proper time points as described in 3.2.6. The cell pellets were resuspended in 600 μl Trizol^{TM} reagent. The samples were either frozen at -20 °C or directly processed. To isolate RNA 200 μl Chloroform was added and samples were vortexed for 15 sec, followed by centrifugation at 14800 rpm for 15 min. After centrifugation different phases are visible. The aqueous supernatant was transferred to a new 1.5 ml tube with 600 μl isopropanol for precipitation of RNA. The samples were thoroughly mixed, followed by centrifugation at 14800 rpm for 15 min. The supernatant was removed and the RNA was washed once with 75 % ethanol. Finally the samples were centrifuged for a last time as described before and the pellet was air dried and rehydrated in

20-50 μl nuclease free water. To determine the amount and purity of total RNA a Nanodrop was used as described in 3.5.3. RNA was stored at -80 °C or further used for reverse transcription for quantitative RT-PCR (3.6.2).

3.6.2 Quantitative reverse transcription (RT) PCR

The RNA was reverse transcribed into complementary DNA (cDNA) using the Reverse transcription kit by Promega. For the reaction 1 μg of RNA was used. To select for processed mRNA the oligo/dt random primers were used. The reaction was performed as described by the manufacturer. The cDNA was stored at -20 °C until further analysis.

3.6.3 Real time PCR

Quantitative reverse transcription (RT)-PCR was measured by a first-strand method in a LightCycler 480 Instrument II (Roche). The cDNA was diluted 1:10. A 10 μl reaction mix was prepared by adding 5 μl of diluted cDNA, 10 pmol forward as well as reverse primers and 5 μl of LightCycler®480 Sybr green I Master (Roche). Measurement was performed in triplicates for each sample and following program was used:

pre denaturing	10 min	95 °C
DNA denaturing	30 sec	95 °C
annealing	30 sec	62 °C
elongation	30 sec/kb	72 °C
	40 cycles	

The average threshold cycle (CT) values were determined from triplicate reactions set relative to a housekeeping gene GAPDH or 18S rRNA. Melting curves were analysed to confirm the identities of the obtained products.

3.7 Protein Methods

3.7.1 Preparation of total cell lysate

To ensure proper solubilization of proteins and to eliminate unspecific or weak protein interactions all total-cell lysates were prepared with highly stringent RIPA lysis buffer. Further, all protein analysis steps were carried out on ice or at 4 °C to reduce the activity of proteases. Cell pellets were harvested as described in 3.2.6 and resuspended in the appropriate volume

of lysis buffer with fresh protease inhibitors 0.2 mM PMSF, 1 mg/ml pepstatin A, 5 mg/ml aprotinin, 20 mg/ml leupeptin, 25 mM iodacetamide and 25 mM N- ethylmaleimide. The samples were incubated for 30 min and vortexed every 10 min. Complete cell disruption as well as genomic DNA shearing was facilitated by sonification for 30 sec (40 pulses, output 0.60; 0.8 impulse/sec). As a means to seperate cell debris and insoluble fraction, the samples were centrifuged at 1100 rpm for 3 min at 4 °C (Heraeus^{TM} Fresco^{TM} 21 Microcentrifuge). The supernatant was transferred to a fresh 1.5 ml tube. Protein concentration was measured by spectrophotometry at 595 nm. Concentrations were determined in relation to the standard curve of several BSA dilutions (3.7.3). Finally, the appropriate dilutions of proteins were denatured by addition of 5x laemmli buffer with a final concentration of 1x laemmli buffer and subsequent boiling at 95 °C for 3 min [330]. Protein lysates were stored at -20 °C until analysis by SDS-PAGE/Western blotting (3.7.7 & 3.7.8).

Ripa Buffer	50 mM Tris-HCl pH 8.0 150 mM NaCl 5 mM EDTA 1 % (v/v) NP-40 0.1 % (w/v) SDS 0.5 % (w/v) Sodium deoxycholate

5x Laemmli Buffer	250 mM Tris-HCl pH 6.8 50 % (v/v) Glycerol 3.75 % (v/v) β-Mercaptoethanol (freshly added) 10 % (w/v) SDS 0.5 % (w/v) Bromphenol blue ad H_2O

3.7.2 Native gel electrophoresis

To determine viral capsid formation, cells were transfected followed by infection (3.2.5, 3.4.1) and harvested at appropriate time points. Samples were resuspended in a low stringent lysis buffer and incubated for 10 min on ice. Samples were centrifuged at 12.000 rpm at 4 ∘C. Samples were mixed with 6xloading buffer and subjected to agarose gel electrophoresis. Proteins were transferred to nitrocellulose blotting membranes (0.2 μm) by capillary transfer using 10x saline sodium citrate (SSC) buffer and visualized by immunoblotting. X-rays were scanned and cropped using power point.

low stringent NP40	50 mM Tris-HCl pH 8.0 100 mM NaCl 1 mM EDTA 1 % (v/v) NP-40

3.7.3 Quantitative determination of protein concentration

Protein concentrations were measured using a Protein Assay according to Bradford [331]. 1 μl of sample was added to 800 μl ddH_2O and 200 μl of Bradford Reagent (Applichem). Measurements were done in a SmartSpec Plus spectrophotometer (BioRad) at 595 nm against a blank. Protein concentrations were determined by interpolation from a standard curve with BSA (New England Biolabs).

Standard curve	1 μg/μl	10 μl of 0.1 μg/μl BSA
	2 μg/μl	20 μl of 0.1 μg/μl BSA
	4 μg/μl	4 μl of 1 μg/μl BSA
	8 μg/μl	8 μl of 1 μg/μl BSA
	16 μg/μl	16 μl of 1 μg/μl BSA

3.7.4 Treatment with the proteasome inhibitor MG132

MG 132 is a chemical that inhibits the proteasome dependent degradation. As described previously cells were seeded (3.2.1), transfected (3.2.5) and/or infected (3.4.1). 4 h before harvesting the cells, 25 μM MG132 was added to the samples.

3.7.5 Nickel-nitrilotriacetic acid (Ni-NTA) pull down

Cells or vectors expressing a 6xHis-SUMO-2 were transfected and/or infected with the appropriate amount of virus/vector and harvested as described in 3.2.6. Before removing the PBS, 20 % were transferred to a new 1.5 ml tube and used for total protein analysis. The remaining 80 % of cells were resuspended in 5 ml of guanidinium containing lysis buffer and either stored at -80 °C till further analysis or immediately sonicated for 30 sec (40 pulses, output 0.60; 0.8 Impulse/s; Branson Sonifier 450). Followed by incubation in a rotator (GFL 3025) over night at 4 °C with in lysis buffer prewashed 25 μl Ni-NTA beads. After incubation, the samples were centrifuged at 4000 rpm and transferred to a new 1.5 ml tube and centrifuged at 2000 rpm for 3 min. The supernatant was removed and 1 ml of denaturing wash buffer pH 8.0 was added followed by centrifugation as mentioned. The samples were washed twice with 1 ml of denaturing wash buffer pH 6.3. Finally, the samples were eluted in 20 μl of elution buffer and boiled at 95 °C for 3 min. Samples were stored at -20 °C till further analysis. Prior to separation by SDS Page, the samples were centrifuged for 10 min at 14800 rpm.

wash buffer pH 6.3	8 M Urea 100 mM Na_2HPO_4 100 mM NaH_2PO_4 10 mM Tris-HCl pH 6.3 20 mM Imizadole 5 mM β-Mercaptoethanol (freshly added) protease inhibitors (freshly added)
wash buffer pH 8.0	8 M Urea 100 mM Na_2HPO_4 100 mM NaH_2PO_4 10 mM Tris-HCl pH 8.0 20 mM Imizadole 5 mM β-Mercaptoethanol (freshly added) protease inhibitors (freshly added)

denaturing guanidin buffer	6 M GuHCl 100 mM Na_2HPO_4 100 mM NaH_2PO_4 10 mM Tris-HCl pH 8.0 20 mM Imizadole 5 mM β-Mercaptoethanol (freshly added) protease inhibitors (freshly added)
Elution buffer	200 mM Imizadole 0.1 % (w/v) SDS 30 % Glyceol 150 mM Tris-HCl pH 6.3 720 mM β-Mercaptoethanol 0.01 % (w/v) Brompenhol blue

3.7.6 Immunoprecipitation

For immunoprecipitation equal amounts (1-5 mg) of total-cell lysates (3.7.1) from each sample were precleared by addition of 30 μl/sample Pansorbin A for 30 min at 4 °C in a rotator (GFL 3025). Prior to antibody coupling of the Sepharose A beads, 3-5 mg/IP had to be incubated at 4 °C for 15 min with 1 ml of RIPA buffer. Followed by coupling of appropriate amounts of antibody to the beads for 1 h at 4 °C. After incubation the beads were centrifuged at 6000 rpm for 3 min (Heraeus^{TM} Fresco^{TM} 21 Microcentrifuge) and washed once with 1 ml RIPA buffer supplemented with fresh protease inhibitors. The precleared samples were transferred to a new 1.5 ml tube and beads with coupled antibody were added to the samples. Immunoprecipitation was performed at 4 °C in a rotator (GFL 3025) for 2 h. The resulting protein complexes were pelleted by centrifugation at 6000 rpm for 3 min (Heraeus^{TM} Fresco^{TM} 21 Microcentrifuge) and washed once with 1 ml RIPA buffer with fresh protease inhibitors. In order to elute the proteins, the appropriate amount of 2x laemmli buffer was added, leading to the final concentration of 1x laemmli buffer [330]. Subsequently, the samples were boiled at 95 °C for 5 min and stored at -20 °C until further analysis. Prior to loading on SDS Page (3.7.7), the samples were centrifuged at 14800 rpm for 10 min and the supernatant was loaded onto the gels.

2x Laemmli-Buffer	100 mM Tris-HCl pH 6.8 20 % (v/v) Glycerol 1.57 % (v/v) β-Mercaptoethanol (freshly added) 4 % (w/v) SDS 0.2 % (w/v) Bromphenol blue ad H_2O

3.7.7 Sodium Dodecylsulfate Polyacrylamide gel electrophoresis

As means to seperate protein samples of lysates (3.7.1), immunoprecipitation (3.7.6) or SUMOylation pull down (3.7.5) SDS Page (Sodium Dodecylsulfate Polyacrylamide gel electrophoresis) was used. All gels were prepared by the Multigel SDS-PAGE system of Biometra according to the manufacturer's instructions and run at 15-20 mA/gel in TGS-buffer. Polyacrylamide gels were made by using 30 % acrylamide/bisacrylamide solution (37.5:1 Rotiphorese Gel 30; Roth) diluted to the final concentration of 8-15 % with ddH_2O. Protein samples were concentrated between the lower pH of the stacking gel in comparison to the higher pH value of the separation gel. Acrylamide polymerization was initiated by addition of ammonium persulfat (APS) (final=0.1%) and tetramethylethylenediamine (TEMED) (final=0.01]%). To determine the molecular weight of proteins, Page Ruler^{TM} Prestained Protein Ladder Plus (Fermentas) was loaded onto the gels. Afterwards, separated proteins were transferred onto nitrocellulose membranes (Amersham Protran®) by western blotting (3.7.8).

30 % Acrylamid stock solution	29 % (w/v) Acrylamid 1 % (w/v) N,N'Methylen-bisacrylamide
5 % stacking gel	17 % (v/v) Acrylamid (30 %) 69 % (v/v)H_2O 13 % (v/v)1 MTris pH 6.8 0.1 % (v/v) SDS 0.1 % (v/v) APS 0.01 % (v/v) TEMED
8 % seperating gel	26 % (v/v) Acrylamid (30 %) 46 % (v/v) H_2O 26 % 1.5 M Tris pH 8.8 0.1 % (v/v) SDS 0.1 % (v/v) APS 0.06 % (v/v) TEMED
10 % seperating gel	34 % (v/v) Acrylamid (30 %) 38 % (v/v) H_2O 26 % (v/v) 1.5 M Tris pH 8.8 0.1 % (v/v) SDS 0.1 % (v/v) APS 0.04 % (v/v) TEMED
15 % seperating gel	50 % Acrylamid (v/v) (30 %) 22 % (v/v) H_2O 26 % (v/v) 1.5 M Tris pH 8.8 0.1 % (v/v) SDS 0.1 % (v/v) APS 0.04 % (v/v) TEMED
TGS	25 mM Tris 192 mM Glycin 0.1 % (w/v) SDS

3.7.8 Western Blot

Protein samples separated by SDS-Page (3.7.7) were transferred onto 0.45 μm or, if the protein is smaller than 20 kDa, 0.2 μm Nitrocellulose membrane (GE Healthcare) using the Trans-Blot Electrophoretic Transfer Cell System (BioRad) in Towbin-buffer. Gels and membranes were soaked in Towbin-buffer, placed upon one another between two soaked blotting papers (Whatman) and two blotting pads in a plastic cassette. The electric transfer was performed in "full wet" mode in a blotting chamber with Towbin-buffer at 400 mA for 90 min. After the transfer, membranes were shortly incubated in Poncaeu-S to exclude air bubbles. In order to saturate unspecific antibody binding areas, nitrocellulose membranes were incubated for 30-60 min in 5 % non fat dry milk at 4 °C. Subsequently, the blocking solution was removed and membranes were washed briefly with PBS-T to remove residual blocking solution. The appropriate dilution of primary antibody was used and membranes were incubated over night at 4 °C. After the removal of the primary antibody, membranes were washed three times for 5 min and incubated overnight with HRP-coupled secondary antibody (1:10,000) diluted in 3 % non fat dry milk solved in PBS-T. Subsequently, after removal of the secondary antibody, membranes were washed three times for 5 min with PBS-T. Protein bands were visualized by enhanced chemiluminescence using a self made solution. 10 ml of solution A were mixed with 100 μl of solution B and 10 μl H_2O_2. Membranes were shortly incubated in the solution and immediately transferred to X-Ray cassettes and X-Ray films were added. The X-Ray films were developed using an Agfa Curix 60. X-Ray films were scanned, cropped and figures were prepared using PowerPoint (Microsoft). For quantification of protein signals the software ImageJ (Wayne Rasband) was used.

PBS-T	0.1 % (v/v) Tween 20 100 ml 10x PBS ad 1 L
ECL-B	7.6 mM p-coumaric acid in DMSO
ECL-A	1.25 mM Luminol Sodium 1 M Tris-HCl pH 8.6 ad ddH_2O
Blocking solution	5 % (w/v) Nonfat dry milk in 1x PBS
Towbin buffer	25 mM Tris-HCl pH 8.3 200 mM Glycin 0.05 % (w/v) SDS 20 % (v/v) Methanol
Ponceau S	0.002 % (w/v) Ponceau S 3 % (v/v) TCA

3.8 Indirect Immunofluoroscence

For indirect immunofluorpscence the appropriate amount of cells were seeded out on glass coverslips (3.2.1) followed by transfection (3.2.5) and/or infection (3.4.1) as described before. According to the experimental setup, samples were fixated at the appropriate time points with 4 % Paraformaldehyd (PFA) and incubated for 10 min at RT. The samples were washed three times and stored with 1x PBS at 4 °C or immediately processed for further analysis.

3.8.1 Antibody staining of immunofluoroscence samples

To stain samples for immunofluorescence (3.8) samples were permeabilized with 0.5 % (v/v) Triton-X100 in PBS for 5 min at RT. Followed by blocking of unspecific antibody binding sites with TBS-BG for 1 h at RT. The appropriate antibody solutions were prepared in PBS-T and put directly onto the glass coverslips. Samples were incubated over night at 4 °C in a damp plastic chamber. After washing the samples three times with PBS-T for 5 min the corresponding fluorescence coupled secondary antibody was added to the samples and incubated overnight in the dark at 4 °C in a damp plastic chamber. Finally, after washing three times with PBS-T, samples were dried and mounted on glass slides with Mowiol. Samples were incubated over night in the dark at RT. Digital images were aquired using a confocal microscope (Axiovert 200 M microscope), which were further processed and analysed using the software Volocity (PerkinElmer).

TBS-BG	20 mMTris-HCl pH 7.6 137 mM NaCl 3 mM KCl 1.5 mM $MgCl_2$ 0.05 %(v/v) Tween 20 0.05 %(w/v) Sodium Azide 5 %(w/v) Glycine 5 %(w/v) BSA
Mowiol	100 mMTris-HCl pH 8.5 24 % (v/v) Glycerol 9.6 % (w/v) Mowiol ad ddH_2O

PBS-Triton	0.5 % (v/v) Triton-X-100

3.9 Reporter gene assay

As a means to quantitatively determine the promoter activities, the Dual-Luciferase®Reporter Assay System (Promega) was used. Luciferases are enzymes with catalytic activity that emit

visible light upon substrate conversion. The firefly luciferase is the most commonly used luciferase catalyzing following reaction:

$$\text{Luciferin} + \text{ATP} \rightarrow \text{luciferyl adenylate} + \text{PPI}$$

$$\text{Luciferyl adenylate} + \text{O}_2 \rightarrow \text{oxyluciferin} + \text{AMP} + \text{light}$$

Transcriptional activity of a promoter of interest was investigated by transiently transfecting cells with a reporter construct harboring a luciferase ORF under the control of this particular promoter and normalized to constitutively expressed renilla luciferase (*Renilla reniformis*) that served as internal transfection control. Cells were seeded out, transfected and/or infected as described previously (3.2.1, 3.2.5, 3.4.1). According to the experimental setup, samples were harvested at the appropriate time points by directly adding 150 μl /well of passive lysis buffer and incubated for 15 min at RT. 5 μl of lysate was transferred to a new 1.5 ml tube with predispensed 20 μl LAR II. Samples were mixed and measured in a GlowMax Multi Jr luminometer (Promega). Subsequently, *renilla* activity was measured by addition of 20 μl 1x Stop and glo buffer. This sequential measurement is possible as *firefly* luciferase activity is blocked by the pH conditions of the *renilla* substrate. The relative luciferase unit (RLU) was calculated through dividing the *firefly*-value by the corresponding *renilla*-value.

Chapter 4

Results

4.1 Hypoxia modulates HAdV infection

4.1.1 HAdV gene expression is suppressed during hypoxia

As described in 1.4.2, PML-NBs are playing an essential role during antiviral defense [220]. Subsequently, different viruses evolved a distinct mechanism to counteract PML-NBs (1.11). For example, the HAdV early viral protein E4orf3 leads to a disruption of the dot like structure to a track-like structure, thus inhibiting the antiviral measurements [152]; [153]; [154]. At the same time replication of the HAdV occurs in close proximity to the PML-NBs, indicating that the HAdV takes advantage of some associated components of the PML-NBs, while antagonizing others [156]; [221]; [222]; [223]; [224]; [225]. Recently it was observed that HIF-1α supports antiviral defense in the host cell [307], but at the same time supports viral replication for different DNA viruses [309]; [302]; [310]; [311]; [313]; [314]. It has been also shown, that HIF-1α leads to the degradation of PML [315]. Until today it is unknown whether hypoxia might affect HAdV replication. Our initial hypothesis was, that HIF-1α supports HAdV infection by suppression of PML-NBs. In order to investigate the influence of extreme hypoxia on HAdV replication, we treated H1299 cells in an O_2-chamber with 0.1 % of oxygen 24 hours prior to infection. Samples were harvested after 24 hours post infection (hpi) and were investigated at the protein, DNA level and viral progeny production. Under physiological normoxia (phys. normoxia) we observed no stabilization of HIF-1α. Infection of cells with an HAdV-wt and staining for selected viral proteins, showed expression of all tested viral proteins (Figure 4.1A lane 1 and 2). During hypoxia we detected stabilized HIF-1α protein levels (Figure 4.1A lanes 3 and 4), but the expression of adenoviral proteins is reduced compared to protein expression under physiological normoxia. We also investigated the influence of extreme hypoxia on the HAdV

DNA synthesis and observed reduced viral DNA levels during hypoxia (Figure 4.1B lanes 2 and 4). To assess the effect on viral progeny production, we determined the total virus yield during hypoxia in comparison to physiological normoxia. Stabilization of HIF-1α reduced viral progeny in H1299 cells five-fold after 24 hpi compared to physiological normoxia (Figure 4.1C). To determine viral replication during mild hypoxia, we treated H1299 cells in an O_2-chamber with 1 % of oxygen. We harvested cells 24 hpi and 48 hpi and determined the protein levels of HIF-1α and selected viral proteins. Our results show that under mild hypoxia HIF-1α is reduced at 48 hpi (Figure 4.1D lane 6) and viral protein expression is comparable to physiological normoxia (Figure 4.1D lanes 2,3 and 5,6).

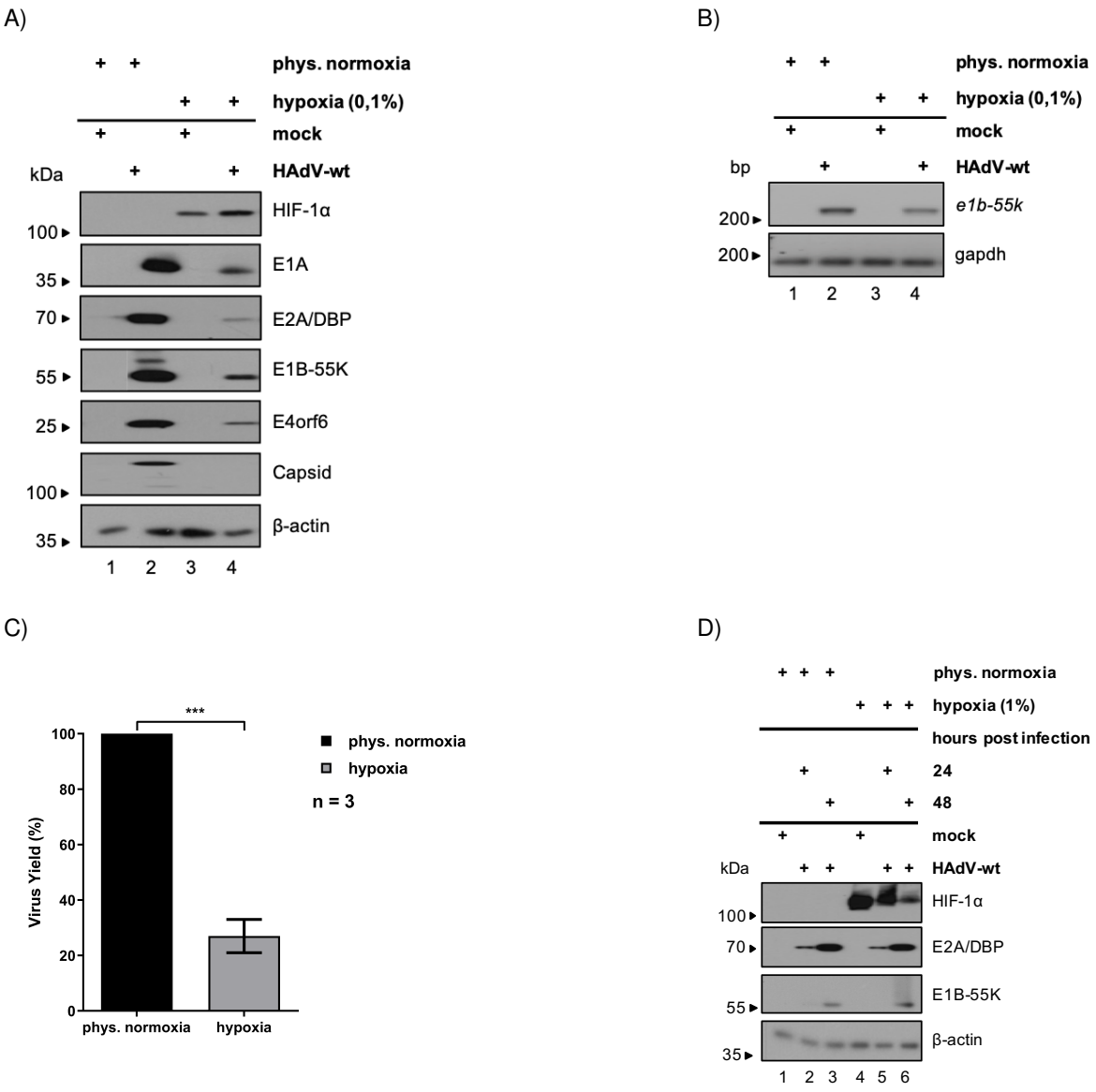

Figure 4.1: Hypoxia is a negative factor for HAdV replication
Prior to infection, cells were treated as described in 3.2.4, shortly 24 h prior to infection H1299 cells were either treated under phys. normoxia, extreme hypoxia (0.1 %) or mild hypoxia (1 %) conditions. Cells were infected with a HAdV-wt with a MOI of 50 and harvested 24 h post infection (hpi). A) Total-cell lysate was extracted as described in 3.7.1 followed by 10 % - 12 % SDS-Page and western blot analysis (3.7.7 ; 3.7.8). Samples were stained for HIF-1α (BD Science), early viral proteins E1A (M73), E2A/DBP (B6-8), E1B-55K (2A6) and E4orf6 (RSA3) and the late viral protein Capsid (L133). As loading control β-actin (AC-15) was used. B) Cells were treated as mentioned in 3.5.2. 10 μg of Protein lysate were treated with Proteinase K to isolate DNA followed by PCR for *e1b-55k* and *gapdh*. C) H1299 cells were infected under hypoxia or phys. normoxia and harvested at appropriate time points. The harvested virus was used to reinfect 293 cells. After fixation with ice cold MeOH cells were stained for E2A/DBP (B6-8) followed by Alexa 488 staining and counted. Bar charts represent average values and standard deviations based on three independent experiments. Statistically significant differences were determined using a two-sided Welch's t-test. *: $P \leq 0.05$, **: $P \leq 0.01$, ***: $P \leq 0.001$, n.s.: no significance. D) HepG2 cells were treated in an hypoxia chamber (1 %) 24 h prior to infection and harvested at appropriate time points and western blot was performed for HIF-1α (BD Science), E2A/DBP (B6-8), E1B-55K and β-actin.

It is known that the PML-NBs play an essential role for the efficient viral replication [221], [156], [222], [223], [224]. Next, we unravel whether the observed negative effects of hypoxia on HAdV gene expression and progeny production are caused by hypoxia-mediated modulation of the PML-NBs. Thus, the number of PML-NBs during physiological normoxia and hypoxia was investigated by immunofluorescence analysis. Here we observed no changes of the quantity of PML-NBs during hypoxia compared to physiological normoxia (Figure 4.2A, 4.2B). Taken together, these results provide evidence that modulation of PML-NBs in number is not affected by hypoxia. Stabilization of HIF-1α and simultanous repression of HAdV gene expression is not dependent on PML-NB mediated effects. .

A)

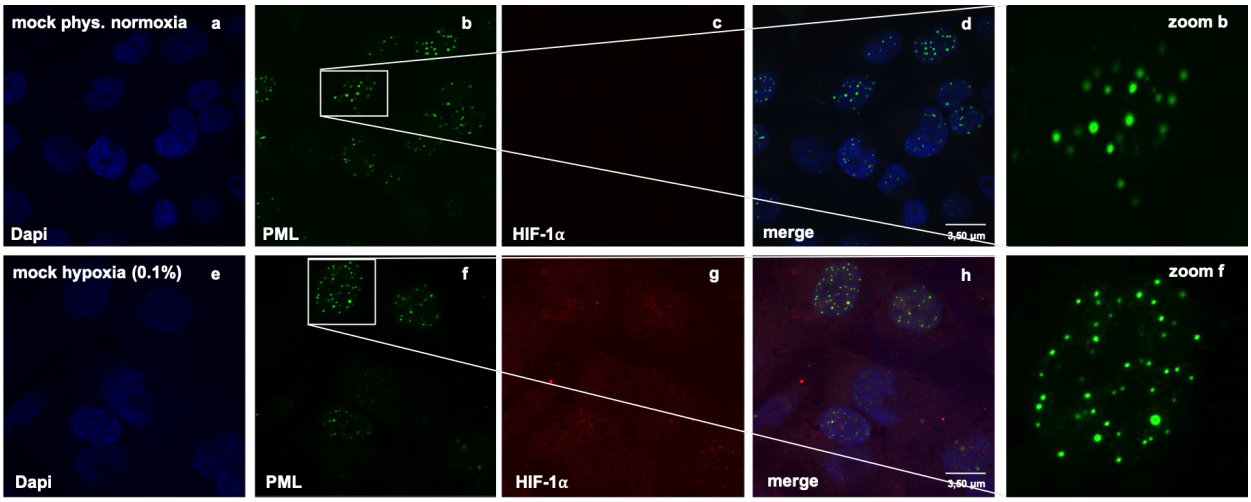

B)

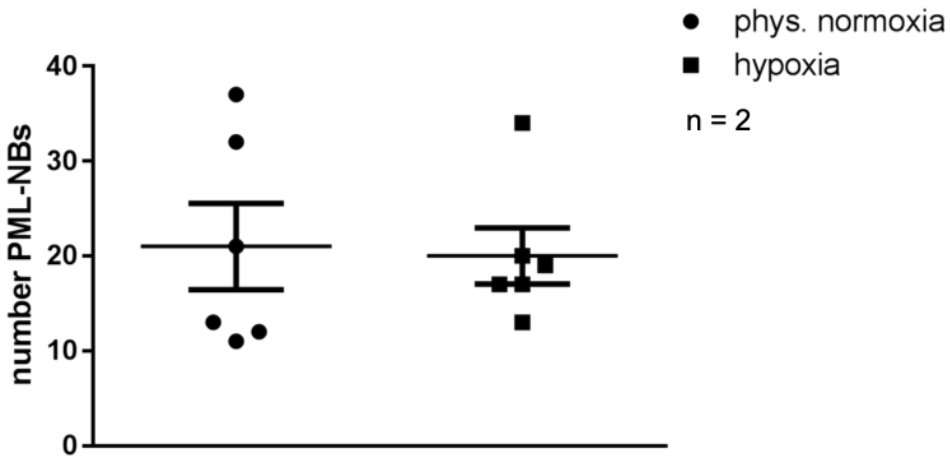

Figure 4.2: Hypoxia does not influence quantity of PML-NBs
Prior to infection, cells were treated as described in 3.2.1, shortly 24 h prior to infection H1299 cells were either treated under phys. normoxia or extreme hypoxia (0.1 %) conditions. Cells were infected with a HAdV-wt with a MOI of 50 and harvested 24 hpi. A) Immunofluorescence analysis was performed for PML (NB100-59787), HIF-1α (Santa Cruz) and Dapi. B) 50 cells were counted for amount of PML-NBs. Graph was established in GraphPad Prism 5.

4.1.2 Overexpression of HIF-1α represses HAdV replication

In order to asses, whether HIF-1α stabilization is responsible for the negative effect on HAdV replication, HIF-1α was overexpressed. In addition, a HIF-1α variant was transfected (3.2.5), comprising mutations at P405A and P531G within the ODD region. These mutations block the capacity of PHDs, thus the pVHL is not able to bind and degrade HIF-1α [297]; [298]; [299]; [300]. Samples were harvested 24 hpi, 48 hpi and western blot analysis was performed. Interestingly HAdV is not able to degrade overexpressed HIF-1α (Figure 4.3 a, lane 3-6). Expression of the early viral protein E1B-55K is four-fold and nine-fold reduced, if HIF-1α or respectively HIF-1α-P405A/P531G is co-expressed (4.3A, lane 4 and 6).Whereas E4orf6 is four-fold reduced if HIF-1α is co-expressed (4.3A, lane 4). To validate the negative effects of HIF-1α on viral replication, viral progeny production was determined after transfection of HIF-1α and HIF-1α P405A/P531G (4.3B; 4.3C). Compared to cells transfected with an empty vector viral progeny production was significantly reduced (five-fold), when HIF-1α was overexpressed (Figure 4.3B). The production of infectious viral particles was proportionally reduced to the increasing concentration of transfected HIF-1α (4.3C). The same effect can be observed for HIF-1α-P405A/P531G (4.3B, 4.3C). Those results are in accordance with the previous hypoxia results (4.1.1), indicating that HIF-1α is a novel restriction factor for HAdV replication.

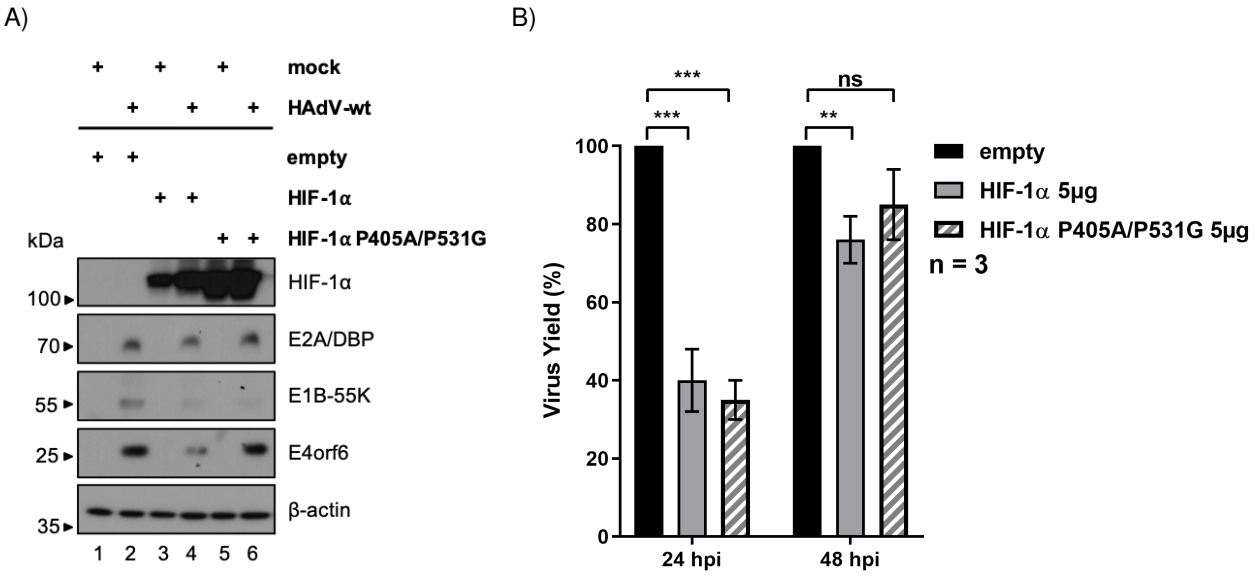

C)

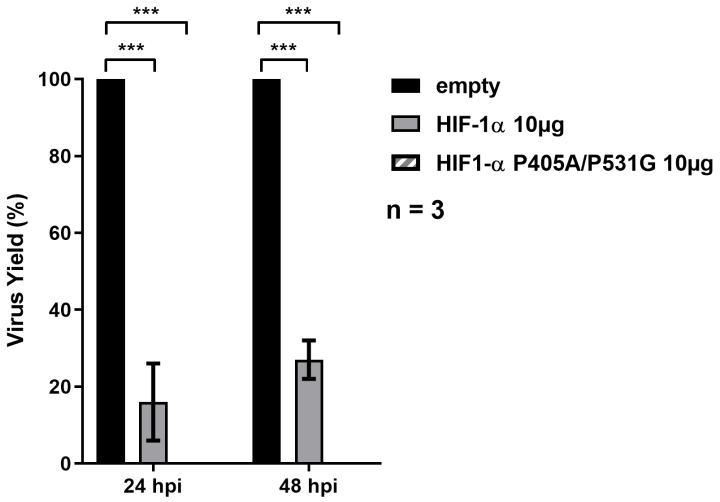

Figure 4.3: Overexpression of HIF-1α represses HAdV gene expression and progeny production
H1299 cells were transfected with either an empty vector or HIF-1α or HIF-1α-P405A/P531G (3.2.5). A) Samples were harvested 48 hpi and total-cell lysates were extracted (3.7.1) and resolved by 10 % - 12 % SDS-PAGE. Samples were stained for HIF-1α (BD Science), E2A/DBP (B6-8), E1B-55K (2A6), E4orf6 (RSA3) and β-actin (AC-15). B)-C) H1299 cells were transfected either with an empty vector, HIF-1α or HIF-1α-P405A/P531G with respectively 5 μg or 10 μg of DNA followed by infection with a HAdV-wt, MOI 50 (3.4.1). Samples were harvested after appropriate time points (3.2.6) and 293 cells were reinfected (3.4.4). 24 hpi samples were fixed with ice cold MeOH and stained for E2A/DBP (B6-8) followed by Alexa 488 staining. Stained samples were counted with a microscope (Zeiss). Statistically significant differences were determined using a two-sided Welch's t-test. *: P $\leq$ 0.05, **: P $\leq$ 0.01, ***: P $\leq$ 0.001, n.s.: no significance.

Next, we performed proliferation assays to exclude any effect of HIF-1α mediated changes on cell proliferation. Samples were transfected as described above and harvested at appropriate time points. Samples were counted in triplicates with trypan blue (3.2.3). Validation of the expression was done by western blot (Figure 4.4B). We observe that all cells grow constantly till 24 h post transfection. While the cell proliferation of the empty control is reduced two-fold at 48 h post transfection, the samples expressing HIF-1α and HIF-1α-P405A/P531G show no impaired cell proliferation, indicating a positive effect of HIF-1α on cell proliferation (4.4A). Together, these data show that stabilization and expression of HIF-1α restricts efficient HAdV gene expression and progeny production.

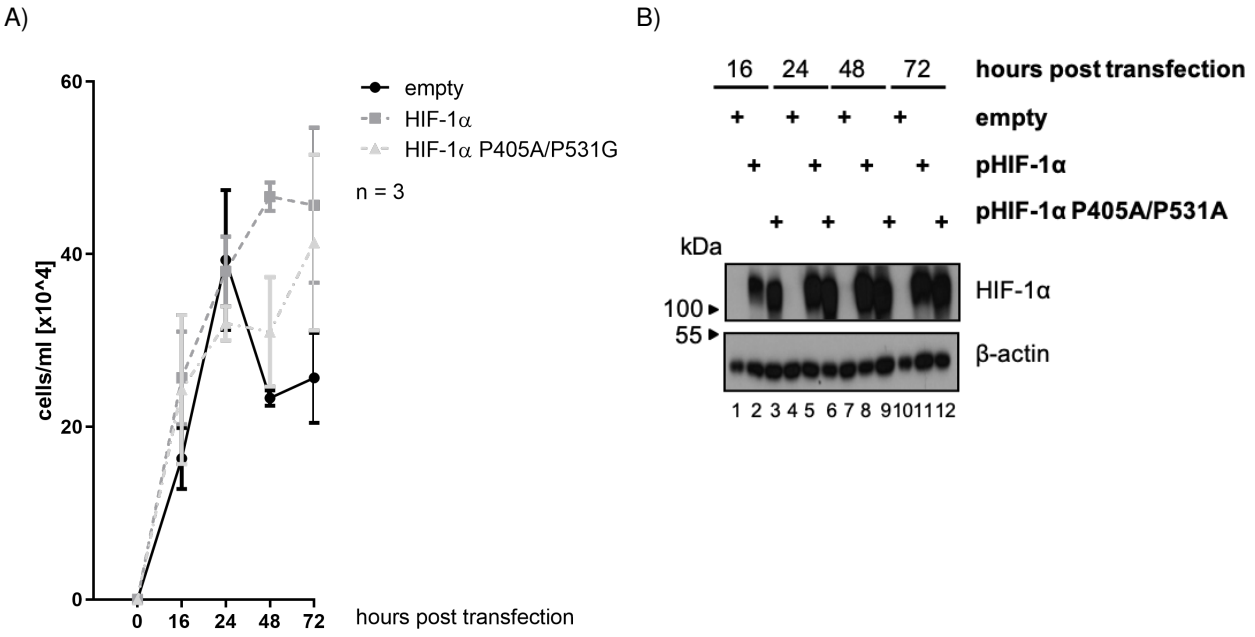

Figure 4.4: HIF-1α promotes cell proliferation
A) H1299 cells were either transfected with an empty vector, HIF-1α or HIF-1α-P405A/P531G and harvested after 16, 24, 48, and 72 h (3.2.5). Samples were counted in triplicates with trypan blue as described in 3.2.3. B) From the same samples as described in A) total-cell lysates were made and resovled by 10 % SDS-PAGE. After western blot analyses was performed samples were stained for HIF-1α and β-actin.

4.1.3 HIF-1α interferes with HAdV capsid formation

After investigating the influence of hypoxia and overexpressed HIF-1α, it was shown that presence of HIF-1α has a negative effect on HAdV replication. To asses a possible molecular mechanism how HIF-1α represses HAdV replication, we screened the HAdV genome for potential hypoxia response element (HRE) sequences. Putative HRE regions contain a highly conserved core sequence (5′-G/ACGTG-3') [301]; [332]. and was found in HAdV serotypes C, D, B and F genomes. In HAdV-C5, we found the HRE sequence twice (Figure 4.5A, blue box), one is located at position 384 bp and the other one at position 11303 bp. The first position is within the packaging signal of HAdV-C5 (Figure 4.5B).

A)

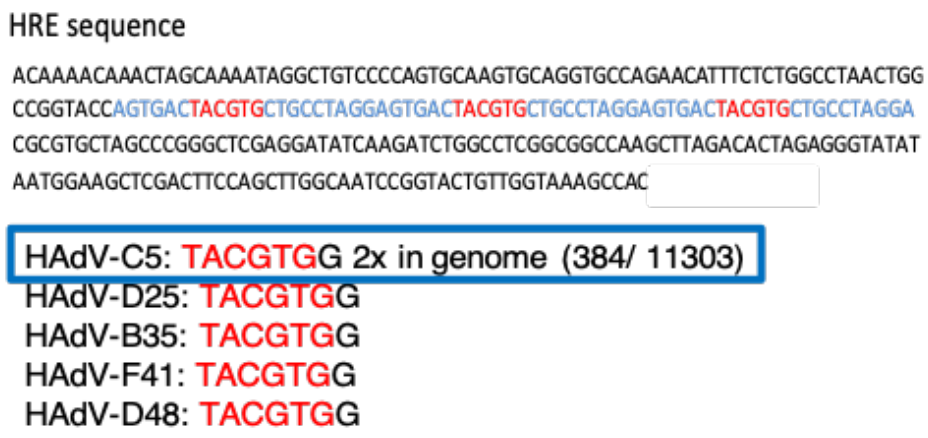

B)

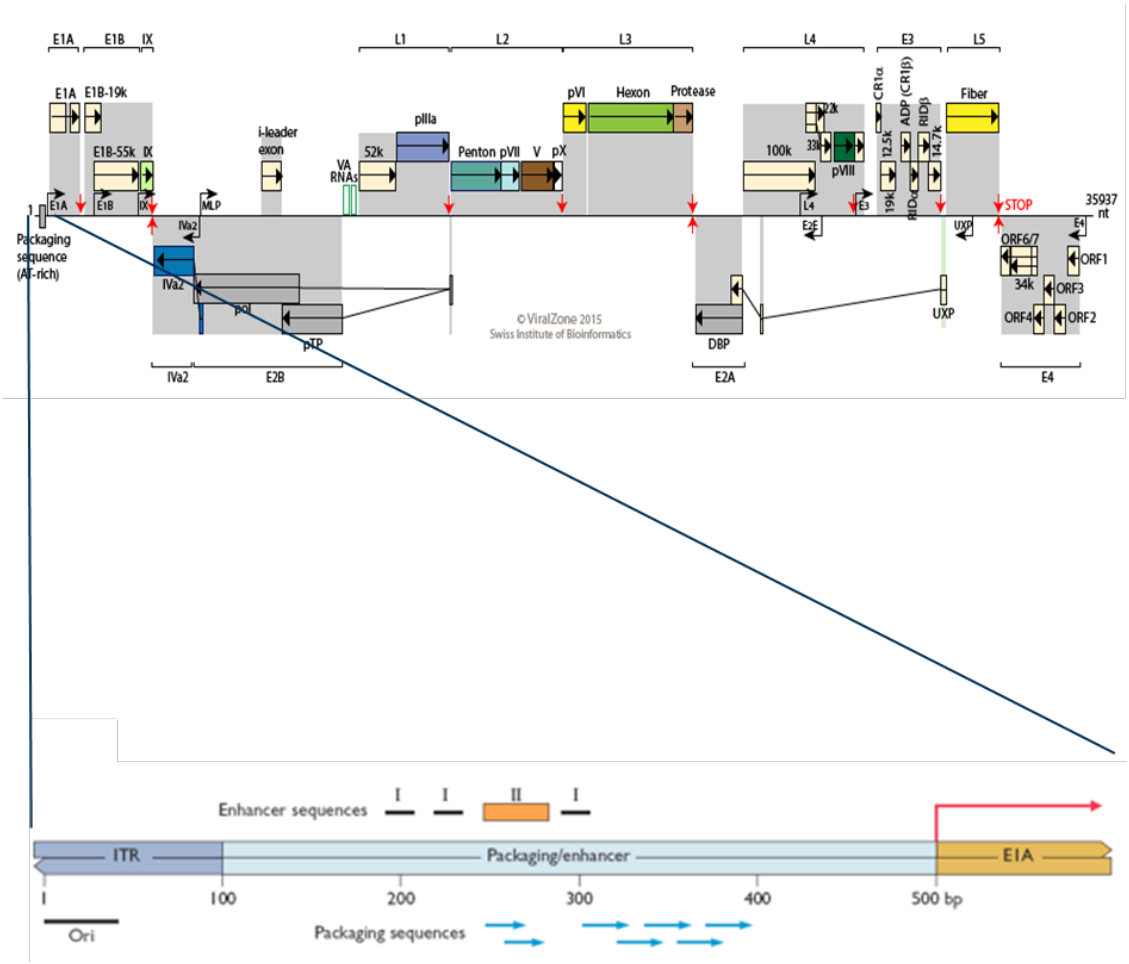

Figure 4.5: Conserved HRE sequence is found in viral genomes of several HAdV serotypes
A) HRE vector was sequenced and the core sequence was determined (5'-G/ACGTG-3' marked in red). B) Closer examination of the HRE sequence and the packaging sequence within HAdV-C5.

Since the packaging signal is essential for the efficient capsid formation (1.2), it was tested whether HIF-1α is capable of inhibiting adenoviral packaging by native gel analysis. H1299 cells were transfected with either an empty vector, HIF-1α or HIF-1α-P405A/P531G followed by infection with HAdV-wt. Samples were harvested 48 hpi as described in 3.7.2. Figure

4.6A confirms the expression of transfected HIF-1α and HIF-1α-P405A/P31G (Figure 4.6A lanes 2 and 3) and infection (Figure 4.6A lanes 1 to 3). As expected, capsid formation is not impaired, if an empty vector is transfected (4.6B, lane 1). However, transfection of HIF-1α reduces packaging two-fold (4.6B, lane 2). The capsid formation is even 3-fold reduced, if HIF-1α-P405A/P531G is co-expressed (4.6B lane 3), confirming that HIF-1α disrupts capsid formation.

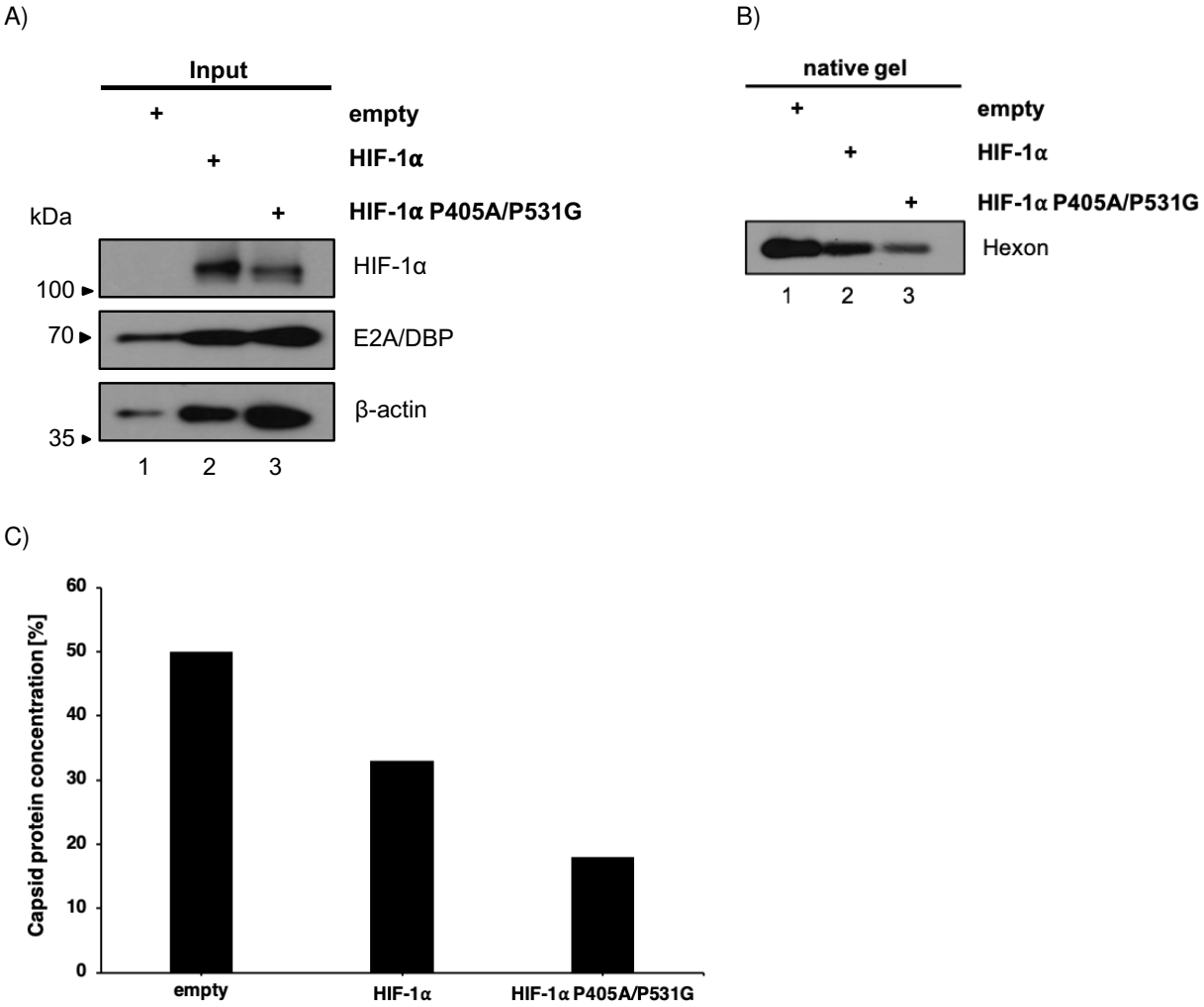

Figure 4.6: HIF1-α inhibits capsid formation of HAdV
A) For determination of protein steady state levels, lysates were denatured using Laemmli buffer, separated by 10 % SDS-PAGE and analysed by western blot against HIF-1α (BD Science), E2A/DBP (B6-8) and β-actin (AC-15). B) Samples were lysed using a low stringent NP-40 lysis buffer. Native lysates were separated by agarose gel electrophoresis and further analysed by immunoblotting stained for Hexon (Abcam). C) Intensity of bands were analysed with ImageJ.

4.2 HAdV counteracts HIF-1α restrictive function

4.2.1 HIF-1α protein levels are repressed during HAdV infection

In order to artificially induce the stabilization of HIF-1α a chemical was used. Cobalt(II)-chloride ($CoCl_2$) inhibits PHDs, which under normoxia mark HIF-1α for degradation (Figure 4.7A) [333]. We treated H1299 with 100 μM $CoCl_2$ 16 h prior to infection. We confirmed that HIF-1α is stabilized up to 48 h after treatment with $CoCl_2$ (Figure 4.7B). Subsequently, the influence of HAdV infection on HIF-1α was investigated.

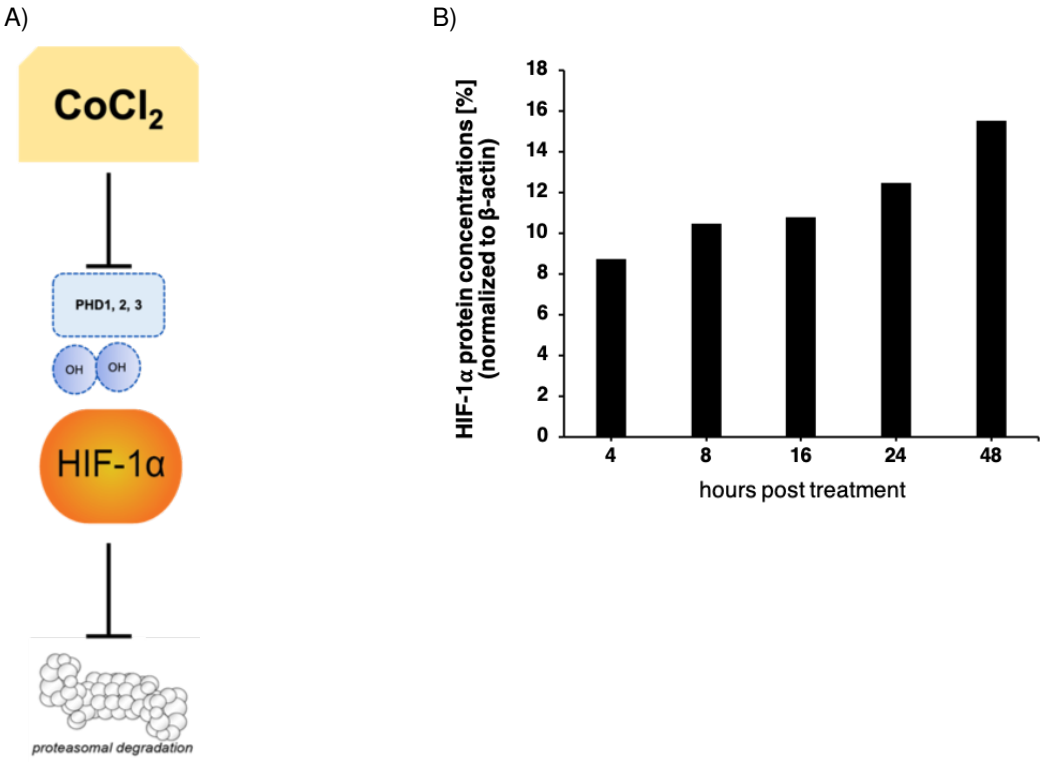

Figure 4.7: $CoCl_2$ is an artificial inducer of HIF-1α
A) Schematic overview of $CoCl_2$ preventing proteasomal degradation of HIF-1α. $CoCl_2$ inhibits the functions of PHDs, thus HIF-1α can not be marked for proteasomal degradation. B) H1299 cells were treated with 100 μM $CoCl_2$ to stabilize HIF-1α. At appropriate times cells were harvested and western blot for HIF-1α (BD Science) and β-actin (AC-15) was performed. Intensity of bands was analysed with ImageJ.

After treatment with $CoCl_2$, the protein levels of HAdV and HIF-1α were investigated. H1299 cells were treated as mentioned above and subsequently infected with HAdV-wt. Samples were harvested at time points 0, 8, 16, 24, 48 and 72 hpi. Whereas 0 hpi served as the uninfected mock control. Here we observed that HIF-1α protein levels are two-fold reduced at 24 hpi leading to a repressed signal after 48 hpi (Figure 4.8 lane 5 and 6).

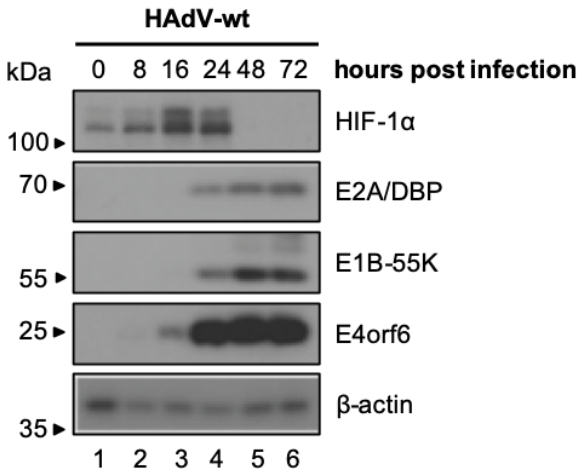

Figure 4.8: HAdV represses HIF-1α during infection
H1299 cells were treated as mentioned above (4.7). Cells were infected with HAdV-wt and harvested at appropriate time points. Lysates were resolved on 10 % - 12 % SDS-PAGE. Western blot analysis was performed for E2A/DBP (B6-8), E1B-55K (2A6), E4orf6 (RSA3), MRE11 (Abcam), HIF-1α (BD Science) and β-actin (AC-15).

4.2.2 HAdV represses HIF-1α transcriptional activity

For the transcriptional activity, HIF-1α requires the presence of the p300 protein [302]; [292]. Previous studies showed, that the cellular transcription factor p300 binds HAdV transcriptional activator E1A-13S [113]. To asses the influence of HAdV infection on the transcriptional activity of HIF-1α, a luciferase-based promoter assay was performed, using a vector containing an HRE sequence. HIF-1α presence would promote transcription of the luciferase gene resulting in a chemiluminescence signal that will be measured (Figure 4.9A). H1299 cells were transfected with a vector containing the luciferase under the control of an HRE promoter as well as HIF-1α, followed by infection with a HAdV-wt at a MOI of 50. If an empty vector control is transfected, no luciferase signal was detected. In contrast, if HIF-1α is present, a signal of 25000 RLU was detected (Figure 4.9B lane 2). If the sample is infected with an HAdV-wt, the promoter activity is reduced 2-fold (Figure 4.9B lane 3). Taken together, it was shown, that HAdV reduces the promoter activity of HRE by reduction of HIF-1α.

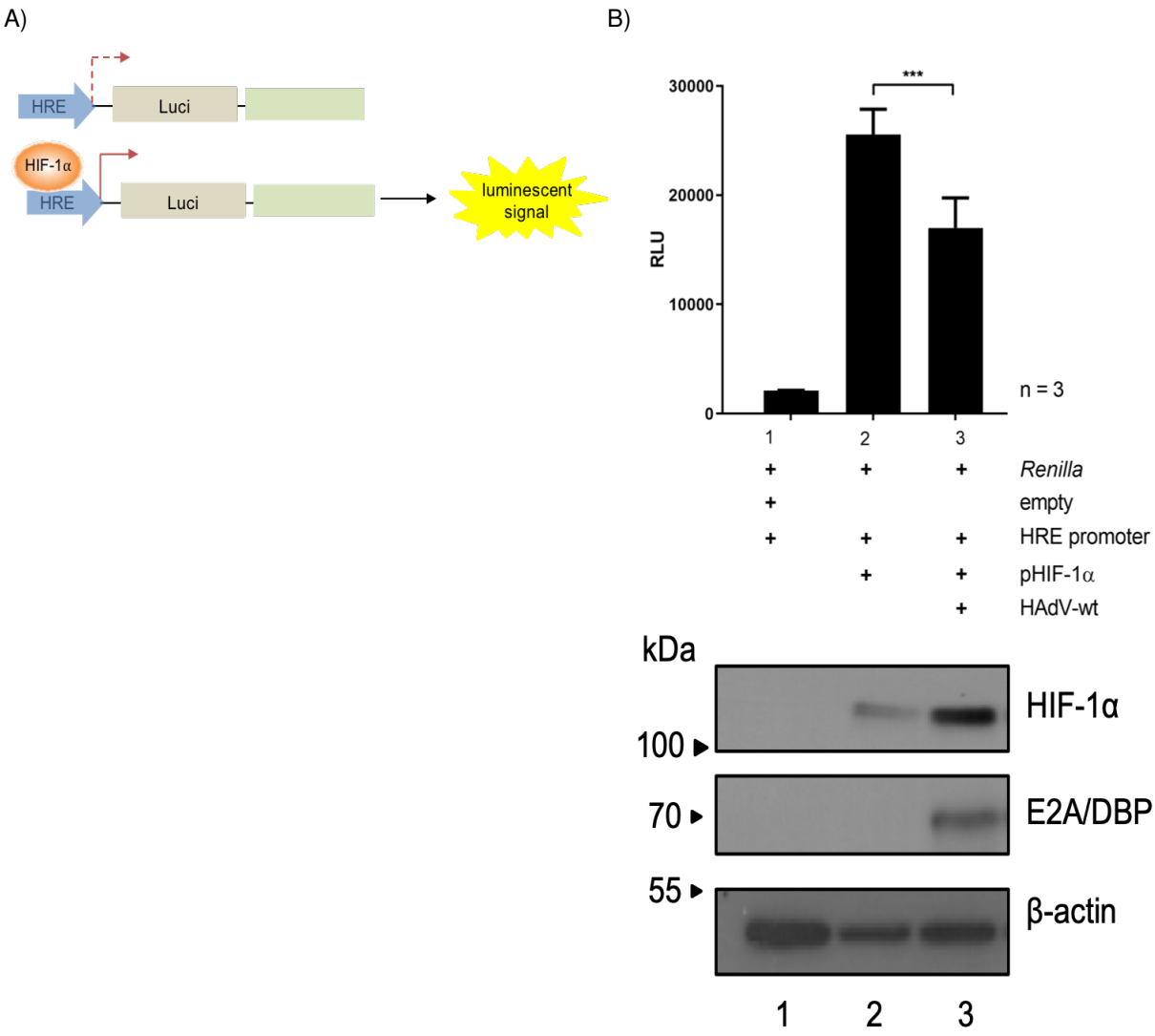

Figure 4.9: HAdV restricts HIF-1α dependent promoter activity during infection
A) Schematic overview of HRE dependent luciferase transcription: The luciferase gene is under the control of an HRE promoter, which is activated by binding of HIF-1α. B) To further investigate the effect of HAdV infection on HIF-1α, H1299 cells were transfected with a luciferase fused to an HRE promoter (1 μg), HIF-1α (5 μg) and *Renilla* (0.2 μg). Additionally, H1299 cells were infected with an HAdV-wt at a MOI of 50. The cells were harvested 48 hpi and luciferase activity was determined (3.9). Bar charts represent average values and standard deviations based on three independent experiments. Statistically significant differences were determined using a two-sided Welch's t-test. *: P $\leq$ 0.05, **: P $\leq$ 0.01, ***: P $\leq$ 0.001. Lysates of the corresponding samples were resolved by a 10 % SDS-PAGE. Western blot analysis was performed for HIF-1α (BD Science), E2A/DBP (B-68) and β-actin (AC-15).

4.2.3 HIF-1α is no target of the viral E3 ubiquitin ligase

It has been shown that the viral E4 and E1B proteins play an important role in the inhibition of the DDR and secure efficient viral replication (1.7). Since HIF-1α is repressed during HAdV infection, the question arose, if HIF-1α is a novel target of the viral E3 ubiquitin ligase. H1299 cells were infected with HAdV-wt and virus mutants lacking either E1B-55K (HAdV-ΔE1B-55K)

or E4orf6 (HAdV-ΔE4orf6) and western blot analysis was performed. First it was validated that the virus mutants are lacking either E1B-55K or E4orf6 respectively and that the infection is equal between all viruses (Figure 4.10A, lanes 2-7). Surprisingly, we observed that HIF-1α is still being repressed, even if the viral E3 ubiquitin ligase complex is not functional (Figure 4.10A, lane 6 and 7). To confirm these results, H1299 cells were transfected either alone or with a mixture of E1B-55K and E4orf6 DNA. Cells were harvested at 24 h and 48 h post transfection (hpt) and protein levels of HIF-1α, E1B-55K, E4orf6, MRE11 and β-actin were detected. MRE11 was used as control for a functional viral E3 ubiquitin ligase since it is known, that MRE11 is a target of the viral E3 ubiquitin ligase (1.7). Again, we observed that the components of the viral E3 ubiquitin ligase are not able to reduce HIF-1α (Figure 4.10B).

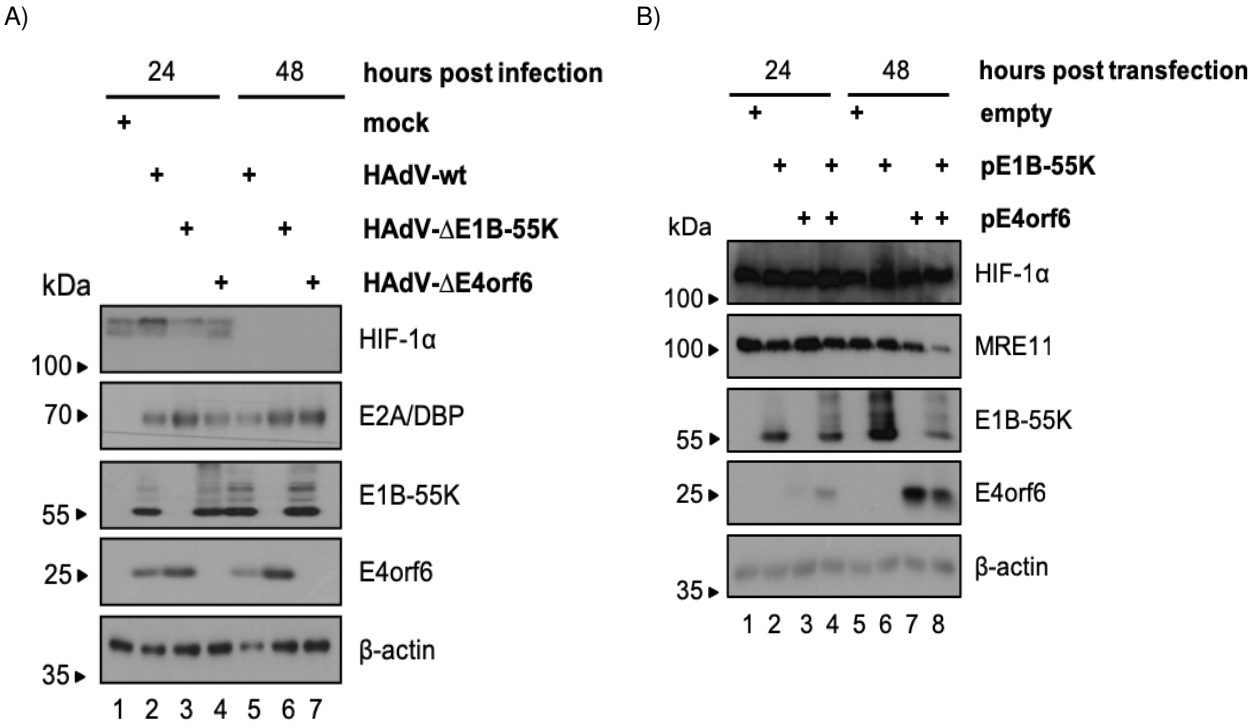

Figure 4.10: HAdV restricts HIF-1α dependent promoter activity during infection
A) Cells were infected with either HAdV-wt, HAdV-ΔE1B-55K or HAdV-ΔE4orf6 at a MOI of 50 and harvested at certain time points. Lysates were resolved by 10 % SDS-PAGE followed by western blot analysis for HIF-1α (BD Science), E2A/DBP (B6-8), E1B-55K (2A6), E4orf6 (RSA3) and β-actin (AC-15). B) For the purpose of validating the previous results, cells were transfected with each or a mixture of 5 μg pE1B-55K and pE4orf6. Samples were harvested 48 h post transfection. Lysates were resolved by 10 % SDS-PAGE followed by western blot analysis for HIF-1α (BD Science), E1B-55K (2A6), E4orf6 (RSA3), MRE11 (Abcam) and β-actin (AC-15).

4.2.4 Proteasomal degradation of HIF-1α during HAdV infection

During normoxia HIF-1α is degraded via the proteasome [298]; [334]. As a means to validate that HIF-1α is degraded by the proteasome during infection, proteasomal degradation was inhibited by MG132. MG132 is a chemical, which is able to inhibit the proteasome via the 26S

(Figure 4.11A). Samples were treated with 25 μM of MG132 4 h before harvest. In order to validate that the proteasome is inhibited, MDM2 was stained for western blot analysis. It is an E3 ligase, which promotes p53 ubiquitinylation and proteasomal degradation. MDM2 itself is ubiquitinylated and degraded by the proteasome [335]. We could validate our previous data, since HIF-1α is repressed during HAdV infection, when the proteasome is fully functional. In contrast, after treatment of MG132 we observed an accumulation of HIF-1α during infection, confirming that HIF-1α is targeted for proteasomal degradation during HAdV infection (Figure 4.11B, lane 3 and 4). Taken together, we showed that HIF-1α is a target for proteasomal degradation, but is no target of the viral E3 ubiquitin ligase complex during infection.

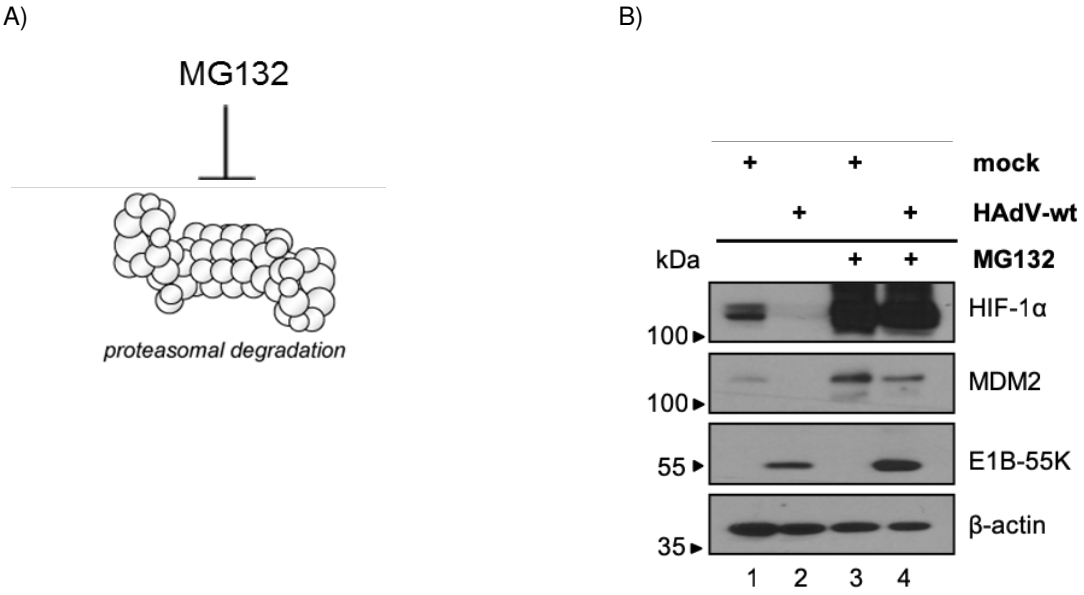

Figure 4.11: HAdV represses HIF-1α via the proteasome
A) MG132 is a chemical inhibiting the proteasome via the 26S. B) H1299 cells were infected with a MOI of 50 and treated with 25 μM MG132 4 h prior to harvesting. Total-cell lysates were prepared (3.7.1) and resolved by 10 % SDS-PAGE. The protein levels for HIF-1α (BD Science), MDM2 (Santa Cruz), E1B-55K (2A6) and β-actin (AC-15) were detected.

4.3 Modulation of hypoxia by the viral E4orf3 protein

4.3.1 HIF-1α is a novel target of the early viral protein E4orf3

HAdV have developed several mechanisms to counteract host antiviral response. Besides the viral E3 ubiquitin ligase complex build with E4orf6 and E1B-55K, the viral protein E4orf3, which is able to inhibit antiviral response through degradation or displacement of host proteins, secures efficient viral replication [135]; [279]; [336]; [337]; [338]. Since HIF-1α is no target of

the viral E3 ubiquitin ligase (Figure 4.10), E4orf3 might play a role in the repression of HIF-1α. To confirm our hypothesis, we compared the protein levels of HIF-1α after infection of HAdV-wt, HAdV-ΔE1B-55K, HAdV-ΔE4orf6 and a mutant virus lacking the E4orf3 protein (HAdV-ΔE4orf3). Recurrent with our previous results, western blot analyses confirmed the reduction of HIF-1α during HAdV-wt, HAdV-ΔE1B-55K and HAdV-ΔE4orf6 infection (Figure 4.10). Interestingly, HAdV is not able to repress HIF-1α anymore, if E4orf3 is depleted (Figure 4.12A, lane 7). To further investigate the role of the early viral protein E4orf3 to repress HIF-1α, H1299 cells were transfected with gradually increasing amounts of E4orf3 DNA. Here we observed that with a higher concentration of E4orf3, HIF-1α is significantly reduced (Figure 4.12B, lanes 4-6).

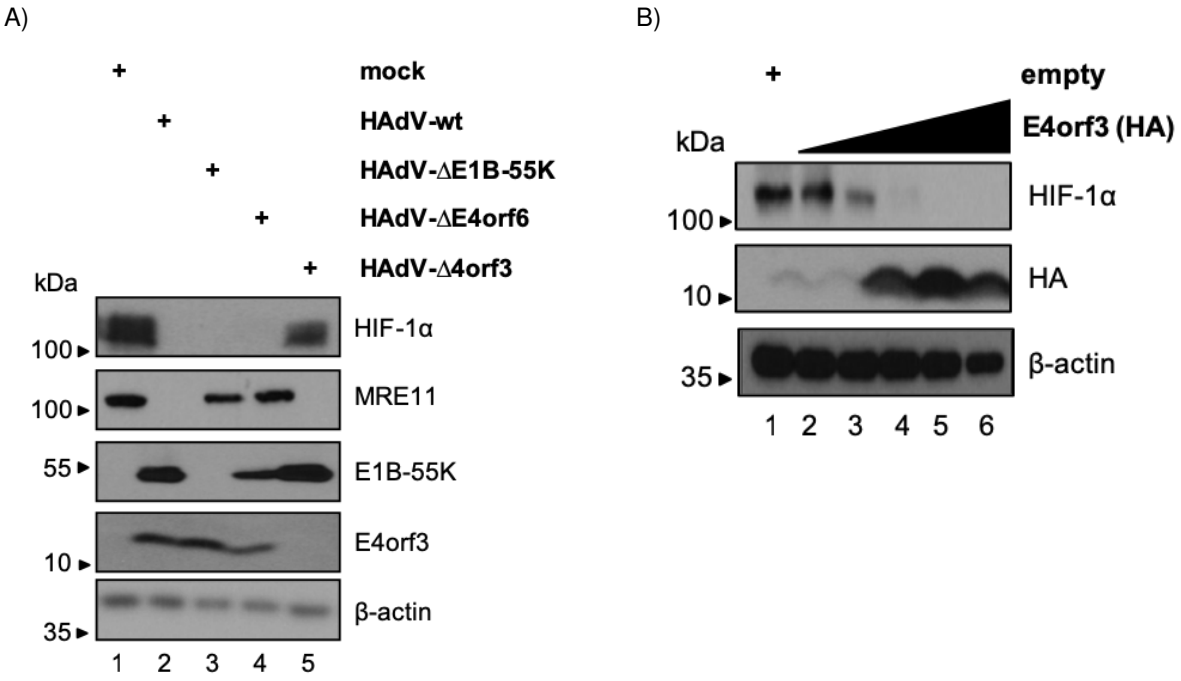

Figure 4.12: HIF-1α is a novel target of E4orf3
A) Cells were treated with 100 μM $CoCl_2$ prior to HAdV-wt, HAdV-ΔE1B-55K, HAdV-ΔE4orf6 and HAdV-ΔE4orf3 infection. Samples were harvested 48 hpi. Total-cell lysates were resolved by 10 % - 15 % SDS-PAGE and western blot was performed for HIF-1α (BD Science), E1B-55K (2A6) and E4orf3 (6A11). B) E4orf3 alone is able to reduce HIF-1α. Gradually more pE4orf3-HA (0.5 μg-20 μg was transfected followed by preparation for total-cell lysate. Protein levels for E4orf3-HA (3F10) and HIF-1α (BD Science) were detected by western blot.

To test, if endogenous HIF-1α is a novel interaction partner of E4orf3 during HAdV infection, a binding assay was performed (3.7.6). Endogenous HIF-1α was immunoprecipitated and subsequently subjected to western blot analysis. Figure 4.13A depicts the steady state level of the samples. Since the samples were harvested 24 hpi HIF-1α is detectable in the mock and infected samples (4.13A, lane 1 and 2). The mock sample is not infected and thus no viral proteins are detectable (4.13A, lane 1). Consistent with the data obtained previously, we

observed that HIF-1α interacts with E4orf3 during infection (Figure 4.13B, lane 2).

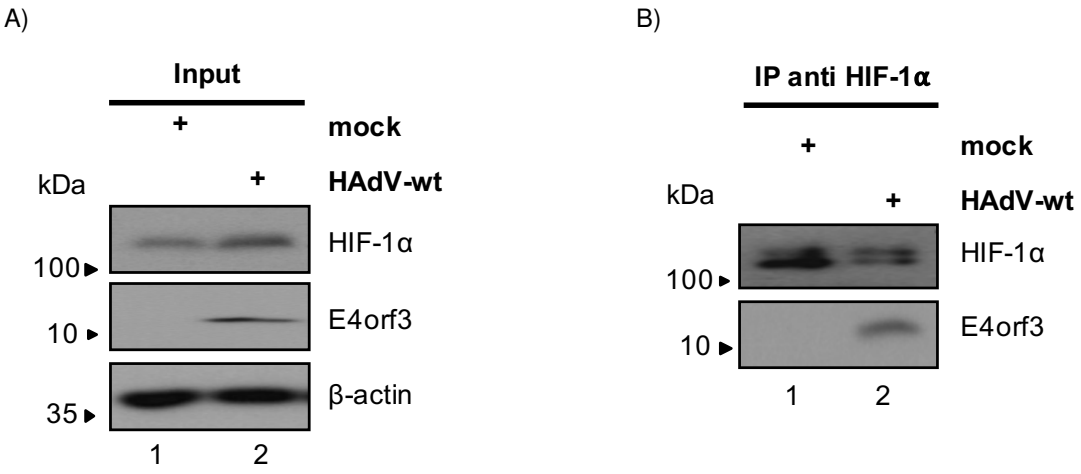

Figure 4.13: HIF-1α novel interaction partner of E4orf3
16 h prior to infection with HAdV-wt, cells were treated with 100 μM $CoCl_2$. A) Samples were harvested 24 hpi and total-cell lysates were resolved by 10 % - 15 % SDS-PAGE. Western blot was performed for HIF-1α (BD Science), β-actin (AC-15) and E4orf3 (6A11). B) E4orf3 alone is able to reduce HIF-1α. Gradually more pE4orf3-HA (0.5 μg-20 μg was transfected followed by preparation for total-cell lysate (3.7.1). Total-cell lysate were resolved by 10 % - 15 % SDS-PAGE. Protein levels for E4orf3-HA (3F10) and HIF-1α (BD Science) were detected by western blot.

Additionally, it was investigated, if E4orf3 influences the transcriptional activity of HIF-1α during infection. H1299 cells were treated as described before (4.2.2). In short, samples were transfected with a vector containing a HRE dependent luciferase and infected with HAdV-wt and HAdVΔE4orf3. Samples were harvested at according time points and a luciferase assay was performed (3.9). Concordant with our previous results HAdV-wt infection leads to a repression of HIF-1α promoter activity (Figure 4.14 lane 3). As anticipated, abscence of the E4orf3 protein leads to a re-establishment of the promoter activity, since HIF-α can not be repressed anymore (Figure 4.14 lane 4). To sum up, for the first time we showed that the early viral protein E4orf3 is exclusively responsible for the degradation of HIF-1α, thus modulating the hypoxia pathway during infection.

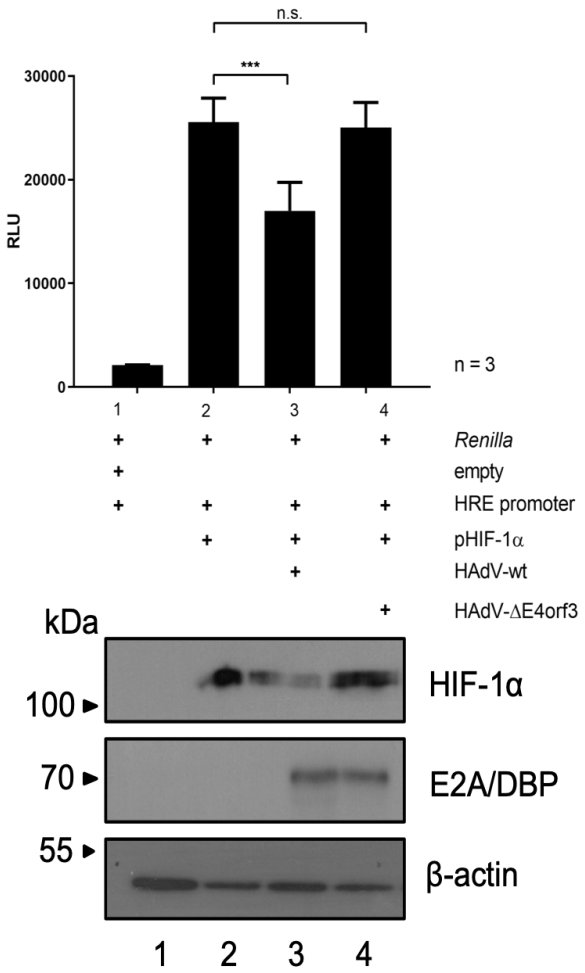

Figure 4.14: E4orf3 represses HIF-1α dependent promoter activity
To further validate the repression of HIF-1α by E4orf3, the gene reporter activity was measured. Samples were transfected with a luciferase fused to an HRE promoter (1 μg), HIF-1α (5 μg) and *Renilla* (0.2 μg)and harvested 24 hpi. Bar charts represent average values and standard deviations based on three independent experiments. Statistically significant differences were determined using a two-sided Welch's t-test. *: P $\leq$ 0.05, **: P $\leq$ 0.01, ***: P $\leq$ 0.001.

4.3.2 Subnuclear localization of HIF-1α and E4orf3

E4orf3 mediates PML-NB disruption via PML-II binding [151]; [154]; [163]; [161]. Furthermore, it recruits several host proteins, into PML containing track-like structures induced by E4orf3 [135]; [279]; [336]; [337]; [338]. To identify, if E4orf3 interferes with the localization of HIF-1α, we treated H1299 with $CoCl_2$ followed by infection with HAdV-wt or HAdV-ΔE4orf3 and performed immunofluorescence analysis (3.8). In mock cells HIF-1α is diffusely distributed in the nucleus (Figure 4.15 f). Notably, E4orf3 shows nuclear localization (Figure 4.15 panels m and p) and is able to relocalize HIF-1α into track-like structures (Figure 4.15 panel p). Calculation of the pearson correlation coefficient (pcc) reveals a factor over 0.5, for 50 counted cells, which concludes that the colocalization of HIF-1α and E4orf3 is significant (Figure 4.15 panel zoom

p). As expected, the capacity of HAdV to relocalize HIF-1α into track-like structures is lost, if the E4orf3 protein is absent (Figure 4.15 panel u). Furthermore, calculation of the pcc shows a value of 0.4, which concludes that no significant colocalization can be found (Figure 4.15 panel zoom x).

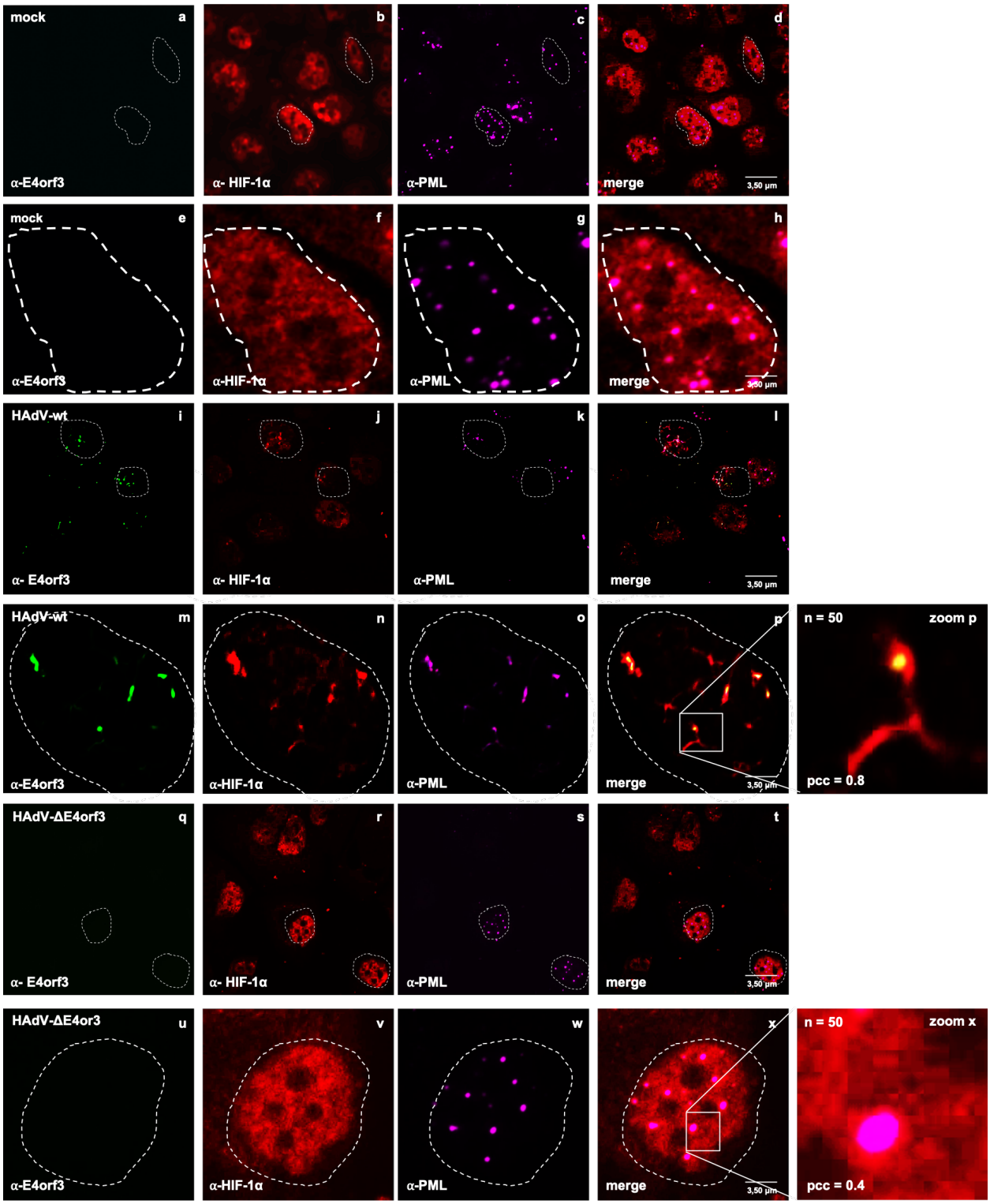

Figure 4.15: HIF-1α is recruited to the track-like structures induced by E4orf3
16 h prior to infection with HAdV-wt or HAdV-ΔE4orf3 (MOI 50) cells were treated with 100 μM $CoCl_2$. Samples were fixed with 4 % PFA 24 hpi and immunofluorescence was performed for HIF-1α (Santa Cruz), PML (NB100-59787), E4orf3 (6A11) and Dapi (3.8). The pearson correlation coefficient (pcc) was calculated for 50 cells.

4.3.3 Posttranslational modification of E4orf3 regulates repression of HIF-1α

Recent studies have shown that E4orf3 functions as a SUMO E3 ligase, thus targeting specific cellular proteins for SUMOylation and proteasomal degradation [278]; [160]. To asses, if E4orf3 SUMOylation is needed to efficiently degrade HIF-1α, an E4orf3, which has a mutation within the predicted SUMO conjugation motif at lysine position 8 (K8R), was used. At the same time, the interaction capacity between HIF-1α and the E4orf3 SCM mutant was investigated. Cells were harvested 48 hpt and prepared for Co-IP (3.7.6). Consistently with our previous results wild type E4orf3 reduces HIF-1α protein levels (4.16A, lane 2). Surprisingly, the K8R mutant of E4orf3 is not able to degrade HIF-1α anymore (Figure 4.16A, lane 3). Likewise, interaction between HIF-1α and the E4orf3 SCM mutant is weaker compared to the wild type E4orf3 (Figure 4.16B, lane 2 and 3).

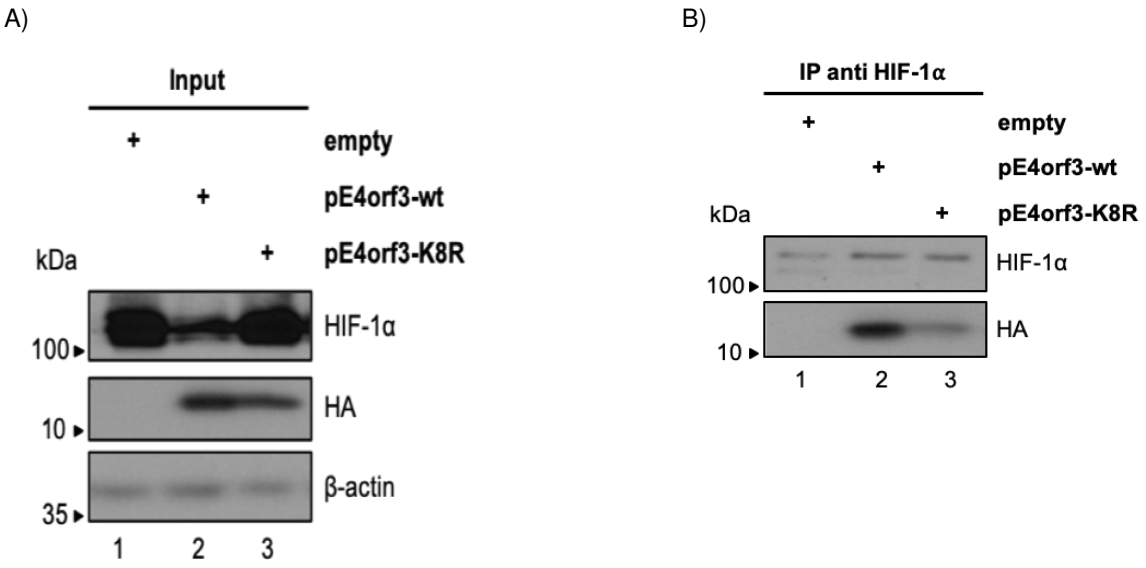

Figure 4.16: SUMOylation is a prerequisite to degrade HIF-1α
16 h prior to transfection cells were treated with 100 μM $CoCl_2$. Cells were transfected with either pE4orf3-HA or pE4orf3-K8R-HA (5 μg). A) Samples were harvested 48 hpt and total-cell lysates were resolved by 10 % - 15 % SDS-PAGE. Western blot was performed for HIF-1α (BD Science), β-actin (AC-15) and HA (3F10). B) SUMOylation of E4orf3 required to interact with HIF-1α. From total-cell lysate Co-IP was performed as described in 3.7.6. Samples were resolved by 10 % - 15 % SDS-PAGE. Protein levels for HA (3F10) and HIF-1α (BD Science) were detected by western blot.

Next it was investigated, if the localization of HIF-1α changes depending on the SCM mutation of E4orf3. Confirming our previous results, wt E4orf3 transfection significantly relocalized HIF-1α (Figure 4.17 panel zoom p, pcc = 0.7). Whereas the SCM mutant of E4orf3 is not able to relocalize HIF-1α (Figure 4.17 panel zoom x, pcc = 0.4). Taken together, we showed for the first time that the repression of HIF-1α by E4orf3 is dependent on the capability of E4orf3 to

be SUMOylated.

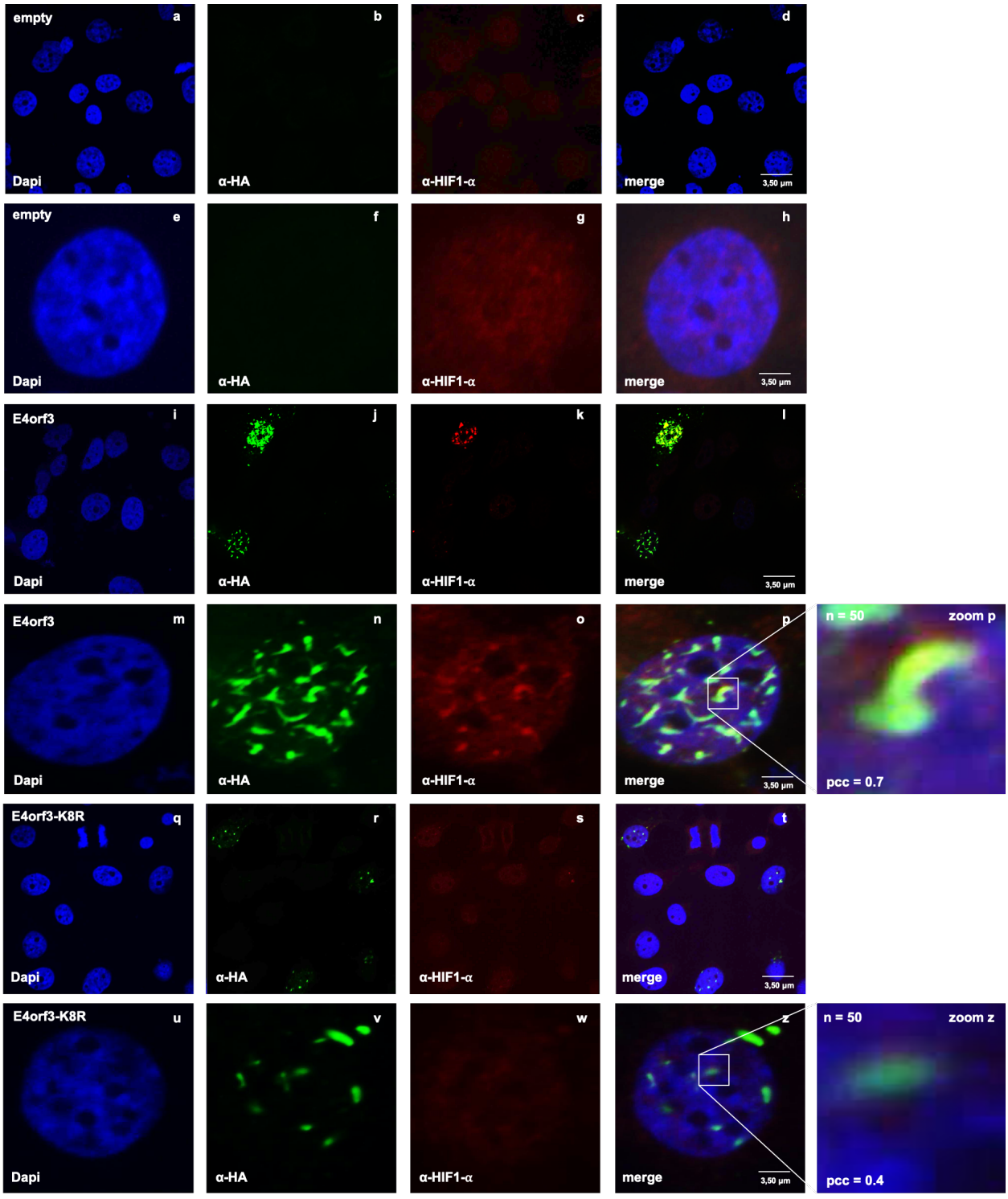

Figure 4.17: SUMOylation of E4orf3 is required to relocalize HIF-1α
16 h prior to transfection cells were treated with 100 μM $CoCl_2$. Cells were transfected with either pE4orf3-HA or pE4orf3-K8R-HA (5 μg). Samples were fixed 48 hpt and immunofluorescence was performed for HIF-1α (Santa Cruz), HA (3F10) and Dapi (3.8). The pcc was calculated for 50 cells.

Additionally, we investigated the capability of the SCM mutant to overcome the transcriptional repression of HIF-1α dependent promoter activity. H1299 cells were transfected with either an empty vector, pE4orf3-wt or pE4orf3-K8R. As anticipated, wildtype E4orf3 is able to re-

press the promoter activity, whereas the SCM mutant is not able to repress HIF-1α dependent promoter activity anymore (Figure 4.18).

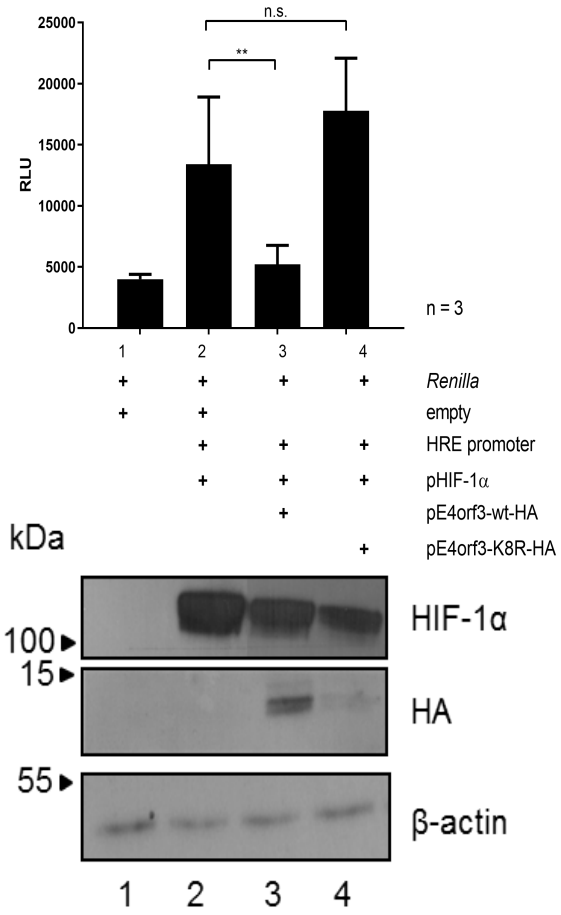

Figure 4.18: E4orf3-K8R loses its repressive function on HIF-1α promoter activity
As a means to further validate the effect of E4orf3 SUMOylation on HIF-1α H1299 cells were transfected with a luciferase fused to an HRE promoter (1 μg), HIF-1α (5 μg) and Renilla (0.2 μg). The cells were harvested 48 hpt and luciferase signal was measured (3.9). Bar charts represent average values and standard deviations based on three independent experiments. Statistically significant differences were determined using a two-sided Welch's t-test. *: P $\leq$ 0.05, **: P $\leq$ 0.01, ***: P $\leq$ 0.001. Total-cell lysates were resolved by 10 % - 15 % SDS-PAGE and western blot analysis for HIF-1α (BD Science), HA (3F10) and β-actin (AC-15) was performed.

4.4 Repression of HIF-1α is independent of PML-NBs

During HAdV infection cellular proteins are targeted and often reorganized into distinct structures. The early viral protein E4orf3 leads to the disruption of the dot like structures to track-like structures of PML-NBs [153]; [152]; [158]; [154]; [151]. To identify, if PML-NBs play a role in the degradation of HIF-1α, a cell line with a knock down of the PML protein was established. The control cell line, which was transduced with an empty scrambled shRNA, and the shPML cell line were infected with a HAdV-wt at a MOI of 50. 48 hpi samples were harvested and western blot analysis was performed. However, we could not observe a change in the degra-

dation of HIF-1α during infection (Fig 4.19 lane 4). These results suggest, that during HAdV infection only E4orf3 is responsible for the degradation of HIF-1α.

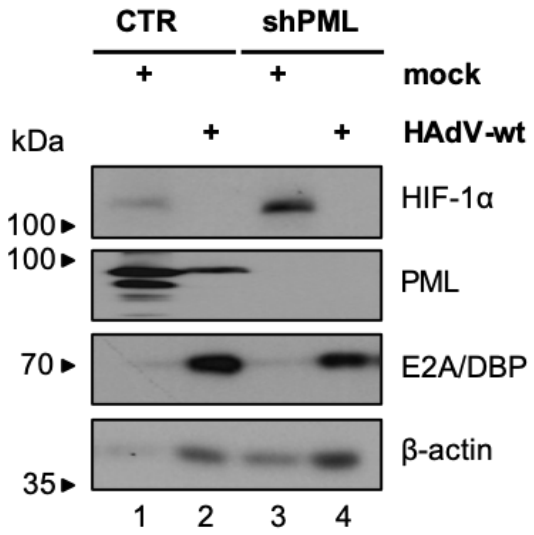

Figure 4.19: E4orf3 represses HIF-1α independent of PML
H1299 cells transduced with either an empty control vector (shScrambled) or shPML were treated with 100 μM of $CoCl_2$ 16 h prior to infection. Total-cell lysates were made as described in 3.7.1 and resolved by 10 % SDS-PAGE followed by western blot analyses. Samples were stained for HIF-1α (BD Science), PML (NB100-59787), E2A/DBP (B6-8) and β-actin (AC-15).

4.4.1 Subnuclear localization of HIF-1α is independent of PML

Furthermore, we investigated, if PML plays a role in relocalization of HIF-1α into the track-like structures induced by E4orf3. To answer this question, the H1299 cell lines mentioned in 4.4) were used. H1299 control cells and cells depleted for PML were treated with 100 μM $CoCl_2$ and infected with a HAdV-wt at a MOI of 50. After 48 hpi cells were fixed with 4 % PFA and immunofluorescence analysis was performed. Figure 4.20A, f and n validate the depletion for PML. For the first time, we could show that the repression and relocalization of HIF-1α to the track-like structures is independent of PML (Figure 4.20B, panel ze and panel zoom ze).

A)

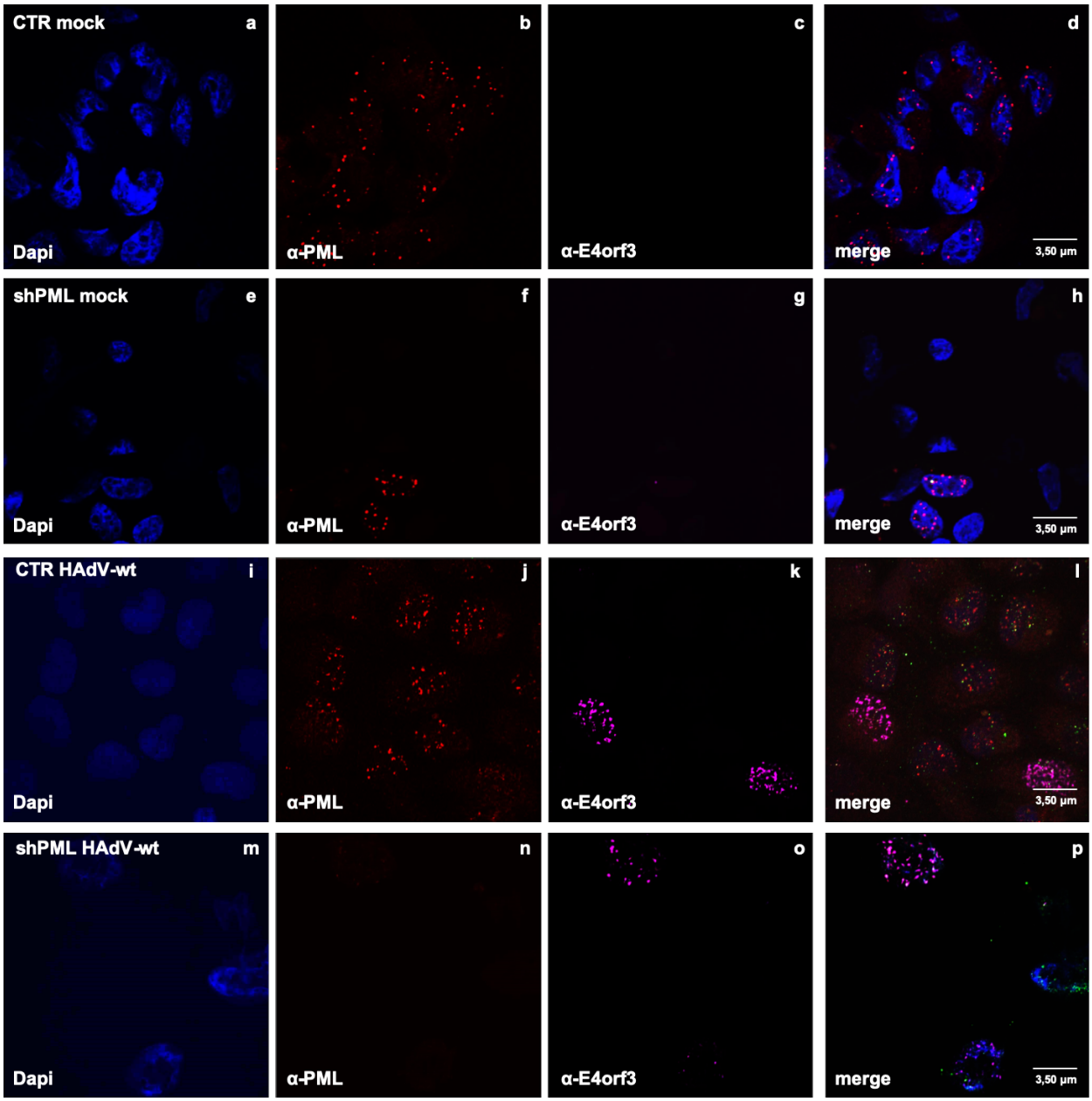
CTR mock
a
b
c
d
Dapi
α-PML
α-E4orf3
merge
3,50 µm
shPML mock
e
f
g
h
Dapi
α-PML
α-E4orf3
merge
3,50 µm
CTR HAdV-wt
i
j
k
l
Dapi
α-PML
α-E4orf3
merge
3,50 µm
shPML HAdV-wt
m
n
o
p
Dapi
α-PML
α-E4orf3
merge
3,50 µm

B)

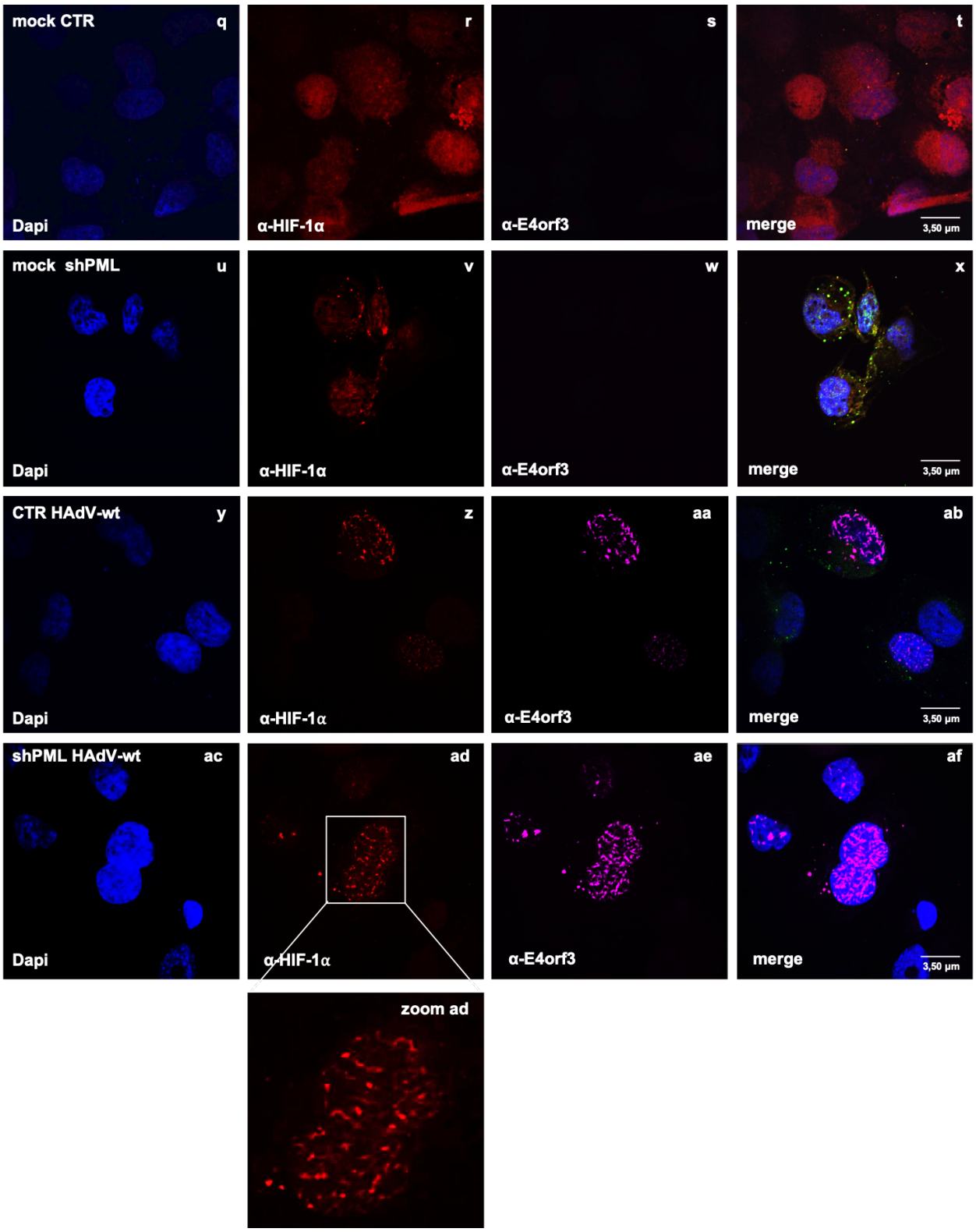

Figure 4.20: HIF-1α is recruited to track-like structures by E4orf3 independent of PML
Prior to infection the control cell line as well as the shPML cell line were treated with 100 μM $CoCl_2$. A) Validation of the depletion of PML. Samples were fixed as described (3.8) and stained for PML and E4orf3. B) Recruitment of HIF-1α to the track-like structure induced by E4orf3 independent of PML. Samples were treated as described in A) and stained for HIF-1α (Santa Cruz) and E4orf3 (6A11).

4.5 SUMOylation modulates functions of HIF-1α

4.5.1 SUMO 2 and 3 change subnuclear localization of HIF-1α

The role of SUMOylation is controversial regarding the function and stabilization of HIF-1α [303]; [304]; [305]; [306]. To further confirm our data, that SUMOylation plays a crucial role on the function and stabilization of HIF-1α, H1299 were transduced with lentiviral vectors containing SUMO 1-3-HA (3.3.2). After the establishment of those cell lines, it was possible to investigate the influence of the different SUMO isoforms on HIF-α. First, it was investigated how the different SUMO isoforms are able to influence the localization of HIF-1α during HAdV-wt and HAdV-ΔE4orf3 infection. After validation that HAdV-wt and HAdV-ΔE4orf3 infect cells homogeneously (4.21 panels a-d), the influence of the different SUMO isoforms on HIF-1α localization was investigated. Surprisingly, all SUMO isoforms are able to relocalize HIF-1α to their specific sites (4.22 panels a-d). During HAdV-wt infection only SUMO 2 and 3, together with HIF-1α are relocalized into the track-like structures induced by E4orf3 (Figure 4.22C, panel zoom ao, 4.22D, panel zoom bd). This relocalization is lost, if the E4orf3 protein is not present during infection (Figure 4.22C panel zoom at, 4.22D, panel zoom bi). Taken together, these data indicate that SUMO 2 and 3 play a role in the localization of HIF-1α during infection.

A)

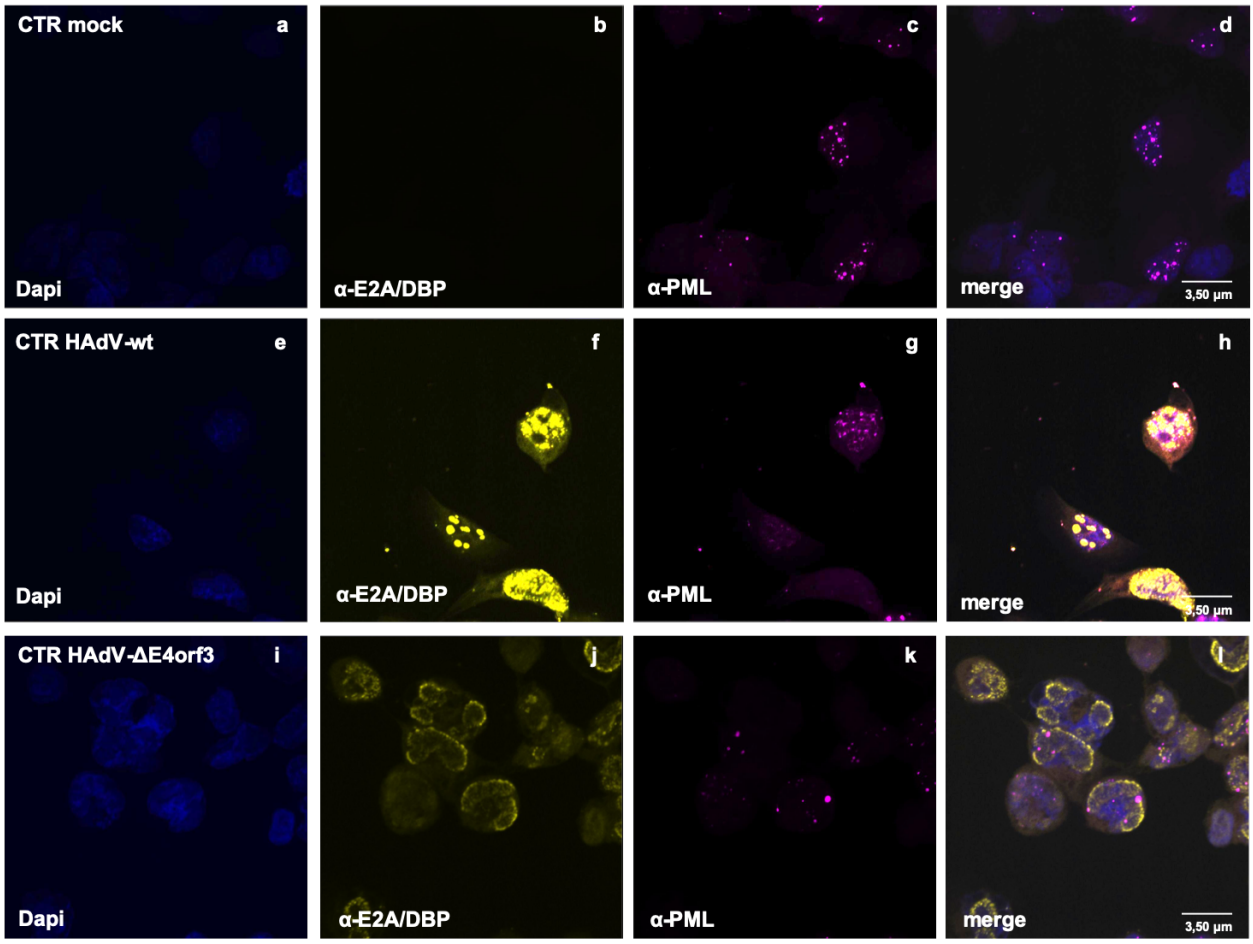
CTR mock
a
Dapi
b
α-E2A/DBP
c
α-PML
d
merge
3,50 µm
CTR HAdV-wt
e
Dapi
f
α-E2A/DBP
g
α-PML
h
merge
3,50 µm
CTR HAdV-ΔE4orf3
i
Dapi
j
α-E2A/DBP
k
α-PML
l
merge
3,50 µm

B)

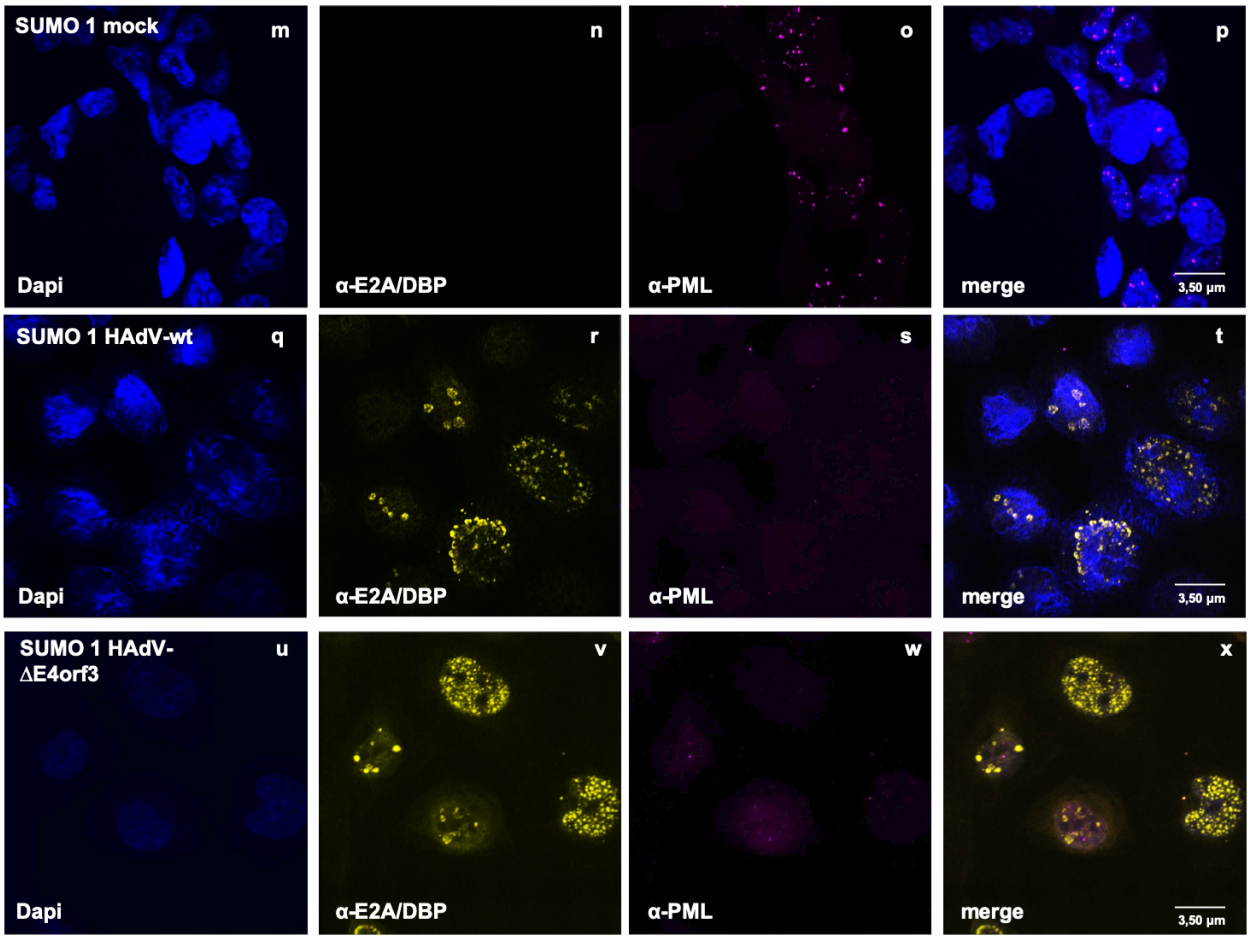
SUMO 1 mock
m
n
o
p
Dapi
α-E2A/DBP
α-PML
merge
3,50 µm
SUMO 1 HAdV-wt
q
r
s
t
Dapi
α-E2A/DBP
α-PML
merge
3,50 µm
SUMO 1 HAdV-ΔE4orf3
u
v
w
x
Dapi
α-E2A/DBP
α-PML
merge
3,50 µm

C)

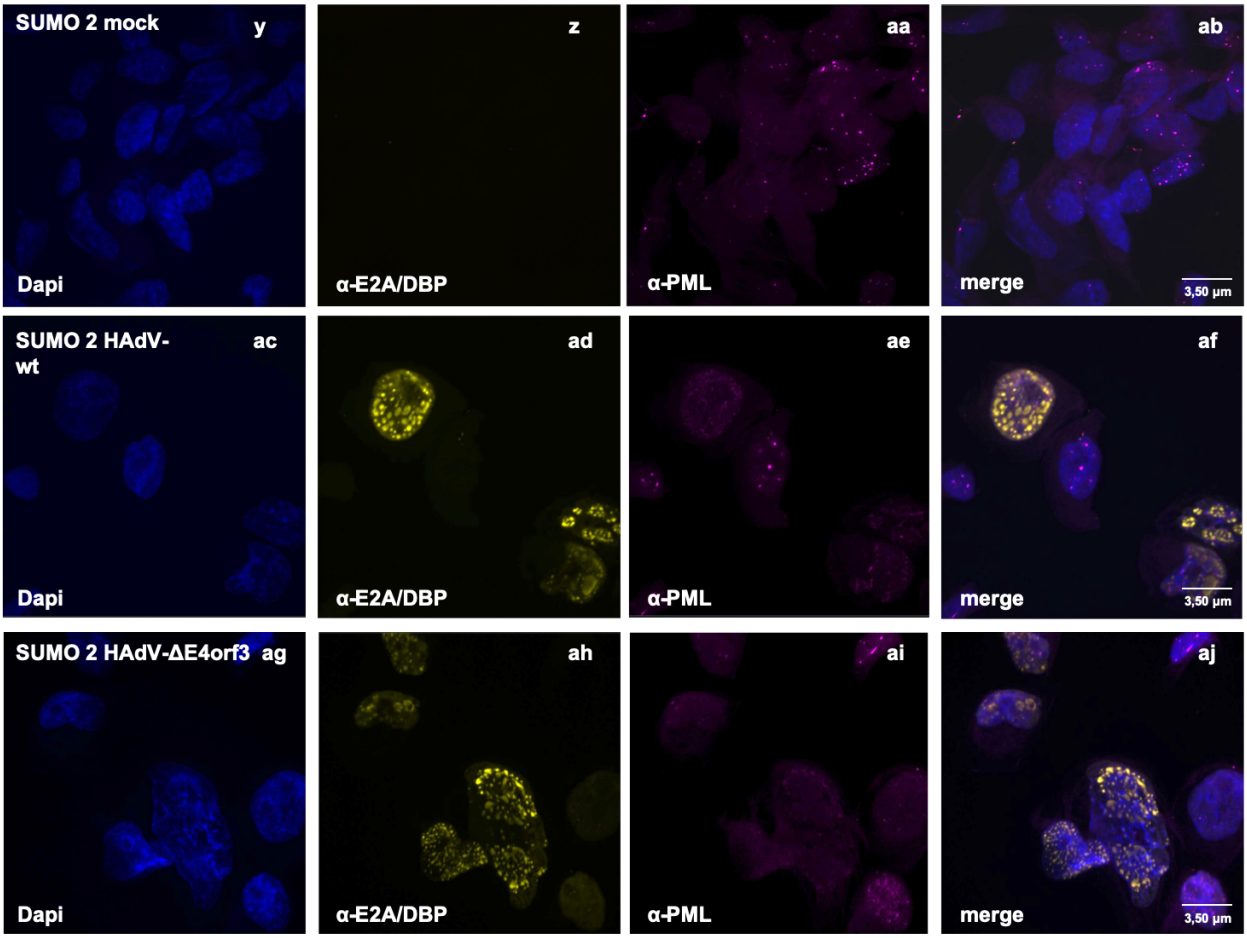
SUMO 2 mock
y
Dapi
z
α-E2A/DBP
aa
α-PML
ab
merge
3,50 µm
SUMO 2 HAdV-wt
ac
Dapi
ad
α-E2A/DBP
ae
α-PML
af
merge
3,50 µm
SUMO 2 HAdV-ΔE4orf3
ag
Dapi
ah
α-E2A/DBP
ai
α-PML
aj
merge
3,50 µm

D)

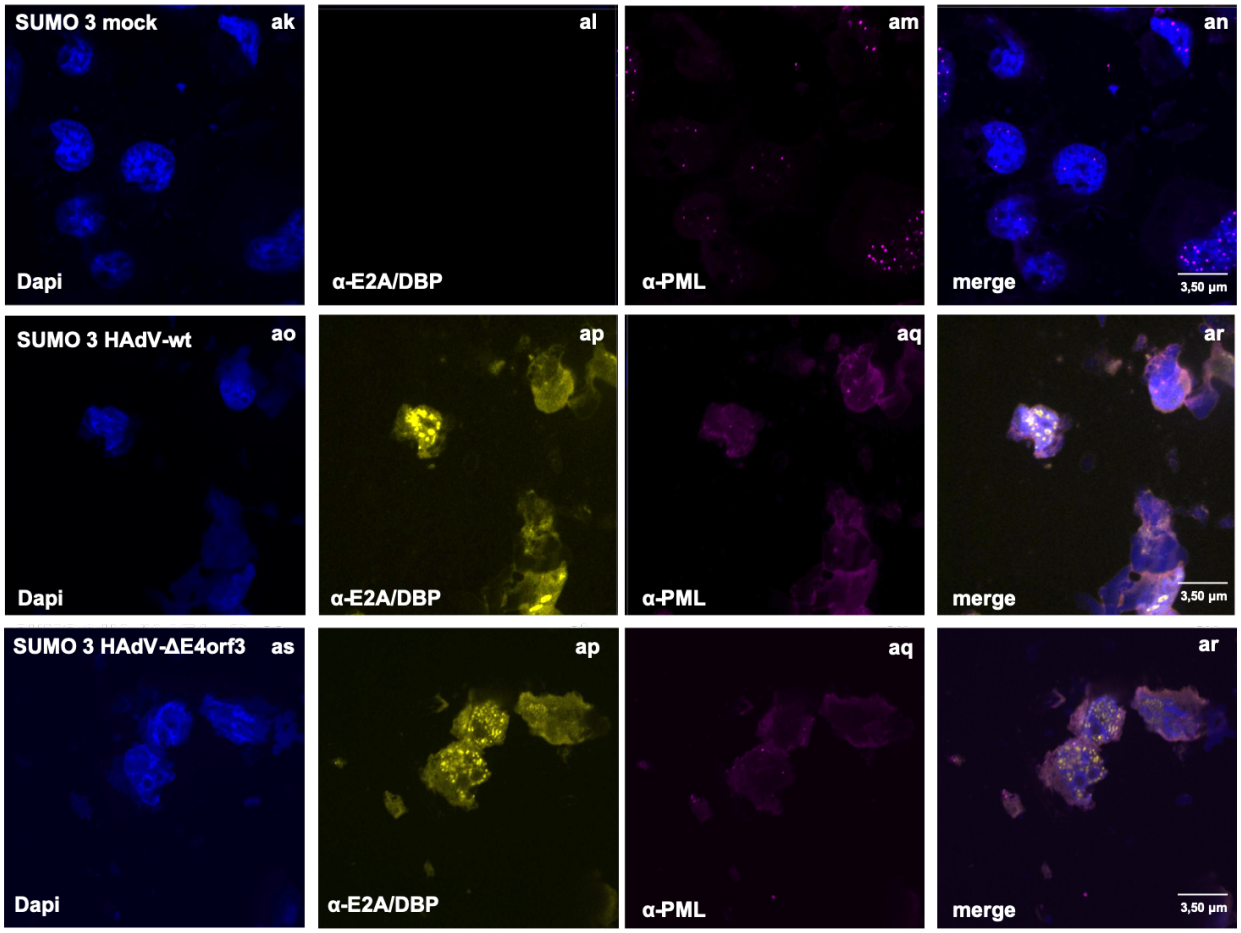

Figure 4.21: HAdV-wt and HAdV-ΔE4orf3 infect cells with the same efficiency
To investigate the influence of different SUMO isoforms, H1299 cells were transduced with either SUMO 1-3-HA. A) - D) First the even infection of the HAdV-wt and HAdV-ΔE4orf3 virus was confirmed by immunofluorescence (3.8). Samples were fixed with 4 % PFA and stained for E2A/DBP (B6-8), PML (NB100-59787) and Dapi.

A)

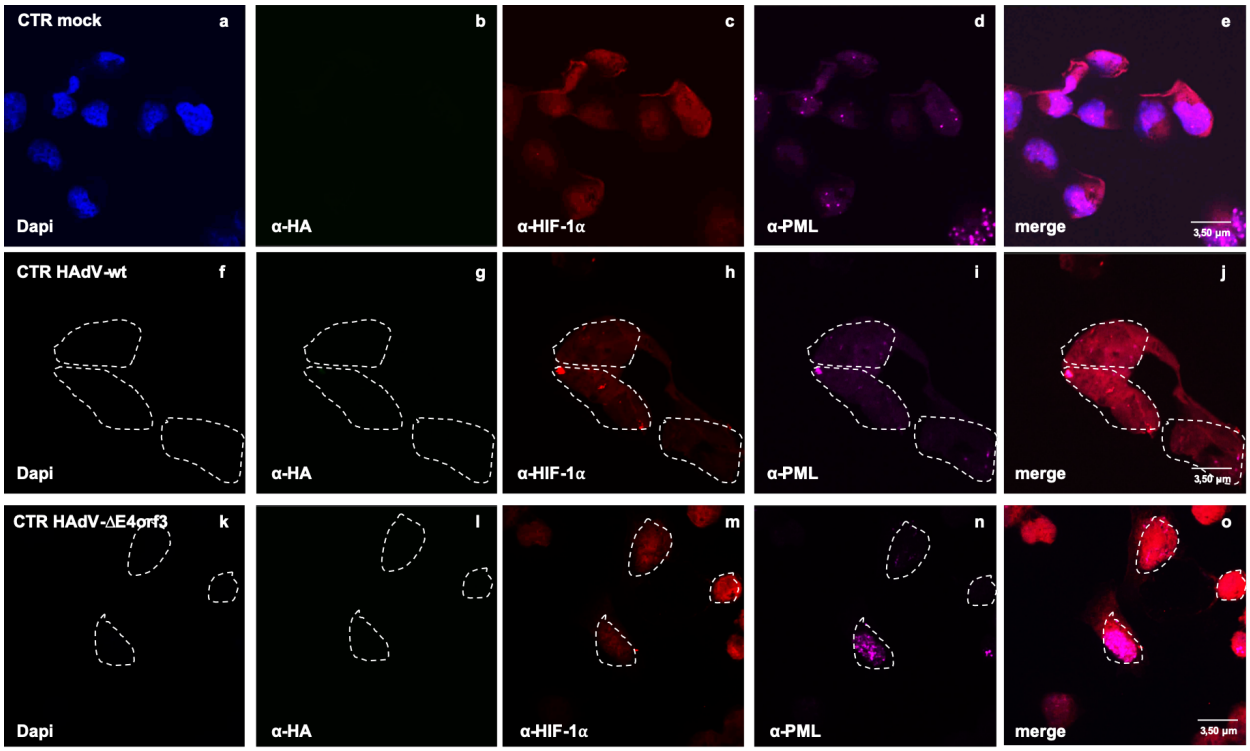
CTR mock
a
Dapi
b
α-HA
c
α-HIF-1α
d
α-PML
e
merge
3,50 µm
CTR HAdV-wt
f
Dapi
g
α-HA
h
α-HIF-1α
i
α-PML
j
merge
3,50 µm
CTR HAdV-ΔE4orf3
k
Dapi
l
α-HA
m
α-HIF-1α
n
α-PML
o
merge
3,50 µm

B)

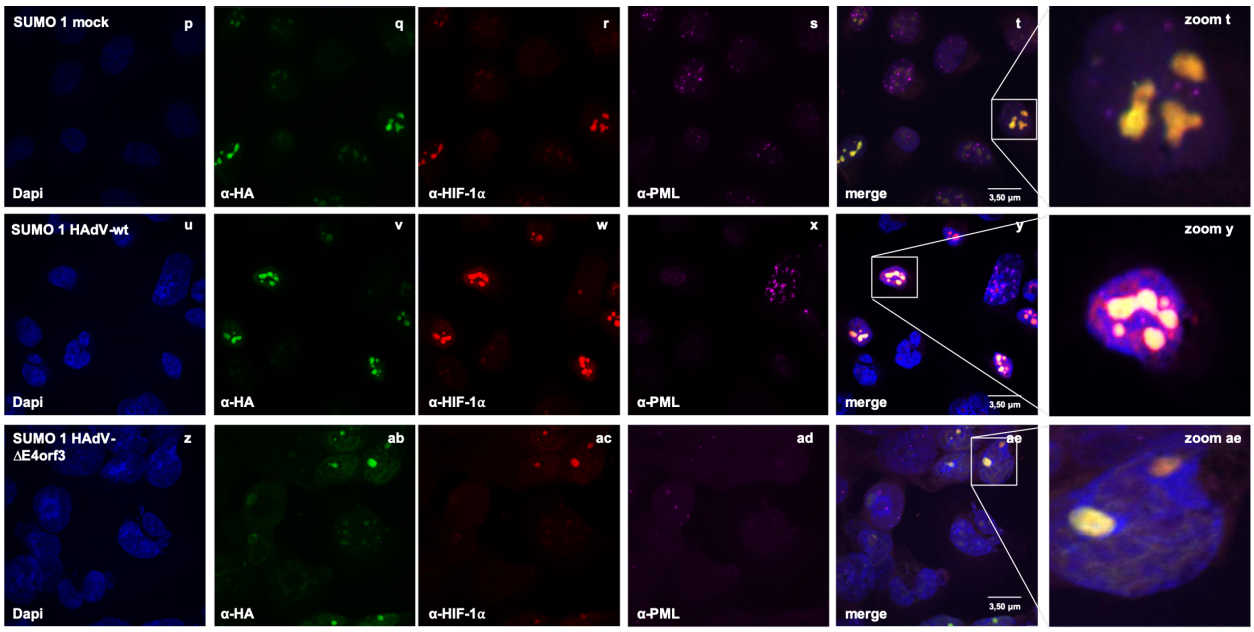
SUMO 1 mock
p
Dapi
q
α-HA
r
α-HIF-1α
s
α-PML
t
merge
3,50 µm
zoom t
SUMO 1 HAdV-wt
u
Dapi
v
α-HA
w
α-HIF-1α
x
α-PML
y
merge
3,50 µm
zoom y
SUMO 1 HAdV-ΔE4orf3
z
Dapi
ab
α-HA
ac
α-HIF-1α
ad
α-PML
ae
merge
3,50 µm
zoom ae

C)

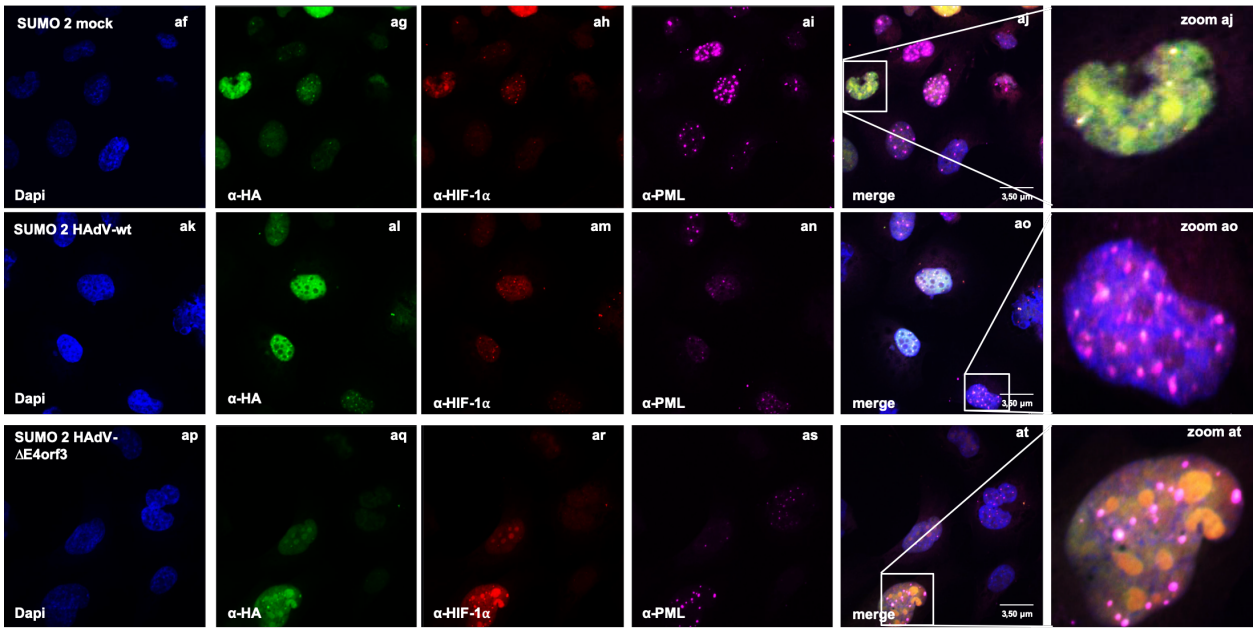

D)

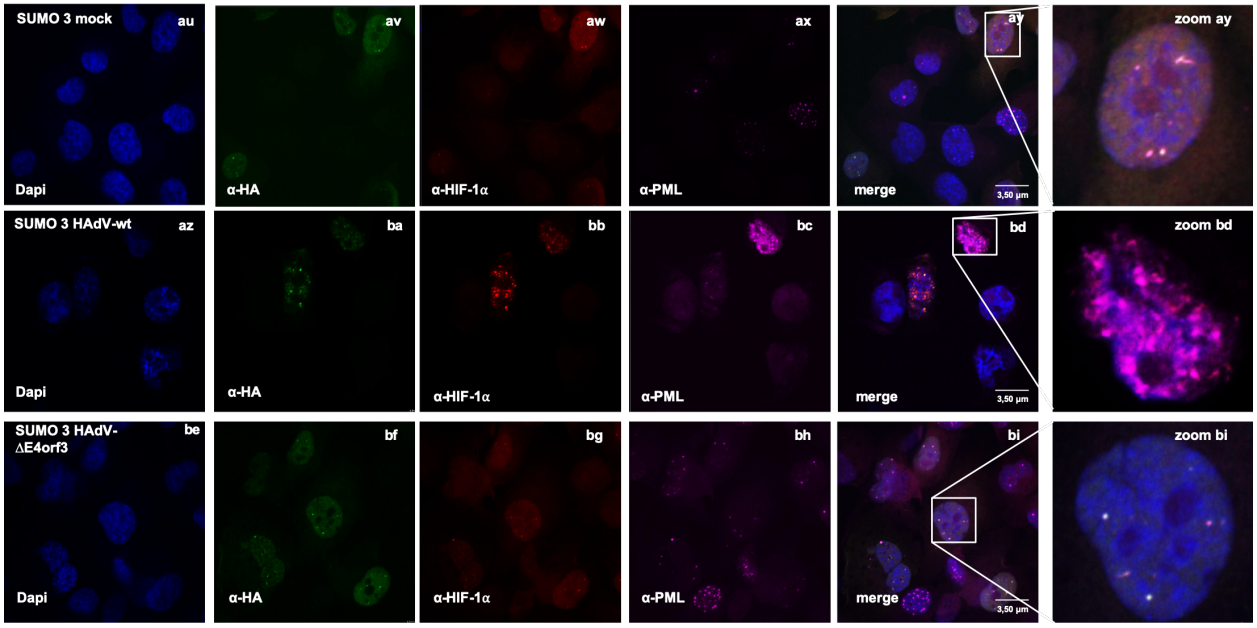

Figure 4.22: Only SUMO 2 and 3 together with HIF-1α are relocalized into the track-like structures induced by E4orf3
To investigate the influence of different SUMO isoforms, H1299 cells were transduced with either SUMO 1-3-HA. 16 h prior to infection (HAdV-wt at a MOI of 50), samples were treated with 100 μM $CoCl_2$. Samples were fixed with 4 % PFA after 24 hpi and stained for E4orf3 (6A11), HIF-1α (Santa Cruz), HA (3F10), PML (NB100-59787) and Dapi (3.8). A) As previously shown HIF-1α relocalizes to the track-like structures induced by E4orf3 in the control cell line. B) SUMO 1 and HIF-1α do not relocalize into track-like structures induced by E4orf3. C) - D) SUMO 2 and 3 together with HIF-1α relocalize into track-like structures induced by E4orf3.

4.5.2 SUMO 1 represses HIF-1α dependent promoter activity

Since we showed that SUMOylation influences the localization of HIF-1α, the question arose, if also the transactivating capacity of HIF-1α is influenced by SUMO 1-3. Therefore, H1299

cells were transfected with an empty vector, HRE, HIF-1α and the different SUMO isoforms. Subsequently, a luciferase-based reporter assay determined the promoter activity (3.9). As expected, SUMO 1 inhibits the transcriptional activity of HIF-1α two-fold, even though the protein levels of HIF-1α do not show any difference to the empty vector control (Figure 4.23, lane 3). In contrast to SUMO 1, SUMO 2 and 3 do not influence the transcriptional activity of HIF-1α, but at the same time the protein levels of HIF-1α are reduced (Figure 4.23, lane 4 and 5). Taken together, we showed, that the different SUMO isoforms have different capabilities to influence HIF-1α. SUMO 1 does not influence the protein stability, but represses HIF-1α dependent transcriptional activity. In contrast, SUMO 2 and 3 do influence the protein stability of HIF-1α, but, transcriptional activity is not repressed.

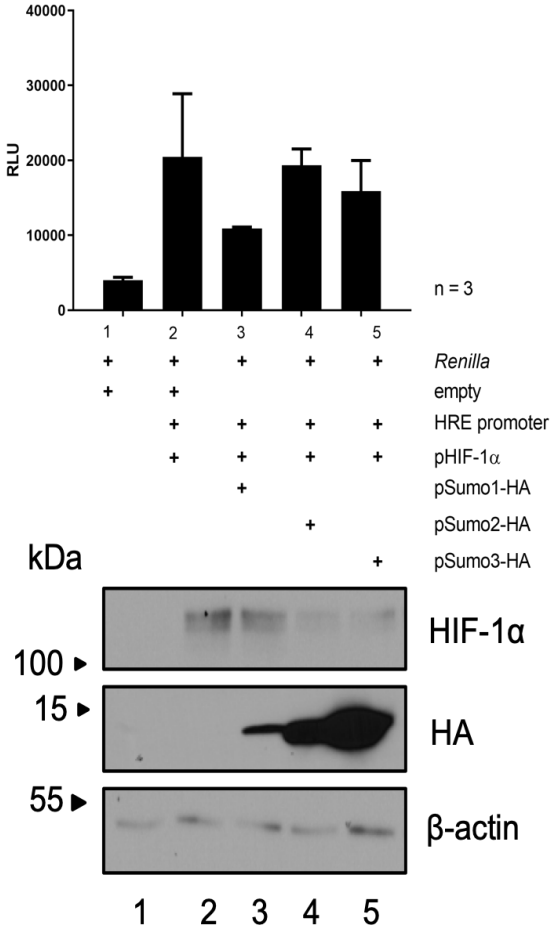

Figure 4.23: SUMO 1 represses transcription activity of HIF-1α
H1299 cells were transfected with 0.2 μg *Renilla* , 5 μg empty vector, 1 μg HRE, 5 μg HIF-1α, 5 μg SUMO 1, -2 or -3 and harvested after 48 hpt. The mean and standard deviations are presented for three independent experiments. Total-cell lysates were resolved by 10 % - 15 % SDS-PAGE and western blot analysis for HIF-1α (BD Science), HA (3F10) and β-actin (AC-15) was performed.

4.6 Different Serotypes E4orf3 differentially manipulate HIF-1α

4.6.1 Conserved repression of HIF-1α by E4orf3

It is known that the E4orf3 protein of different serotypes have different abilities to relocalize proteins [338]. Additionally, the comparison of the HRE core sequence and genome sequence of different HAdV serotpyes, revealed that the core sequence can be found in all investigated HAdV serotypes (4.6, Figure 4.5A). To elucidate the competence of the different serotypes to influence HRE dependent promoter activity, a luciferase assay was performed. H1299 cells were transfected with HRE, HIF-1α and the pE4orf3-HA of different serotypes. Despite the different capabilities to influence HIF-1α protein stability (4.25), all serotypes tested are able to inhibit HIF-1α dependent promoter activity (4.24). For the first time, we showed that different serotypes have different repression capacity to repress HIF-1α transcriptional activity.

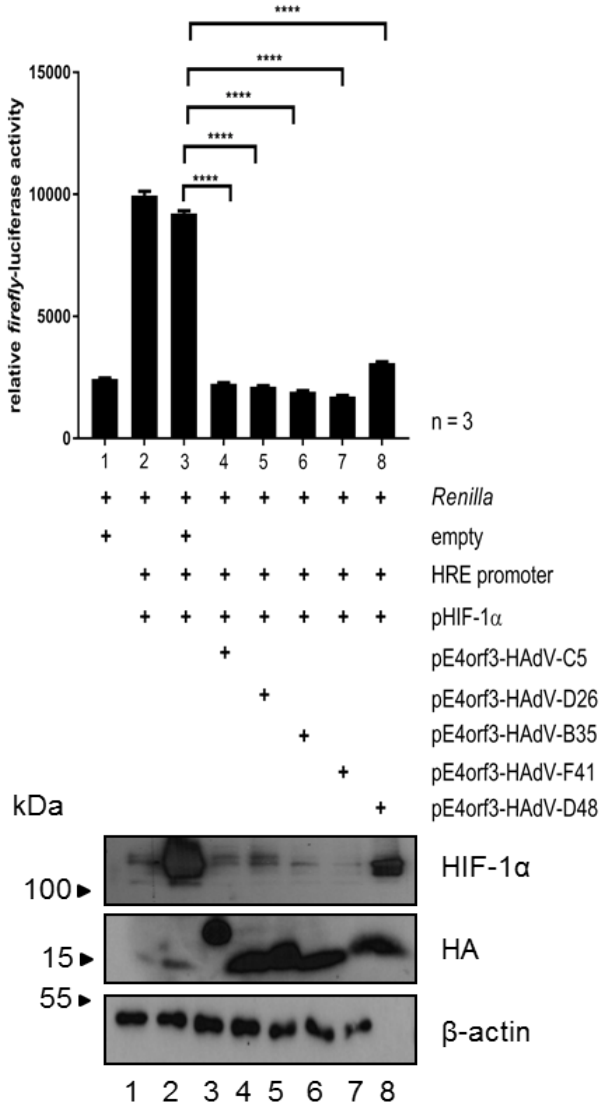

Figure 4.24: All HAdV serotypes E4orf3 inhibit HIF-1α dependent promoter activity
H1299 cells were transfected with either an empty vector, HRE, HIF-1α and pE4orf3-HA of the HAdV serotypes B, C, D and F as described in 3.2.5. 48 hpt samples were harvested as described in 3.9. Bar charts represent average values and standard deviations based on three independent experiments. Statistically significant differences were determined using a two-sided Welch's t-test. *: P $\leq$ 0.05, **: P $\leq$ 0.01, ***: P $\leq$ 0.001, ****: P $\leq$ 0.0001. Total-cell lysates were resolved by 10 % - 15 % SDS-PAGE and western blot analysis for HIF-1α (BD Science), HA (3F10) and β-actin (AC-15) was performed.

Next, we investigated the influence of different serotypes on HIF-1α protein stability. Thus, 16 h prior H1299 cells were treated with 100 μM $CoCl_2$ and transfected with E4orf3 of B, C, D and F serotypes. Western blot analysis revealed that all serotypes, except for HAdV-D48, are able to degrade HIF-1α. Compared to the empty control HAdV-C5 decreases HIF-1α protein levels 6-fold. The viral protein E4orf3 of HAdV-D26 decreases HIF-1α protein levels 5-fold. HAdV-B35 and -F41 decrease HIF-1α protein levels 3-fold (Figure 4.25C). Additional sequence analysis revealed that not all serotypes share the same lysine at position 8 (Figure 4.25B, first red marked box), indicating a different mechanism to repress HIF-1α.

A)

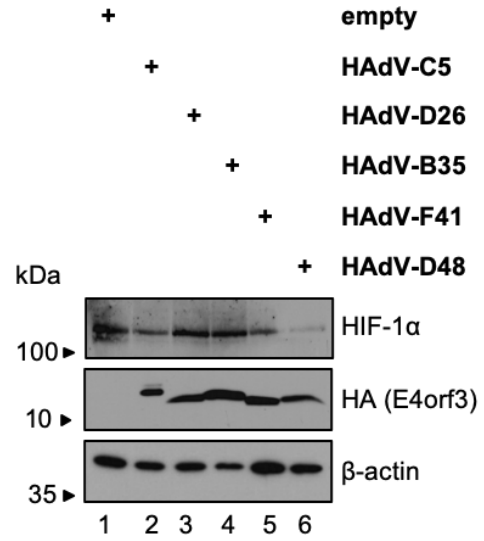

B)

```
HAdV-C5   1   MIRCLRLKVEGALEQIFTMAGLNIRDLLRDILRRWRDENYLGMVEGAGMFIEEIHP-EGF
HAdV-D26  1   MKVCLIMKVEGALWELFHMCGVDLHQQFVEIIQGWKNENYLGMVNECNLMIDEIDGGPAF
HAdV-B35  1   MRVCLRMVVEGALRDLFVMCGLDLPQELTRIIQGWKAENYLGMVQECNMMIEELENAPSF
HAdV-F41  1   MKVCLRMTVEGALNKLFELHGASLQEILMDVLRGWQAENYLGVIQDCSLMFEDFEE-NAF
HAdV-D48  1   MKVCLIMKVEGALWELFHMCGVDLHQQFVEIIQGWKNENYLGMVNECNLMIDEIDGGPAF
              *  ** :*****.:* : * .: : :  ::: *: *****::: ..:::::::.   .*

HAdV-C5   60  SLYVHLDVRAVCLLEAIVQHLTNAIICSLAVEFDHATGGERVHLIDLHFEVLDNLLE
HAdV-D26  61  NVILMLDVRVEPLLEATVEHLENRVGFDLAVCFHQHSGGERCHLRDLHFIVLRDRLE
HAdV-B35  61  GILLFLDVRVEALLEATVEHLENRISFDLAVLFHQHSGGERCHLRDLQFEVLRDRLE
HAdV-F41  60  AMFVFLEVRVSALVEAVIGNLENRIFFDLAVIFYQRSGGERCDLRDLHFGWLYNRLE
HAdV-D48  61  NVILMLDVRVEPLLEATVEHLENRVGFDLAVCFHQHSGGERCHLRDLHFIVLRDRLE
               : : *:**.  *:** : :* * :  .*** * : :**** .* **:*  * : **
```

C)

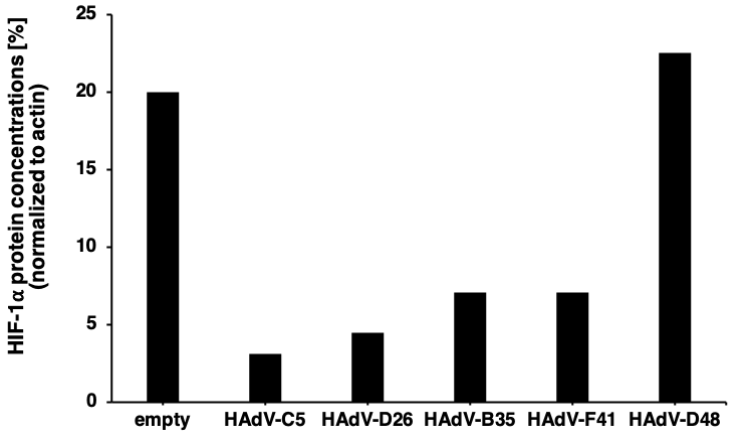

Figure 4.25: Different serotypes E4orf3 are able to modify HIF-1α
16 h prior to transfection cells were treated with 100 μM $CoCl_2$. A) Cells were transfected with either an empty vector or pE4orf3-HA of B, C, D and F serotypes (5 μg, 3.2.5). Samples were harvested 48 hpt. Total-cell lysates were resolved by 10 % - 15 % SDS-PAGE. Western blot analyses was performed for HIF-1α (BD Science), HA (3F10) and β-actin (AC-15). B) Protein sequences of the different serotypes were compared. C) Intensity of bands from A) were analysed with ImageJ.

Chapter 5

Discussion

5.1 HAdV counteracts HIF-1α during infection

Over the last years investigating the role of HIF1-α during viral infection became more prominent. Several viruses, including HBV, EBV and HPV stabilize HIF-1α and exploit its function to secure efficient viral replication [307], [309], [312], [314]. However, until now it remains elusive, which influence HIF-1α has on the HAdV replication. Our initial hypothesis proposed a supportive role of HIF-1α on HAdV infection, as HIF-1α is a known repressor of PML [315]. In contrast to our hypothesis, this study showed for the first time, that stabilized HIF-1α and thus hypoxia has a negative effect on the HAdV replication, concluding that HIF-1α is a novel restriction factor (Figure 4.2). During extreme hypoxia (0.1 %) HAdV is not able to counteract the restrictive functions of HIF-1α (Figure 4.1A, lane 4). HIF-1α leads to the reduced expression of early and late viral proteins. This reduction was also observed on the viral DNA and viral progeny production (Figure 4.1B, 4.1C). This negative effect is not obliqued to the repression of PML-NBs, since we showed that the quantity of PML-NBs is not changed during hypoxia. Additionally, we validated the hypoxia results by overexpression of HIF-α. Here we observed that HIF-1α has a negative effect on the viral progeny production in a concentration dependent manner (Figure 4.3B, 4.3C). This negative effect was enhanced, if the ODD (oxygen dependent degradation) of HIF-1α was mutated (Figure 4.3B, 4.3C). The ODD region of HIF-1α is hydroxylated by PHDs and subsequently proteasomal degraded by pVHL. Figure 4.3A lane 5 and 6 show a further enhanced signal of HIF-1α, compared to lanes 3 and 4, indicating that the ODD region is targeted by the HAdV to counteract the restrictive functions of HIF-1α. It is of particular interest how HIF-1α is able to restrict the HAdV replication. To asses this question, the genomes of several HAdV serotypes were investigated for the highly conserved HRE

sequence (4.6). Astonishingly, all serotypes contain the conserved HRE sequence. In the case of HAdV-C5 the viral genome comprises two HRE sequences (Figure 4.5A), among others at the packaging signal of HAdV. Therefore, we hypothesized that binding of HIF-1α could interfere with adenoviral packaging and could indeed show, that HIF-1α interferes with efficient capsid formation (Figure 4.6B). Intriguingly, HAdV is able to counteract HIF-1α during mild hypoxia (1 %), as well as stabilized HIF-1α by $CoCl_2$ (Figure 4.8, lane 5 and 6). Consistent with these observations, HAdV counteracts hypoxia by reducing HIF-1α dependent HRE promoter activity (Figure 4.9B, lane 3). These data indicate that the virus evolved a very efficient mechanism to counteract HIF-1α. Surprisingly, this mechanism does not involve the well studied viral E3 ubiquitin ligase built by E1B-55K and E4orf6, but involves a novel target for the viral protein E4orf3 (Figure 4.10). We showed for the first time, that HIF-1α protein levels are still repressed, even if the viral E3 ubiquitin ligase is not functional (Figure 4.10A; Figure 4.10B). During normoxia HIF-1α is proteasomal degraded. To validate that HIF-1α is proteasomal degraded during HAdV infection, H1299 cells were treated with the proteasomal inhibitor MG132. Indeed we could prove that HIF-1α is degraded via the proteasome during HAdV infection (Figure 4.11B). To asses which viral factor is responsible for the degradation of HIF-1α, H1299 cells were infected with HAdV-wt, HAdV-ΔE1B-55K, HAdV-ΔE4orf6 and HAdV-ΔE4orf3. Intriguingly, if HAdV is depleted for the early viral protein E4orf3, HIF1-α can not be degraded anymore. Indicating that HIF-1α is a novel target for proteasomal degradation by E4orf3. Taken together we could show for the first time, that HIF-1α is a novel restriction factor for HAdV replication and that the early viral protein E4orf3 is responsible for the degradation of HIF-1α and thus plays a crucial role in efficient replication.

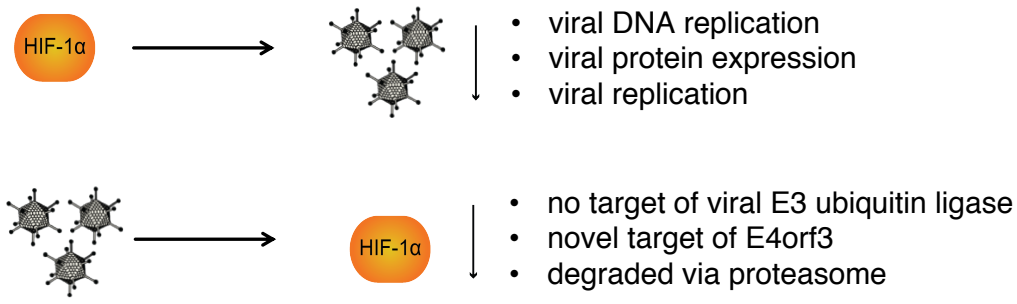

Figure 5.1: Summary of results.
This work revealed that HIF-1α is a novel restriction factor for HAdV replication. HAdV is able to counteract the restriction by repression of HIF-1α through E4orf3.

5.2 Modulation of hypoxia by E4orf3

Several studies demonstrated that the early viral protein E4orf3 induces the reorganization of the dot like PML-NBs into distinct track-like structures during early stages of infection. For instance, the antiviral host protein MRE11 is also located at those track-like structures and dislocated to the cytoplasm for degradation by the viral E3 ubiquitin ligase built by the early viral proteins E1B-55K and E4orf6 [336], [339]. Our work identifies a novel function for E4orf3, the ability to target HIF-1α for proteasomal degradation. Immunofluorescence studies revealed that HIF-1α is relocalized to the track-like structures induced by E4or3 and not to cytoplasmic aggresomes. In accordance with this, we showed, that during HAdV infection HIF-1α interacts with E4orf3 in vitro (Figure 4.13B, 4.16B). Since HIF-1α is recruited to the E4orf3 induced PML track-like structures, we investigated the role of PML-NBs on HIF-1α degradation Based on our data, PML does not contribute to the degradation of HIF-1α, but supports the idea that HIF-1α inhibition is exclusively dependent on the early viral E4orf3 protein. (Figure 4.19). Even though we showed that PML does not contribute to the repression of HIF-1α, it would be very fascinating, if relocalization of HIF-1α into the nucleus induces a change in the composition of PML isoforms in the PML-NBs. It has been shown that the specific PML isoforms have different functions [192], [340], [195]. Additionally, it has been shown that E4orf3 interacts with PML II, leading to the disruption of the dot like structure into the track-like structures [154]. Previously published data demonstrate, that HIF-1α increases interferon response upon VSV infection [307]. It would be very intriguingly, if HIF-1α plays a role in the recruitment of specific PML isoforms. This would explain why HIF-1α is only degraded at the late phase of HAdV infection.

We can support our hypothesis, that solely E4orf3 is responsible for the degradation of HIF-1α, with our data on the E4orf3-K8R, which is no longer capable of degrading HIF-1α (Figure 4.16A, lane 3). Additionally, we observe that the SCM mutant of E4orf3 is not able to suppress HIF-1α dependent promoter activity (Figure 4.18, lane 4) and loses the ability to recruit HIF-1α to the track-like structures (Figure 4.17). Our results offer a new perspective on the function of E4orf3. Even though from structure analysis E4orf3 does not seem to have the features for a SUMO or Ubiquitin ligase [163], we suggest that E4orf3 is a viral E3 SUMO ligase. There is the possibility that E4orf3 functions similar to RanBP2 [278]. RanBP2 is known to SUMOylate HIF-1α and thus reduces its activity [341]. Previously, it was shown that the early viral protein E1A interacts with Ubc9 to interfere with SUMOylation of host proteins [271], but recently it was suggested that also E4orf3 is exploiting Ubc9 to recruit SUMO 2 and 3 to the track-like

structures induced by E4orf3 [342]. Our data indicate that SUMOylation is a prerequisite to repress HIF-1α by the viral protein E4orf3 (Figure 4.16A; Figure 4.17). We propose that E4orf3 is exploiting Ubc9 during infection and is able to influence the SUMOylation status of several proteins, including HIF-1α. Until today the role of SUMOylation is controversial regarding the function and stabilization of HIF-1α [341], [303], [304], [305]. To further analyse the role of SUMO on HIF-1α, we established a cell line with transduced SUMO 1-3. Immunofluorescence analysis revealed that all SUMO isoforms are able to relocalize HIF-α to their respective localization (Figure 4.22). However, during HAdV infection, just SUMO 2 and 3 are relocalized to the E4orf3 induced track-like structures together with HIF-1α (Figure 4.22C, 4.22D). Transcriptional activity of HIF-1α is also influenced by the different SUMO isoforms. Our data revealed that SUMO 1 is repressing transcriptional activity of HIF-1α without influencing the stability of the protein (Figure 4.23, lane 3). In contrast SUMO 2 and 3 do not influence the transcriptional activity of HIF-1α, but change localization of HIF-1α (Figure 4.22C zoom aj; Figure 4.22D, zoom ay) which leads to a reduced signal on the protein level (Figure 4.23, lane 4 and 5). Even though we detect a reduced protein signal in the presence of SUMO 2 and 3, the transcriptional activity analysis does not measure a reduced luciferase signal, indicating that SUMO 2 and 3 alone are not capable to target HIF-1α for proteasomal degradation.

For the first time we showed, that SUMOylation plays a crucial role for HIF-1α stability, location and function, which is manipulated during HAdV infection by E4orf3. We suggest that E4orf3, together with Ubc9, recruits SUMO 2 and 3 into the track-like structures and thus is able to change the SUMOylation of HIF-1α. Due to the change of SUMOylation HIF-1α is subsequently degraded via the proteasome (Figure 5.2A). It is possible that the interaction of SUMO isoforms, Ubc9 and E4orf3 is at the lysine at position 8 of E4orf3, which is supported by our results, that E4orf3 is not able to suppress HIF-1α anymore, if the K8 is mutated (Figure 4.16A, 5.2B).

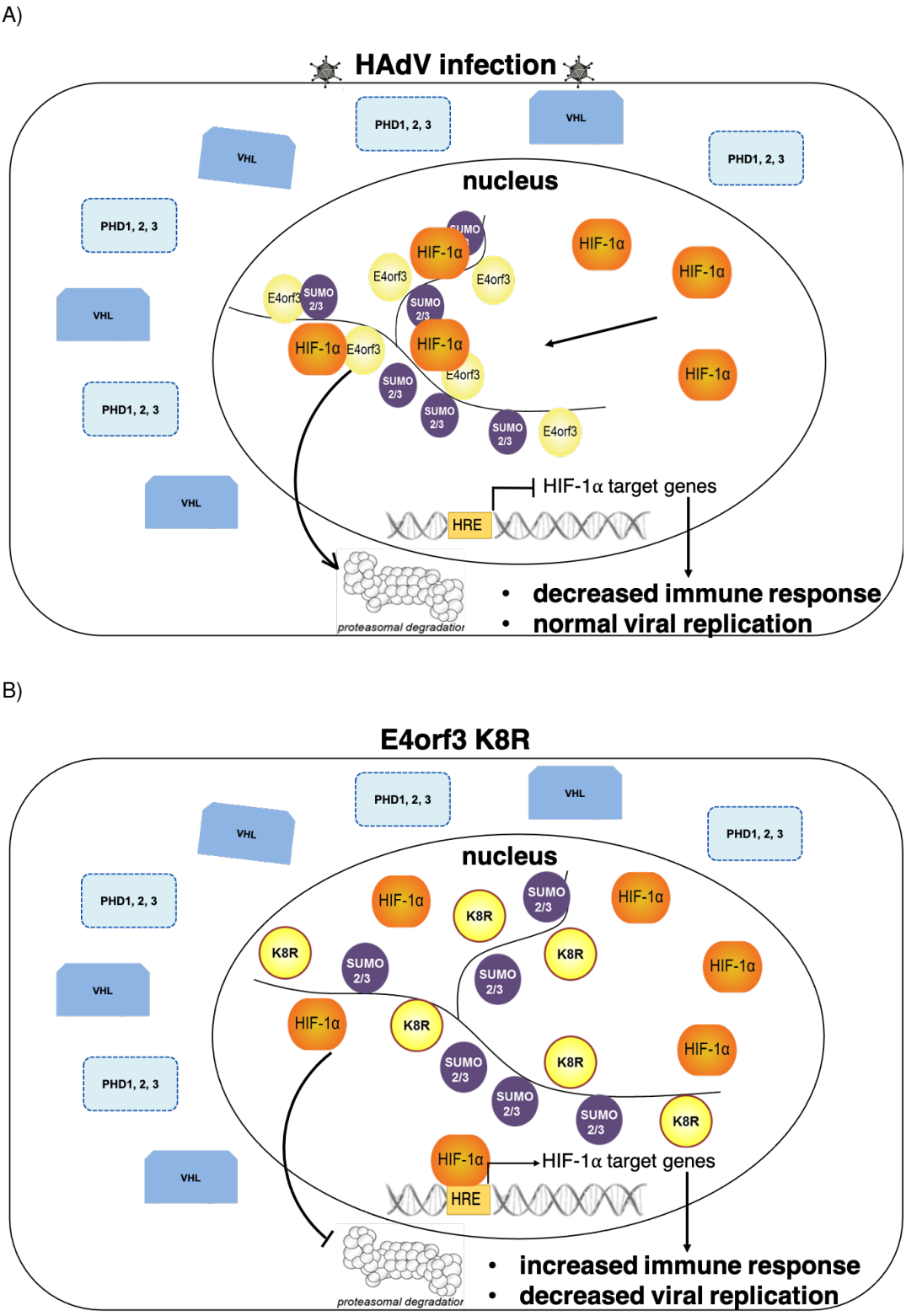

Figure 5.2: Schematic overview of working hypothesis
A) HAdV modulates hypoxia pathways by E4orf3. Our data indicate that HAdV is modulating hypoxia pathways during infection. The early viral protein E4orf3 is able to recruit HIF-1α into the track-like structures, independent of PML (4.4). Recently it was shownt hat with Ubc9 SUMO 2 and 3 are recruited to the track-like structures [342]. Thus E4orf3 is able to change the SUMOylation of HIF-1α subsequently leading to the degradation. For the first time we showed that HIF-1α is a restrictive factor for the HAdV replication (4.3). Since HIF-1α is no target of the viral E3 ubiquitin ligase built by E1B-55K and E4orf6, E4orf3 is crucial for the successful HAdV replication. B) SUMOylation of E4orf3 is a prerequisite to modulate hypoxia pathways. For the first time we showed, that if the lysine at position 8 is mutated, E4orf3 is not able to recruit HIF-1α into the track-like structures and inhibit transcriptional activity of HIF-1α (4.3.1) Scheme of DNA modified from https://www.somersault1824.com.

5.3 Conserved repression of HIF-1α by E4orf3

It is known that the disruption of the DDR plays a central role for several HAdV serotypes and E4orf3 is essential for the inhibition of the antiviral response [338], [343]. Our data presented here indicate that E4orf3 plays an essential role in the suppression of HIF-1α during infection (1.6.3, 4.3.1). Furthermore, we showed that several HAdV serotypes contain the highly conserved HRE sequence within their genome (4.6). To investigate the influence of other HAdV serotypes on HIF-1α, we transfected E4orf3 of serotypes B, C, D, and F. Interestingly, we showed for the first time that the serotypes C5, F41 and D48 efficiently repress HIF-1α, while HAdV-B35 does not repress HIF-1α protein level. This repression is independent of the conserved lysine at the position 8, for instance the HAdV-F41 does not contain a lysine at position 8, but a threonin (Figure 4.25B). Despite the differences in sequence, all serotypes are able to repress transcriptional activity of HIF-1α, indicating that HIF-1α repression is conserved for different HAdV serotypes. Albeit at first glance it seems like the different HAdV serotypes developed different mechanisms to suppress HIF-1α. There are publications, indicating that SUMOylation is the mutual factor for all serotypes [338]. Previous studies showed that not all serotypes are able to relocalize MRE11 into the track-like structures, but all investigated serotypes relocalize proteins that are highly SUMOylated [338]. It would be very intriguingly, if the common factor of the recruitment of the different SUMO isoforms is Ubc9. This hypothesis is supported by our finding of the influence of the different SUMO isoforms on HIF-1α dependent transcriptional activity (Figure 4.23). In addition it would explain why HIF-1α transcriptional activity is repressed, but not all serotypes are able to repress HIF-1α on the protein level (Figure 4.25A). It is very fascinating to observe that E4orf3 of the serotype F41 is able to repress HIF-1α protein level and transcriptional activity. HAdV-F41 infects enteric cells, where low oxygen is present and HIF-1α stabilized. This stabilization could be the reason for the enhanced protection of enteric cells from viral infection [344]. Additionally, NF-κB is stabilized during hypoxia, indicating a antiviral role of hypoxia in enteric cells [344], [345], [346]. These observations are supporting our finding, that hypoxia is a negative effect on HAdV replication. Due to poor infection efficiency we could not preform infection assays with HAdV-F41. Nevertheless, our findings can improve the experimental settings and the influence of different HAdV serotypes on HIF-1α can be investigated.

5.4 Clinical relevance

It is very intriguing to consider our findings to improve HAdV vector-based cancer therapy. Adenoviral vectors are the most used vectors in the field of gene therapy, which are used as a delivery vehicle, to transfer therapeutic genes for the treatment of genetic or acquired diseases. For instance the HAdV based transfer of exogenous p53 into patients suffering from glioma [347], [348], [349]. Especially in solid tumours a low efficacy of HAdV vector-based cancer therapy is observed. It is known that in solid tumours, HIF-1α is stabilized [350], [351], [282], [352], [353]. Our data shows that different approaches must be taken to develop an efficient HAdV vector for cancer therapy. With our findings HIF-1α is a very potent target for cancer therapy. Reducing HIF-1α by the early viral protein E4orf3 in target cells will improve the efficiency of HAdV vectors in cancer therapy. To apply HAdV for cancer therapy it has to be considered, that several early viral proteins are able to induce oncogenicity in humans (Figure 1.2) and are able to transform rodent cells [354], [165], [355], [356], [357]. We observed that E4orf3 SUMOylation is a prerequisite to repress HIF-1α. It is tempting to ask whether the SUMO status of E4orf3 plays an important role during transformation of primary rodent cells.
Furthermore, with our data we can specify the range of tissues infected by the different HAdV serotypes. Our data suggest that the repression of HIF-1α is conserved in different HAdV serotypes (4.24), indicating that HIF-1α is a restrictive factor in different tissues, like for example in the gut. Enteric cells express HIF-1α, which leads to an enhanced protection of enteric cells from viral infection [344], [345], [346]. HAdV-F41 infects enteric cells and our obtained data show that also E4orf3 of HAdV-F41 represses HIF-1α on the transcriptional and protein level (Figure 4.24, Figure 4.25A). With these findings HAdV vector-based cancer therapy can be further specified for the respective tissues and increase efficiency. Nevertheless ongoing studies are dedicated to elucidate the mechanism how different HAdV regulate HIF-1α during infection.
With this study we can not only improve the HAdV vector-based cancer therapy, but also the treatment of HAdV infection. Typically HAdV infections are mild and self limiting in immunocompetent patients, but in immunocompromised patienst HAdV infections are fatal [358], [20], [23], [22]. Intriguingly, the repressive functions of HIF-1α can be used to disrupt HAdV infection. We show that overexpressed HIF-1α significantly reduces viral progeny production in a concentration dependent manner (4.3). Furthermore, we showed that mutations in the ODD region of HIF-1α enhances the repressive effect on viral progeny production (Figure 4.3B, 4.3C). Since we observed that all serotypes investigated in this study contain an HRE

sequence, it is possible to enhance HIF-1α in an amount, that is repressive or aborts HAdV infection without leading to oncogenecity.

These findings can also be applied to improve HAdV vector based vaccination [359], [360], [361]. In enteric cells stabilized HIF-1α leads to an enhanced immune response and activation of NF-κB [344], [345], [346]. Taken together the results of this study significantly improve HAdV therapeutic application.

Bibliography

[1] W. P. ROWE, R. J. HUEBNER, L. K. GILMORE, R. H. PARROTT, and T. G. WARD, "Isolation of a cytopathogenic agent from human adenoids undergoing spontaneous degeneration in tissue culture.," *Proceedings of the Society for Experimental Biology and Medicine. Society for Experimental Biology and Medicine (New York, N.Y.)*, vol. 84, pp. 570–573, Dec. 1953.

[2] M. R. HILLEMAN and J. H. WERNER, "Recovery of new agent from patients with acute respiratory illness.," *Proceedings of the Society for Experimental Biology and Medicine. Society for Experimental Biology and Medicine (New York, N.Y.)*, vol. 85, pp. 183–188, Jan. 1954.

[3] H. S. GINSBERG, E. GOLD, W. S. JORDAN, S. KATZ, G. F. BADGER, and J. H. DINGLE, "Relation of the new respiratory agents to acute respiratory diseases.," *American journal of public health and the nation's health*, vol. 45, pp. 915–922, July 1955.

[4] J. H. Dingle and A. D. Langmuir, "Epidemiology of acute, respiratory disease in military recruits.," *The American review of respiratory disease*, vol. 97, pp. Suppl:1–65, June 1968.

[5] E. JAWETZ, L. HANNA, M. SONNE, and P. THYGESON, "A laboratory infection with adenovirus type 8; laboratory and epidemiologic observations.," *American journal of hygiene*, vol. 69, pp. 13–20, Jan. 1959.

[6] R. H. Yolken, F. Lawrence, F. Leister, H. E. Takiff, and S. E. Strauss, "Gastroenteritis associated with enteric type adenovirus in hospitalized infants.," *The Journal of pediatrics*, vol. 101, pp. 21–26, July 1982.

[7] M. Retter, P. J. Middleton, J. S. Tam, and M. Petric, "Enteric adenoviruses: detection, replication, and significance.," *Journal of clinical microbiology*, vol. 10, pp. 574–578, Oct. 1979.

[8] M. Benkö and B. Harrach, "A proposal for a new (third) genus within the family Adenoviridae.," *Archives of virology*, vol. 143, no. 4, pp. 829–837, 1998.

[9] M. Benkó, P. Elo, K. Ursu, W. Ahne, S. E. LaPatra, D. Thomson, and B. Harrach, "First molecular evidence for the existence of distinct fish and snake adenoviruses.," *Journal of virology*, vol. 76, pp. 10056–10059, Oct. 2002.

[10] A. J. Davison, M. Benko, and B. Harrach, "Genetic content and evolution of adenoviruses.," *Journal of General Virology*, vol. 84, pp. 2895–2908, Nov. 2003.

[11] S.-P. Chen, Y.-C. Huang, C.-H. Chiu, K.-S. Wong, Y.-L. Huang, C.-G. Huang, K.-C. Tsao, and T.-Y. Lin, "Clinical features of radiologically confirmed pneumonia due to adenovirus in children.," *Journal of clinical virology : the official publication of the Pan American Society for Clinical Virology*, vol. 56, pp. 7–12, Jan. 2013.

[12] S. Esposito, C. Daleno, G. Prunotto, A. Scala, C. Tagliabue, I. Borzani, E. Fossali, C. Pelucchi, and N. Principi, "Impact of viral infections in children with community-acquired pneumonia: results of a study of 17 respiratory viruses.," *Influenza and other respiratory viruses*, vol. 7, pp. 18–26, Jan. 2013.

[13] P. F. Lewis, M. A. Schmidt, X. Lu, D. D. Erdman, M. Campbell, A. Thomas, P. R. Cieslak, L. D. Grenz, L. Tsaknardis, C. Gleaves, B. Kendall, and D. Gilbert, "A community-based outbreak of severe respiratory illness caused by human adenovirus serotype 14.," *The Journal of infectious diseases*, vol. 199, pp. 1427–1434, May 2009.

[14] F. de Ory, A. Avellón, J. E. Echevarría, M. P. Sánchez-Seco, G. Trallero, M. Cabrerizo, I. Casas, F. Pozo, G. Fedele, D. Vicente, M. J. Pena, A. Moreno, J. Niubo, N. Rabella, G. Rubio, M. Pérez-Ruiz, M. Rodríguez-Iglesias, C. Gimeno, J. M. Eiros, S. Melón, M. Blasco, I. López-Miragaya, E. Varela, A. Martinez-Sapiña, G. Rodríguez, M. Á. Marcos, M. I. Gegúndez, G. Cilla, I. Gabilondo, J. M. Navarro, J. Torres, C. Aznar, A. Castellanos, M. E. Guisasola, A. I. Negredo, A. Tenorio, and S. Vázquez-Morón, "Viral infections of the central nervous system in Spain: a prospective study.," *Journal of medical virology*, vol. 85, pp. 554–562, Mar. 2013.

[15] C. Savón, B. Acosta, O. Valdés, A. Goyenechea, G. Gonzalez, A. Piñón, P. Más, D. Rosario, V. Capó, V. Kourí, P. A. Martínez, J. J. Marchena, G. González, H. Rodriguez, and M. G. Guzmán, "A myocarditis outbreak with fatal cases associated with

adenovirus subgenera C among children from Havana City in 2005.," *Journal of clinical virology : the official publication of the Pan American Society for Clinical Virology*, vol. 43, pp. 152–157, Oct. 2008.

[16] A. Shauer, I. Gotsman, A. Keren, D. R. Zwas, Y. Hellman, R. Durst, and D. Admon, "Acute viral myocarditis: current concepts in diagnosis and treatment.," *The Israel Medical Association journal : IMAJ*, vol. 15, pp. 180–185, Mar. 2013.

[17] A. Treacy, M. J. Carr, L. Dunford, G. Palacios, G. A. Cannon, A. O'Grady, J. Moran, J. Hassan, A. Loy, J. Connell, D. Devaney, P. Kelehan, and W. W. Hall, "First report of sudden death due to myocarditis caused by adenovirus serotype 3.," *Journal of clinical microbiology*, vol. 48, pp. 642–645, Feb. 2010.

[18] M. Detrait, S. De Prophetis, J.-P. Delville, and M. Komuta, "Fulminant isolated adenovirus hepatitis 5 months after haplo-identical HSCT for AML.," *Clinical case reports*, vol. 3, pp. 802–805, Oct. 2015.

[19] S. Berciaud, F. Rayne, S. Kassab, C. Jubert, M. Faure-Della Corte, F. Salin, H. Wodrich, M. E. Lafon, and Typadeno Study Members, "Adenovirus infections in Bordeaux University Hospital 2008-2010: clinical and virological features.," *Journal of clinical virology : the official publication of the Pan American Society for Clinical Virology*, vol. 54, pp. 302–307, Aug. 2012.

[20] J. C. Hierholzer, "Adenoviruses in the immunocompromised host.," *Clinical microbiology reviews*, vol. 5, pp. 262–274, July 1992.

[21] L. R. Krilov, "Adenovirus infections in the immunocompromised host.," *The Pediatric infectious disease journal*, vol. 24, pp. 555–556, June 2005.

[22] T. Lion, "Adenovirus infections in immunocompetent and immunocompromised patients.," *Clinical microbiology reviews*, vol. 27, pp. 441–462, July 2014.

[23] L. Lenaerts, E. De Clercq, and L. Naesens, "Clinical features and treatment of adenovirus infections.," *Reviews in medical virology*, vol. 18, pp. 357–374, Nov. 2008.

[24] T. Lion, R. Baumgartinger, F. Watzinger, S. Matthes-Martin, M. Suda, S. Preuner, B. Futterknecht, A. Lawitschka, C. Peters, U. Potschger, and H. Gadner, "Molecular monitoring of adenovirus in peripheral blood after allogeneic bone marrow transplantation permits early diagnosis of disseminated disease.," *Blood*, vol. 102, pp. 1114–1120, Aug. 2003.

[25] T. Lion, K. Kosulin, C. Landlinger, M. Rauch, S. Preuner, D. Jugovic, U. Pötschger, A. Lawitschka, C. Peters, G. Fritsch, and S. Matthes-Martin, "Monitoring of adenovirus load in stool by real-time PCR permits early detection of impending invasive infection in patients after allogeneic stem cell transplantation.," *Leukemia*, vol. 24, pp. 706–714, Apr. 2010.

[26] S. Esposito, V. Preti, S. Consolo, E. Nazzari, and N. Principi, "Adenovirus 36 infection and obesity.," *Journal of clinical virology : the official publication of the Pan American Society for Clinical Virology*, vol. 55, pp. 95–100, Oct. 2012.

[27] Q. Shang, H. Wang, Y. Song, L. Wei, C. Lavebratt, F. Zhang, and H. Gu, "Serological data analyses show that adenovirus 36 infection is associated with obesity: a meta-analysis involving 5739 subjects.," *Obesity (Silver Spring, Md.)*, vol. 22, pp. 895–900, Mar. 2014.

[28] T. E. SHENK, "Adenoviridae : The Viruses and Their Replication," *FUNDAMENTAL VIROLOGY*, pp. 1053–1088, 2001.

[29] Y. YABE, J. J. TRENTIN, and G. TAYLOR, "Cancer induction in hamsters by human type 12 adenovirus. Effect of age and of virus dose.," *Proceedings of the Society for Experimental Biology and Medicine. Society for Experimental Biology and Medicine (New York, N.Y.)*, vol. 111, pp. 343–344, Nov. 1962.

[30] A. B. F. virology and 2007, "Adenoviridae: the viruses and their replication."

[31] P. L. Stewart, R. M. Burnett, M. Cyrklaff, and S. D. Fuller, "Image reconstruction reveals the complex molecular organization of adenovirus.," *Cell*, vol. 67, pp. 145–154, Oct. 1991.

[32] J. van Oostrum and R. M. Burnett, "Molecular composition of the adenovirus type 2 virion.," *Journal of virology*, vol. 56, pp. 439–448, Nov. 1985.

[33] R. M. Burnett, M. G. Grütter, and J. L. White, "The structure of the adenovirus capsid. I. An envelope model of hexon at 6 A resolution.," *Journal of molecular biology*, vol. 185, pp. 105–123, Sept. 1985.

[34] C. San Martín, "Latest insights on adenovirus structure and assembly.," *Viruses*, vol. 4, pp. 847–877, May 2012.

[35] A. Gaggar, D. M. Shayakhmetov, and A. Lieber, “CD46 is a cellular receptor for group B adenoviruses.,” *Nature medicine*, vol. 9, pp. 1408–1412, Nov. 2003.

[36] P. W. Roelvink, A. Lizonova, J. G. Lee, Y. Li, J. M. Bergelson, R. W. Finberg, D. E. Brough, I. Kovesdi, and T. J. Wickham, “The coxsackievirus-adenovirus receptor protein can function as a cellular attachment protein for adenovirus serotypes from subgroups A, C, D, E, and F.,” *Journal of virology*, vol. 72, pp. 7909–7915, Oct. 1998.

[37] D. M. Shayakhmetov, A. M. Eberly, Z.-Y. Li, and A. Lieber, “Deletion of penton RGD motifs affects the efficiency of both the internalization and the endosome escape of viral particles containing adenovirus serotype 5 or 35 fiber knobs.,” *Journal of virology*, vol. 79, pp. 1053–1061, Jan. 2005.

[38] E. Everitt, L. Lutter, and L. Philipson, “Structural proteins of adenoviruses. XII. Location and neighbor relationship among proteins of adenovirion type 2 as revealed by enzymatic iodination, immunoprecipitation and chemical cross-linking.,” *Virology*, vol. 67, pp. 197–208, Sept. 1975.

[39] H. Liu, L. Jin, S. B. S. Koh, I. Atanasov, S. Schein, L. Wu, and Z. H. Zhou, “Atomic structure of human adenovirus by cryo-EM reveals interactions among protein networks.,” *Science (New York, N.Y.)*, vol. 329, pp. 1038–1043, Aug. 2010.

[40] S. Schreiner, R. Martinez, P. Groitl, F. Rayne, R. Vaillant, P. Wimmer, G. Bossis, T. Sternsdorf, L. Marcinowski, Z. Ruzsics, T. Dobner, and H. Wodrich, “Transcriptional activation of the adenoviral genome is mediated by capsid protein VI.,” *PLoS pathogens*, vol. 8, p. e1002549, Feb. 2012.

[41] C. M. Wiethoff, H. Wodrich, L. Gerace, and G. R. Nemerow, “Adenovirus protein VI mediates membrane disruption following capsid disassembly.,” *Journal of Virology*, vol. 79, pp. 1992–2000, Feb. 2005.

[42] P. K. Chatterjee, M. E. Vayda, and S. J. Flint, “Interactions among the three adenovirus core proteins.,” *Journal of virology*, vol. 55, pp. 379–386, Aug. 1985.

[43] P. K. Chatterjee, M. E. Vayda, and S. J. Flint, “Identification of proteins and protein domains that contact DNA within adenovirus nucleoprotein cores by ultraviolet light crosslinking of oligonucleotides 32P-labelled in vivo.,” *Journal of molecular biology*, vol. 188, pp. 23–37, Mar. 1986.

[44] P. K. Chatterjee, M. E. Vayda, S. F. T. E. journal, and 1986, "Adenoviral protein VII packages intracellular viral DNA throughout the early phase of infection.," *embopress.org*.

[45] P. K. Chatterjee, U. C. Yang, and S. J. Flint, "Comparison of the interactions of the adenovirus type 2 major core protein and its precursor with DNA.," *Nucleic acids research*, vol. 14, pp. 2721–2735, Mar. 1986.

[46] J. Corden, H. M. Engelking, and G. D. Pearson, "Chromatin-like organization of the adenovirus chromosome.," *Proceedings of the National Academy of Sciences of the United States of America*, vol. 73, pp. 401–404, Feb. 1976.

[47] G. R. Nemerow, L. Pache, V. Reddy, and P. L. Stewart, "Insights into adenovirus host cell interactions from structural studies.," *Virology*, vol. 384, pp. 380–388, Feb. 2009.

[48] viral zone, "Mastadenovirus: Virion."

[49] A. J. Davison, M. B. J. o. General, and 2003, "Genetic content and evolution of adenoviruses," *jgv.microbiologyresearch.org*.

[50] M. B. Mathews and T. Shenk, "Adenovirus virus-associated RNA and translation control.," *Journal of virology*, vol. 65, pp. 5657–5662, Nov. 1991.

[51] R. Weinmann, H. J. Raskas, and R. G. Roeder, "Role of DNA-dependent RNA polymerases II and III in transcription of the adenovirus genome late in productive infection.," *Proceedings of the National Academy of Sciences*, vol. 71, pp. 3426–3439, Sept. 1974.

[52] J. R. Nevins and J. E. Darnell, "Groups of adenovirus type 2 mRNA's derived from a large primary transcript: probable nuclear origin and possible common 3' ends.," *Journal of Virology*, vol. 25, pp. 811–823, Mar. 1978.

[53] G. A. Beltz and S. J. Flint, "Inhibition of HeLa cell protein synthesis during adenovirus infection: Restriction of cellular messenger RNA sequences to the nucleus," *Journal of Molecular Biology*, vol. 131, pp. 353–373, June 1979.

[54] S. S. Hong, E. Szolajska, G. Schoehn, L. Franqueville, S. Myhre, L. Lindholm, R. W. H. Ruigrok, P. Boulanger, and J. Chroboczek, "The 100K-chaperone protein from adenovirus serotype 2 (Subgroup C) assists in trimerization and nuclear localization of hexons from subgroups C and B adenoviruses.," *Journal of molecular biology*, vol. 352, pp. 125–138, Sept. 2005.

[55] M. S. Horwitz, M. D. Scharff, and J. V. Maizel, “Synthesis and assembly of adenovirus 2. I. Polypeptide synthesis, assembly of capsomeres, and morphogenesis of the virion.,” *Virology*, vol. 39, pp. 682–694, Dec. 1969.

[56] E. V. Koonin, “A common set of conserved motifs in a vast variety of putative nucleic acid-dependent ATPases including MCM proteins involved in the initiation of eukaryotic DNA replication.,” *Nucleic acids research*, vol. 21, pp. 2541–2547, June 1993.

[57] J. B. Christensen, S. A. Byrd, A. K. Walker, J. R. Strahler, P. C. Andrews, and M. J. Imperiale, “Presence of the adenovirus IVa2 protein at a single vertex of the mature virion.,” *Journal of virology*, vol. 82, pp. 9086–9093, Sept. 2008.

[58] C. M. Crosby and M. A. Barry, “IIIa deleted adenovirus as a single-cycle genome replicating vector.,” *Virology*, vol. 462-463, pp. 158–165, Aug. 2014.

[59] D. Guimet and P. Hearing, “The adenovirus L4-22K protein has distinct functions in the posttranscriptional regulation of gene expression and encapsidation of the viral genome.,” *Journal of virology*, vol. 87, pp. 7688–7699, July 2013.

[60] H.-C. Ma and P. Hearing, “Adenovirus structural protein IIIa is involved in the serotype specificity of viral DNA packaging.,” *Journal of virology*, vol. 85, pp. 7849–7855, Aug. 2011.

[61] P. Ostapchuk, M. Almond, P. H. J. o. virology, and 2011, “Characterization of empty adenovirus particles assembled in the absence of a functional adenovirus IVa2 protein,” *Am Soc Microbiol*.

[62] P. Perez-Romero, R. E. Tyler, J. R. Abend, M. D. J. of, and 2005, “Analysis of the interaction of the adenovirus L1 52/55-kilodalton and IVa2 proteins with the packaging sequence in vivo and in vitro,” *Am Soc Microbiol*.

[63] K. Wu, D. Orozco, P. H. J. o. virology, and 2012, “The adenovirus L4-22K protein is multifunctional and is an integral component of crucial aspects of infection,” *Am Soc Microbiol*.

[64] K. Wu, D. Guimet, and P. Hearing, “The adenovirus L4-33K protein regulates both late gene expression patterns and viral DNA packaging.,” *Journal of virology*, vol. 87, pp. 6739–6747, June 2013.

[65] W. Zhang, J. A. Low, J. C. J. o. virology, and 2001, "Role for the adenovirus IVa2 protein in packaging of viral DNA," *Am Soc Microbiol*.

[66] W. Zhang, R. A. Virology, and 2005, "Interaction of the adenovirus major core protein precursor, pVII, with the viral DNA packaging machinery," *Elsevier*.

[67] W. Zhang, M. I. J. o. virology, and 2007, "Interaction of the Adenovirus IVa2 Protein with Viral Packaging Sequences," *ncbi.nlm.nih.gov*.

[68] W. Zhang, M. I. J. o. virology, and 2003, "Requirement of the adenovirus IVa2 protein for virus assembly," *Am Soc Microbiol*.

[69] C. W. Anderson, P. R. Baum, and R. F. Gesteland, "Processing of adenovirus 2-induced proteins.," *Journal of virology*, vol. 12, pp. 241–252, Aug. 1973.

[70] M. Ishibashi and J. V. Maizel, "The polypeptides of adenovirus. V. Young virions, structural intermediate between top components and aged virions.," *Virology*, vol. 57, pp. 409–424, Feb. 1974.

[71] W. F. Mangel and C. S. Martin, "Structure, function and dynamics in adenovirus maturation. Viruses 6: 4536–4570," 2014.

[72] K. E. Gustin and M. J. Imperiale, "Encapsidation of viral DNA requires the adenovirus L1 52/55-kilodalton protein.," *Journal of virology*, vol. 72, pp. 7860–7870, Oct. 1998.

[73] T. B. Hasson, P. D. Soloway, D. A. Ornelles, W. Doerfler, and T. Shenk, "Adenovirus L1 52- and 55-kilodalton proteins are required for assembly of virions.," *Journal of virology*, vol. 63, pp. 3612–3621, Sept. 1989.

[74] T. B. Hasson, D. A. Ornelles, and T. Shenk, "Adenovirus L1 52- and 55-kilodalton proteins are present within assembling virions and colocalize with nuclear structures distinct from replication centers.," *Journal of virology*, vol. 66, pp. 6133–6142, Oct. 1992.

[75] G. Khittoo and J. Weber, "Genetic analysis of adenovirus type 2. VI. A temperature-sensitive mutant defective for DNA encapsidation.," *Virology*, vol. 81, pp. 126–137, Aug. 1977.

[76] C. Stephens and E. Harlow, "Differential splicing yields novel adenovirus 5 E1A mRNAs that encode 30 kd and 35 kd proteins.," *The EMBO journal*, vol. 6, pp. 2027–2035, July 1987.

[77] P. J. Ulfendahl, S. Linder, J. P. Kreivi, K. Nordqvist, C. Sevensson, H. Hultberg, and G. Akusjärvi, "A novel adenovirus-2 E1A mRNA encoding a protein with transcription activation properties.," *The EMBO journal*, vol. 6, pp. 2037–2044, July 1987.

[78] D. Kimelman, J. S. Miller, D. Porter, and B. E. Roberts, "E1a regions of the human adenoviruses and of the highly oncogenic simian adenovirus 7 are closely related.," *Journal of virology*, vol. 53, pp. 399–409, Feb. 1985.

[79] H. van Ormondt, J. Maat, and R. Dijkema, "Comparison of nucleotide sequences of the early E1a regions for subgroups A, B and C of human adenoviruses.," *Gene*, vol. 12, pp. 63–76, Dec. 1980.

[80] A. J. Berk, F. Lee, T. Harrison, J. Williams, and P. A. Sharp, "Pre-early adenovirus 5 gene product regulates synthesis of early viral messenger RNAs.," *Cell*, vol. 17, pp. 935–944, Aug. 1979.

[81] N. Jones and T. Shenk, "An adenovirus type 5 early gene function regulates expression of other early viral genes.," *Proceedings of the National Academy of Sciences of the United States of America*, vol. 76, pp. 3665–3669, Aug. 1979.

[82] F. Liu and M. R. Green, "Promoter targeting by adenovirus E1a through interaction with different cellular DNA-binding domains.," *Nature*, vol. 368, pp. 520–525, Apr. 1994.

[83] L. C. Webster and R. P. Ricciardi, "trans-dominant mutants of E1A provide genetic evidence that the zinc finger of the trans-activating domain binds a transcription factor.," *Molecular and cellular biology*, vol. 11, pp. 4287–4296, Sept. 1991.

[84] Z. Arany, D. Newsome, E. Oldread, D. M. Livingston, and R. Eckner, "A family of transcriptional adaptor proteins targeted by the E1A oncoprotein.," *Nature*, vol. 374, pp. 81–84, Mar. 1995.

[85] M. L. Avantaggiati, M. Carbone, A. Graessmann, Y. Nakatani, B. Howard, and A. S. Levine, "The SV40 large T antigen and adenovirus E1a oncoproteins interact with distinct isoforms of the transcriptional co-activator, p300.," *The EMBO journal*, vol. 15, pp. 2236–2248, May 1996.

[86] R. Eckner, M. E. Ewen, D. Newsome, M. Gerdes, J. A. DeCaprio, J. B. Lawrence, and D. M. Livingston, "Molecular cloning and functional analysis of the adenovirus E1A-

associated 300-kD protein (p300) reveals a protein with properties of a transcriptional adaptor.," *Genes & development*, vol. 8, pp. 869–884, Apr. 1994.

[87] J. R. Lundblad, R. Kwok, M. E. Laurance, M. H. Nature, and 1995, "Adenoviral EIA-associated protein p300 as a functional homologue of the transcriptional co-activator CBP," *nature.com*.

[88] K. Somasundaram and W. S. El-Deiry, "Inhibition of p53-mediated transactivation and cell cycle arrest by E1A through its p300/CBP-interacting region.," *Oncogene*, vol. 14, pp. 1047–1057, Mar. 1997.

[89] X. J. Yang, V. V. Ogryzko, J. Nishikawa, B. H. Howard, and Y. Nakatani, "A p300/CBP-associated factor that competes with the adenoviral oncoprotein E1A.," *Nature*, vol. 382, pp. 319–324, July 1996.

[90] J. L. Stevens, "Transcription Control by E1A and MAP Kinase Pathway via Sur2 Mediator Subunit," *Science*, vol. 296, pp. 755–758, Apr. 2002.

[91] A. W. Braithwaite, B. F. Cheetham, P. Li, C. R. Parish, L. K. Waldron-Stevens, and A. J. Bellett, "Adenovirus-induced alterations of the cell growth cycle: a requirement for expression of E1A but not of E1B.," *Journal of virology*, vol. 45, pp. 192–199, Jan. 1983.

[92] K. R. Spindler, D. S. Rosser, and A. J. Berk, "Analysis of adenovirus transforming proteins from early regions 1A and 1B with antisera to inducible fusion antigens produced in Escherichia coli.," *Journal of virology*, vol. 49, pp. 132–141, Jan. 1984.

[93] B. Zerler, R. J. Roberts, M. B. Mathews, and E. Moran, "Different functional domains of the adenovirus E1A gene are involved in regulation of host cell cycle products.," *Molecular and cellular biology*, vol. 7, pp. 821–829, Feb. 1987.

[94] K. Buchkovich, N. Dyson, P. Whyte, and E. Harlow, "Cellular proteins that are targets for transformation by DNA tumour viruses.," *Ciba Foundation symposium*, vol. 150, pp. 262–71– discussion 271–8, 1990.

[95] N. Dyson, K. Buchkovich, P. W. P. Takamatsu, and 1989, "Cellular proteins that are targetted by DNA tumor viruses for transformation.," *europepmc.org*.

[96] A. Giordano, C. McCall, P. Whyte, J. F. Oncogene, and 1991, "Human cyclin A and the retinoblastoma protein interact with similar but distinguishable sequences in the adenovirus E1A gene product.," *europepmc.org*.

[97] D. Barbeau, R. C. Marcellus, S. B. Biology, Cell, and 1992, "Quantitative analysis of regions of adenovirus E1A products involved in interactions with cellular proteins," *NRC Research Press*.

[98] M. Classon and N. Dyson, "p107 and p130: versatile proteins with interesting pockets.," *Experimental cell research*, vol. 264, pp. 135–147, Mar. 2001.

[99] N. Dyson, P. Guida, K. Münger, and E. Harlow, "Homologous sequences in adenovirus E1A and human papillomavirus E7 proteins mediate interaction with the same set of cellular proteins.," *Journal of Virology*, vol. 66, pp. 6893–6902, Dec. 1992.

[100] J. A. Howe, J. S. Mymryk, C. E. P. o. the, and 1990, "Retinoblastoma growth suppressor and a 300-kDa protein appear to regulate cellular DNA synthesis.," *National Acad Sciences*.

[101] G. H. Stein, M. Beeson, and L. Gordon, "Failure to phosphorylate the retinoblastoma gene product in senescent human fibroblasts.," *Science (New York, N.Y.)*, vol. 249, pp. 666–669, Aug. 1990.

[102] R. Ferrari, A. J. Berk, and S. K. Kurdistani, "Viral manipulation of the host epigenome for oncogenic transformation.," *Nature reviews. Genetics*, vol. 10, pp. 290–294, May 2009.

[103] R. Ferrari, M. Pellegrini, G. A. Horwitz, W. Xie, A. J. Berk, and S. K. Kurdistani, "Epigenetic reprogramming by adenovirus e1a.," *Science (New York, N.Y.)*, vol. 321, pp. 1086–1088, Aug. 2008.

[104] S. M. Frisch and J. S. Mymryk, "Adenovirus-5 E1A: paradox and paradigm," *Nature Reviews Molecular Cell Biology*, vol. 3, pp. 441–452, June 2002.

[105] I. Savelyeva and M. Dobbelstein, "Infection with E1B-mutant adenovirus stabilizes p53 but blocks p53 acetylation and activity through E1A.," *Oncogene*, vol. 30, pp. 865–875, Feb. 2011.

[106] S. W. Lowe and H. E. Ruley, "Stabilization of the p53 tumor suppressor is induced by adenovirus 5 E1A and accompanies apoptosis.," *Genes & development*, vol. 7, pp. 535–545, Apr. 1993.

[107] X. Zhang, R. Hussain, A. S. Turnell, J. M. Virology, and 2005, "Accumulation of p53 in response to adenovirus early region 1A sensitizes human cells to tumor necrosis factor alpha-induced apoptosis," *Elsevier*.

[108] M. Debbas and E. White, “Wild-type p53 mediates apoptosis by E1A, which is inhibited by E1B.,” *Genes & Development*, vol. 7, pp. 546–554, Apr. 1993.

[109] L. Rao, M. Debbas, P. Sabbatini, D. Hockenbery, S. Korsmeyer, and E. White, “The adenovirus E1A proteins induce apoptosis, which is inhibited by the E1B 19-kDa and Bcl-2 proteins.,” *Proceedings of the National Academy of Sciences of the United States of America*, vol. 89, pp. 7742–7746, Aug. 1992.

[110] M. Yageta, H. Tsunoda, T. Yamanaka, T. Nakajima, Y. Tomooka, N. Tsuchida, and K. Oda, “The adenovirus E1A domains required for induction of DNA rereplication in G2/M arrested cells coincide with those required for apoptosis.,” *Oncogene*, vol. 18, pp. 4767–4776, Aug. 1999.

[111] A. Cuconati, C. Mukherjee, D. Perez, and E. White, “DNA damage response and MCL-1 destruction initiate apoptosis in adenovirus-infected cells.,” *Genes & development*, vol. 17, pp. 2922–2932, Dec. 2003.

[112] A. Cuconati, K. Degenhardt, R. Sundararajan, A. Anschel, and E. White, “Bak and Bax Function To Limit Adenovirus Replication through Apoptosis Induction,” *Journal of Virology*, vol. 76, pp. 4547–4558, May 2002.

[113] P. Pelka, J. N. G. Ablack, G. J. Fonseca, A. F. Yousef, and J. S. Mymryk, “Intrinsic structural disorder in adenovirus E1A: a viral molecular hub linking multiple diverse processes.,” *Journal of virology*, vol. 82, pp. 7252–7263, Aug. 2008.

[114] Y. Liu, A. Shevchenko, A. Shevchenko, and A. J. Berk, “Adenovirus Exploits the Cellular Aggresome Response To Accelerate Inactivation of the MRN Complex,” *Journal of Virology*, vol. 79, pp. 14004–14016, Oct. 2005.

[115] P. Sarnow, C. A. Sullivan, and A. J. Levine, “A monoclonal antibody detecting the adenovirus type 5-E1b-58Kd tumor antigen: characterization of the E1b-58Kd tumor antigen in adenovirus-infected and -transformed cells.,” *Virology*, vol. 120, pp. 510–517, July 1982.

[116] A. Zantema, P. I. Schrier, A. Davis-Olivier, T. van Laar, R. T. Vaessen, and A. J. van der EB, “Adenovirus serotype determines association and localization of the large E1B tumor antigen with cellular tumor antigen p53 in transformed cells.,” *Molecular and cellular biology*, vol. 5, pp. 3084–3091, Nov. 1985.

[117] R. Garcia-Mata, Y.-S. Gao, and E. Sztul, "Hassles with taking out the garbage: aggravating aggresomes.," *Traffic (Copenhagen, Denmark)*, vol. 3, pp. 388–396, June 2002.

[118] R. R. Kopito, "Aggresomes, inclusion bodies and protein aggregation.," *Trends in cell biology*, vol. 10, pp. 524–530, Dec. 2000.

[119] M. E. Martin and A. J. Berk, "Corepressor required for adenovirus E1B 55,000-molecular-weight protein repression of basal transcription.," *Molecular and cellular biology*, vol. 19, pp. 3403–3414, May 1999.

[120] E. Querido, R. C. Marcellus, A. Lai, R. Charbonneau, J. G. Teodoro, G. Ketner, and P. E. Branton, "Regulation of p53 levels by the E1B 55-kilodalton protein and E4orf6 in adenovirus-infected cells.," *Journal of virology*, vol. 71, pp. 3788–3798, May 1997.

[121] J. G. Teodoro and P. E. Branton, "Regulation of p53-dependent apoptosis, transcriptional repression, and cell transformation by phosphorylation of the 55-kilodalton E1B protein of human adenovirus type 5.," *Journal of virology*, vol. 71, pp. 3620–3627, May 1997.

[122] P. R. Yew and A. J. Berk, "Inhibition of p53 transactivation required for transformation by adenovirus early 1B protein.," *Nature*, vol. 357, pp. 82–85, May 1992.

[123] M. A. Pennella, Y. Liu, J. L. Woo, C. A. Kim, and A. J. Berk, "Adenovirus E1B 55-kilodalton protein is a p53-SUMO1 E3 ligase that represses p53 and stimulates its nuclear export through interactions with promyelocytic leukemia nuclear bodies.," *Journal of Virology*, vol. 84, pp. 12210–12225, Dec. 2010.

[124] P. R. Yew, X. Liu, and A. J. Berk, "Adenovirus E1B oncoprotein tethers a transcriptional repression domain to p53.," *Genes & Development*, vol. 8, pp. 190–202, Jan. 1994.

[125] P. Sarnow, P. Hearing, C. W. Anderson, D. N. Halbert, T. Shenk, and A. J. Levine, "Adenovirus early region 1B 58,000-dalton tumor antigen is physically associated with an early region 4 25,000-dalton protein in productively infected cells.," *Journal of virology*, vol. 49, pp. 692–700, Mar. 1984.

[126] P. Blanchette, C. Y. Cheng, Q. Yan, G. Ketner, D. A. Ornelles, T. Dobner, R. C. Conaway, J. W. Conaway, and P. E. Branton, "Both BC-box motifs of adenovirus protein E4orf6 are required to efficiently assemble an E3 ligase complex that degrades p53.," *Molecular and Cellular Biology*, vol. 24, pp. 9619–9629, Nov. 2004.

[127] J. N. Harada, A. Shevchenko, D. C. Pallas, and A. J. Berk, "Analysis of the Adenovirus E1B-55K-Anchored Proteome Reveals Its Link to Ubiquitination Machinery," *Journal of Virology*, vol. 76, pp. 9194–9206, Sept. 2002.

[128] E. Querido, "Degradation of p53 by adenovirus E4orf6 and E1B55K proteins occurs via a novel mechanism involving a Cullin-containing complex," *Genes & Development*, vol. 15, pp. 3104–3117, Dec. 2001.

[129] A. Gupta, S. Jha, D. A. Engel, D. A. Ornelles, and A. Dutta, "Tip60 degradation by adenovirus relieves transcriptional repression of viral transcriptional activator EIA.," *Oncogene*, vol. 32, pp. 5017–5025, Oct. 2013.

[130] T. H. Stracker, C. T. Carson, and M. D. Weitzman, "Adenovirus oncoproteins inactivate the Mre11-Rad50-NBS1 DNA repair complex.," *Nature*, vol. 418, pp. 348–352, July 2002.

[131] C. T. Carson, R. A. Schwartz, T. H. Stracker, C. E. Lilley, D. V. Lee, and M. D. Weitzman, "The Mre11 complex is required for ATM activation and the G2/M checkpoint.," *The EMBO journal*, vol. 22, pp. 6610–6620, Dec. 2003.

[132] D. D'Amours and S. P. Jackson, "The MRE11 complex: at the crossroads of DNA repair and checkpoint signalling," *Nature Reviews Molecular Cell Biology*, vol. 3, pp. 317–327, May 2002.

[133] J. H. J. Petrini and T. H. Stracker, "The cellular response to DNA double-strand breaks: defining the sensors and mediators.," *Trends in cell biology*, vol. 13, pp. 458–462, Sept. 2003.

[134] M. van den Bosch, R. T. Bree, and N. F. Lowndes, "The MRN complex: coordinating and mediating the response to broken chromosomes.," *EMBO reports*, vol. 4, pp. 844–849, Sept. 2003.

[135] A. Baker, K. J. Rohleder, L. A. Hanakahi, and G. Ketner, "Adenovirus E4 34k and E1b 55k oncoproteins target host DNA ligase IV for proteasomal degradation.," *Journal of virology*, vol. 81, pp. 7034–7040, July 2007.

[136] S. Schreiner, C. Bürck, M. Glass, P. Groitl, P. Wimmer, S. Kinkley, A. Mund, R. D. Everett, and T. Dobner, "Control of human adenovirus type 5 gene expression by cel-

lular Daxx/ATRX chromatin-associated complexes.," *Nucleic acids research*, vol. 41, pp. 3532–3550, Apr. 2013.

[137] S. Schreiner, S. Kinkley, C. Bürck, A. Mund, P. Wimmer, T. Schubert, P. Groitl, H. Will, and T. Dobner, "SPOC1-mediated antiviral host cell response is antagonized early in human adenovirus type 5 infection.," *PLoS pathogens*, vol. 9, no. 11, p. e1003775, 2013.

[138] S. Schreiner, P. Wimmer, and T. Dobner, "Adenovirus degradation of cellular proteins.," *Future microbiology*, vol. 7, pp. 211–225, Feb. 2012.

[139] E. Bridge, K. Mattsson, A. Aspegren, A. S. Virology, and 2003, "Adenovirus early region 4 promotes the localization of splicing factors and viral RNA in late-phase interchromatin granule clusters," *Elsevier*.

[140] K. Nordqvist and G. Akusjärvi, "Adenovirus early region 4 stimulates mRNA accumulation via 5' introns.," *Proceedings of the National Academy of Sciences of the United States of America*, vol. 87, pp. 9543–9547, Dec. 1990.

[141] K. Nordqvist, K. Ohman, and G. Akusjärvi, "Human adenovirus encodes two proteins which have opposite effects on accumulation of alternatively spliced mRNAs.," *Molecular and cellular biology*, vol. 14, pp. 437–445, Jan. 1994.

[142] M. M. Huang, P. H. G. development, and 1989, "The adenovirus early region 4 open reading frame 6/7 protein regulates the DNA binding activity of the cellular transcription factor, E2F, through a direct complex.," *genesdev.cshlp.org*.

[143] J. S. Orlando and D. A. Ornelles, "An arginine-faced amphipathic alpha helix is required for adenovirus type 5 e4orf6 protein function.," *Journal of virology*, vol. 73, pp. 4600–4610, June 1999.

[144] S. Weigel and M. Dobbelstein, "The nuclear export signal within the E4orf6 protein of adenovirus type 5 supports virus replication and cytoplasmic accumulation of viral mRNA.," *Journal of virology*, vol. 74, pp. 764–772, Jan. 2000.

[145] T. Dobner, N. Horikoshi, S. Rubenwolf, and T. Shenk, "Blockage by adenovirus E4orf6 of transcriptional activation by the p53 tumor suppressor.," *Science (New York, N.Y.)*, vol. 272, pp. 1470–1473, June 1996.

[146] M. J. Imperiale, G. Akusjnärvi, and K. N. Leppard, "Post-transcriptional control of adenovirus gene expression.," *Current topics in microbiology and immunology*, vol. 199 (Pt 2), pp. 139–171, 1995.

[147] F. Dallaire, P. Blanchette, and P. E. Branton, "A proteomic approach to identify candidate substrates of human adenovirus E4orf6-E1B55K and other viral cullin-based E3 ubiquitin ligases.," *Journal of virology*, vol. 83, pp. 12172–12184, Dec. 2009.

[148] A. M. Soriano, L. Crisostomo, M. Mendez, D. Graves, J. R. Frost, O. Olanubi, P. F. Whyte, P. Hearing, and P. Pelka, "Adenovirus 5 E1A Interacts with E4orf3 To Regulate Viral Chromatin Organization.," *Journal of virology*, vol. 93, May 2019.

[149] J. Boyer, K. Rohleder, and G. Ketner, "Adenovirus E4 34k and E4 11k inhibit double strand break repair and are physically associated with the cellular DNA-dependent protein kinase.," *Virology*, vol. 263, pp. 307–312, Oct. 1999.

[150] R. N. Shepard and D. A. Ornelles, "Diverse Roles for E4orf3 at Late Times of Infection Revealed in an E1B 55-Kilodalton Protein Mutant Background," *Journal of Virology*, vol. 78, pp. 9924–9935, Aug. 2004.

[151] T. Carvalho, J. S. Seeler, K. Ohman, P. Jordan, U. Pettersson, G. Akusjärvi, M. Carmo-Fonseca, and A. Dejean, "Targeting of adenovirus E1A and E4-ORF3 proteins to nuclear matrix-associated PML bodies.," *The Journal of Cell Biology*, vol. 131, pp. 45–56, Oct. 1995.

[152] V. Doucas, A. M. Ishov, A. Romo, H. Juguilon, M. D. Weitzman, R. M. Evans, and G. G. Maul, "Adenovirus replication is coupled with the dynamic properties of the PML nuclear structure.," *Genes & Development*, vol. 10, pp. 196–207, Jan. 1996.

[153] F. Puvion-Dutilleul, M. K. Chelbi-Alix, M. Koken, F. Quignon, E. Puvion, and H. de Thé, "Adenovirus infection induces rearrangements in the intranuclear distribution of the nuclear body-associated PML protein.," *Experimental cell research*, vol. 218, pp. 9–16, May 1995.

[154] A. Hoppe, S. J. Beech, J. Dimmock, K. L. J. o. virology, and 2006, "Interaction of the adenovirus type 5 E4 Orf3 protein with promyelocytic leukemia protein isoform II is required for ND10 disruption," *Am Soc Microbiol*.

[155] R. E. Oncogene and 2001, "DNA viruses and viral proteins that interact with PML nuclear bodies," *nature.com*.

[156] R. D. Everett and M. K. Chelbi-Alix, "PML and PML nuclear bodies: implications in antiviral defence.," *Biochimie*, vol. 89, pp. 819–830, June 2007.

[157] J. Berscheminski, P. Groitl, T. Dobner, P. Wimmer, and S. Schreiner, "The adenoviral oncogene E1A-13S interacts with a specific isoform of the tumor suppressor PML to enhance viral transcription.," *Journal of virology*, vol. 87, pp. 965–977, Jan. 2013.

[158] A. J. Ullman and P. Hearing, "Cellular proteins PML and Daxx mediate an innate antiviral defense antagonized by the adenovirus E4 ORF3 protein.," *Journal of virology*, vol. 82, pp. 7325–7335, Aug. 2008.

[159] M. A. Yondola and P. Hearing, "The adenovirus E4 ORF3 protein binds and reorganizes the TRIM family member transcriptional intermediary factor 1 alpha.," *Journal of virology*, vol. 81, pp. 4264–4271, Apr. 2007.

[160] R. G. Bridges, S.-Y. Sohn, J. Wright, K. N. Leppard, and P. Hearing, "The Adenovirus E4-ORF3 Protein Stimulates SUMOylation of General Transcription Factor TFII-I to Direct Proteasomal Degradation.," *mBio*, vol. 7, pp. e02184–15, Jan. 2016.

[161] E. I. Vink, Y. Zheng, R. Yeasmin, T. Stamminger, L. T. Krug, and P. Hearing, "Impact of Adenovirus E4-ORF3 Oligomerization and Protein Localization on Cellular Gene Expression.," *Viruses*, vol. 7, pp. 2428–2449, May 2015.

[162] V. Patsalo, M. A. Yondola, B. Luan, I. Shoshani, C. Kisker, D. F. Green, D. P. Raleigh, and P. Hearing, "Biophysical and functional analyses suggest that adenovirus E4-ORF3 protein requires higher-order multimerization to function against promyelocytic leukemia protein nuclear bodies.," *The Journal of biological chemistry*, vol. 287, pp. 22573–22583, June 2012.

[163] H. D. Ou, W. Kwiatkowski, T. J. Deerinck, A. Noske, K. Y. Blain, H. S. Land, C. Soria, C. J. Powers, A. P. May, X. Shu, R. Y. Tsien, J. A. J. Fitzpatrick, J. A. Long, M. H. Ellisman, S. Choe, and C. C. O'Shea, "A structural basis for the assembly and functions of a viral polymer that inactivates multiple tumor suppressors.," *Cell*, vol. 151, pp. 304–319, Oct. 2012.

[164] M. Nevels, B. Täuber, E. Kremmer, T. Spruss, H. Wolf, and T. Dobner, “Transforming potential of the adenovirus type 5 E4orf3 protein.,” *Journal of virology*, vol. 73, pp. 1591–1600, Feb. 1999.

[165] M. Nevels, B. Tauber, T. Spruss, H. Wolf, and T. Dobner, “"Hit-and-Run" Transformation by Adenovirus Oncogenes,” *Journal of Virology*, vol. 75, pp. 3089–3094, Apr. 2001.

[166] M. Nevels, T. Spruss, H. Wolf, and T. Dobner, “The adenovirus E4orf6 protein contributes to malignant transformation by antagonizing E1A-induced accumulation of the tumor suppressor protein p53,” *Oncogene*, vol. 18, pp. 9–17, Jan. 1999.

[167] R. T. Javier, “Adenovirus type 9 E4 open reading frame 1 encodes a transforming protein required for the production of mammary tumors in rats.,” *Journal of virology*, vol. 68, pp. 3917–3924, June 1994.

[168] W. H. Ip and T. Dobner, “Cell transformation by the adenovirus oncogenes E1 and E4.,” *FEBS letters*, Dec. 2019.

[169] D. Ewald, M. Li, S. Efrat, G. Auer, R. J. Wall, P. A. Furth, and L. Hennighausen, “Time-sensitive reversal of hyperplasia in transgenic mice expressing SV40 T antigen.,” *Science (New York, N.Y.)*, vol. 273, pp. 1384–1386, Sept. 1996.

[170] Y. Shen, H. Zhu, and T. Shenk, “Human cytomagalovirus IE1 and IE2 proteins are mutagenic and mediate "hit-and-run" oncogenic transformation in cooperation with the adenovirus E1A proteins.,” *Proceedings of the National Academy of Sciences of the United States of America*, vol. 94, pp. 3341–3345, Apr. 1997.

[171] S.-Y. Sohn and P. Hearing, “Adenovirus Early Proteins and Host Sumoylation.,” *mBio*, vol. 7, p. 570, Sept. 2016.

[172] R. Bernardi, P. P. N. r. M. c. biology, and 2007, “Structure, dynamics and functions of promyelocytic leukaemia nuclear bodies,” *nature.com*.

[173] D. Plehn-Dujowich, P. Bell, A. M. Ishov, C. Baumann, and G. G. Maul, “Non-apoptotic chromosome condensation induced by stress: delineation of interchromosomal spaces.,” *Chromosoma*, vol. 109, pp. 266–279, July 2000.

[174] C. A. Ascoli and G. G. Maul, “Identification of a novel nuclear domain.,” *The Journal of cell biology*, vol. 112, pp. 785–795, Mar. 1991.

[175] G. Dellaire, R. W. Ching, H. Dehghani, Y. Ren, and D. P. Bazett-Jones, "The number of PML nuclear bodies increases in early S phase by a fission mechanism.," *Journal of cell science*, vol. 119, pp. 1026–1033, Mar. 2006.

[176] G. Dellaire, C. H. Eskiw, H. Dehghani, R. W. Ching, and D. P. Bazett-Jones, "Mitotic accumulations of PML protein contribute to the re-establishment of PML nuclear bodies in G1.," *Journal of cell science*, vol. 119, pp. 1034–1042, Mar. 2006.

[177] J. A. Dyck, G. G. Maul, W. H. Miller, J. D. Chen, A. Kakizuka, and R. M. Evans, "A novel macromolecular structure is a target of the promyelocyte-retinoic acid receptor oncoprotein.," *Cell*, vol. 76, pp. 333–343, Jan. 1994.

[178] M. H. Koken, F. Puvion-Dutilleul, M. C. Guillemin, A. Viron, G. Linares-Cruz, N. Stuurman, L. de Jong, C. Szostecki, F. Calvo, and C. Chomienne, "The t(15;17) translocation alters a nuclear body in a retinoic acid-reversible fashion.," *The EMBO journal*, vol. 13, pp. 1073–1083, Mar. 1994.

[179] V. Lallemand-Breitenbach and H. de Thé, "PML nuclear bodies.," *Cold Spring Harbor perspectives in biology*, vol. 2, p. a000661, May 2010.

[180] G. G. Maul, E. Yu, A. I. J. o. cellular, and 1995, "Nuclear domain 10 (ND10) associated proteins are also present in nuclear bodies and redistribute to hundreds of nuclear sites after stress," *Wiley Online Library*.

[181] P. Salomoni and P. P. Pandolfi, "The role of PML in tumor suppression.," *Cell*, vol. 108, pp. 165–170, Jan. 2002.

[182] K. Weis, S. Rambaud, C. Lavau, J. Jansen, T. Carvalho, M. Carmo-Fonseca, A. Lamond, and A. Dejean, "Retinoic acid regulates aberrant nuclear localization of PML-RAR alpha in acute promyelocytic leukemia cells.," *Cell*, vol. 76, pp. 345–356, Jan. 1994.

[183] F. M. Boisvert, M. J. Hendzel, and D. P. Bazett-Jones, "Promyelocytic leukemia (PML) nuclear bodies are protein structures that do not accumulate RNA.," *The Journal of cell biology*, vol. 148, pp. 283–292, Jan. 2000.

[184] G. Dellaire and D. P. Bazett-Jones, "PML nuclear bodies: dynamic sensors of DNA damage and cellular stress," *BioEssays*, vol. 26, no. 9, pp. 963–977, 2004.

[185] J. Borrow, A. D. Goddard, B. Gibbons, F. Katz, D. Swirsky, T. Fioretos, I. Dube, D. A. Winfield, J. Kingston, and A. Hagemeijer, "Diagnosis of acute promyelocytic leukaemia

by RT-PCR: detection of PML-RARA and RARA-PML fusion transcripts.," *British journal of haematology*, vol. 82, pp. 529–540, Nov. 1992.

[186] Z. Chen and S. J. Chen, "RARA and PML genes in acute promyelocytic leukemia.," *Leukemia & lymphoma*, vol. 8, pp. 253–260, Nov. 1992.

[187] C. Nervi, E. C. Poindexter, F. Grignani, P. P. Pandolfi, F. Lo Coco, G. Avvisati, P. G. Pelicci, and A. M. Jetten, "Characterization of the PML-RAR alpha chimeric product of the acute promyelocytic leukemia-specific t(15;17) translocation.," *Cancer research*, vol. 52, pp. 3687–3692, July 1992.

[188] P. P. Pandolfi, M. Alcalay, M. Fagioli, D. Zangrilli, A. Mencarelli, D. Diverio, A. Biondi, F. Lo Coco, A. Rambaldi, and F. Grignani, "Genomic variability and alternative splicing generate multiple PML/RAR alpha transcripts that encode aberrant PML proteins and PML/RAR alpha isoforms in acute promyelocytic leukaemia.," *The EMBO journal*, vol. 11, pp. 1397–1407, Apr. 1992.

[189] H. de Thé, C. Lavau, A. Marchio, C. Chomienne, L. Degos, and A. Dejean, "The PML-RAR alpha fusion mRNA generated by the t(15;17) translocation in acute promyelocytic leukemia encodes a functionally altered RAR.," *Cell*, vol. 66, pp. 675–684, Aug. 1991.

[190] G. Meroni and G. Diez-Roux, "TRIM/RBCC, a novel class of 'single protein RING finger' E3 ubiquitin ligases.," *BioEssays : news and reviews in molecular, cellular and developmental biology*, vol. 27, pp. 1147–1157, Nov. 2005.

[191] A. Reymond, G. Meroni, A. Fantozzi, G. Merla, S. Cairo, L. Luzi, D. Riganelli, E. Zanaria, S. Messali, S. Cainarca, A. Guffanti, S. Minucci, P. G. Pelicci, and A. Ballabio, "The tripartite motif family identifies cell compartments.," *The EMBO journal*, vol. 20, pp. 2140–2151, May 2001.

[192] K. Jensen, C. Shiels, and P. S. Freemont, "PML protein isoforms and the RBCC/TRIM motif.," *Oncogene*, vol. 20, pp. 7223–7233, Oct. 2001.

[193] M. Fagioli, M. Alcalay, P. P. Pandolfi, L. Venturini, A. Mencarelli, A. Simeone, D. Acampora, F. Grignani, and P. G. Pelicci, "Alternative splicing of PML transcripts predicts coexpression of several carboxy-terminally different protein isoforms.," *Oncogene*, vol. 7, pp. 1083–1091, June 1992.

[194] P. Brand, T. Lenser, and P. Hemmerich, "Assembly dynamics of PML nuclear bodies in living cells.," *PMC biophysics*, vol. 3, p. 3, Mar. 2010.

[195] W. Condemine, Y. Takahashi, J. Zhu, F. Puvion-Dutilleul, S. Guegan, A. Janin, and H. de Thé, "Characterization of endogenous human promyelocytic leukemia isoforms.," *Cancer research*, vol. 66, pp. 6192–6198, June 2006.

[196] S. Nisole, M. A. Maroui, X. H. Mascle, M. Aubry, and M. K. Chelbi-Alix, "Differential Roles of PML Isoforms.," *Frontiers in oncology*, vol. 3, p. 125, 2013.

[197] S. Weidtkamp-Peters, T. Lenser, D. Negorev, N. Gerstner, T. G. Hofmann, G. Schwanitz, C. Hoischen, G. Maul, P. Dittrich, and P. Hemmerich, "Dynamics of component exchange at PML nuclear bodies.," *Journal of cell science*, vol. 121, pp. 2731–2743, Aug. 2008.

[198] R. Bernardi, I. Guernah, D. Jin, S. Grisendi, A. Alimonti, J. Teruya-Feldstein, C. Cordon-Cardo, M. C. Simon, S. Rafii, and P. P. Pandolfi, "PML inhibits HIF-1alpha translation and neoangiogenesis through repression of mTOR.," *Nature*, vol. 442, pp. 779–785, Aug. 2006.

[199] A. M. Ishov, A. G. Sotnikov, D. Negorev, O. V. Vladimirova, N. Neff, T. Kamitani, E. T. Yeh, J. F. Strauss, and G. G. Maul, "PML is critical for ND10 formation and recruits the PML-interacting protein daxx to this nuclear structure when modified by SUMO-1.," *The Journal of cell biology*, vol. 147, pp. 221–234, Oct. 1999.

[200] E. Duprez, A. J. Saurin, J. M. Desterro, V. Lallemand-Breitenbach, K. Howe, M. N. Boddy, E. Solomon, H. de Thé, R. T. Hay, and P. S. Freemont, "SUMO-1 modification of the acute promyelocytic leukaemia protein PML: implications for nuclear localisation.," *Journal of cell science*, vol. 112 (Pt 3), pp. 381–393, Feb. 1999.

[201] V. Lallemand-Breitenbach, J. Zhu, F. Puvion, M. Koken, N. Honoré, A. Doubeikovsky, E. Duprez, P. P. Pandolfi, E. Puvion, P. Freemont, and H. de Thé, "Role of promyelocytic leukemia (PML) sumolation in nuclear body formation, 11S proteasome recruitment, and As2O3-induced PML or PML/retinoic acid receptor alpha degradation.," *The Journal of experimental medicine*, vol. 193, pp. 1361–1371, June 2001.

[202] T. H. Shen, H.-K. Lin, P. P. Scaglioni, T. M. Yung, and P. P. Pandolfi, "The Mechanisms of PML-Nuclear Body Formation.," *Molecular cell*, vol. 24, p. 805, Dec. 2006.

[203] S. Zhong, S. Müller, S. Ronchetti, P. S. Freemont, A. Dejean, and P. P. Pandolfi, "Role of SUMO-1-modified PML in nuclear body formation.," *Blood*, vol. 95, pp. 2748–2752, May 2000.

[204] Y. Geng, S. Monajembashi, A. Shao, D. Cui, W. He, Z. Chen, P. Hemmerich, and J. Tang, "Contribution of the C-terminal regions of promyelocytic leukemia protein (PML) isoforms II and V to PML nuclear body formation.," *The Journal of biological chemistry*, vol. 287, pp. 30729–30742, Aug. 2012.

[205] U. Sahin, O. Ferhi, M. Jeanne, S. Benhenda, C. Berthier, F. Jollivet, M. Niwa-Kawakita, O. Faklaris, N. Setterblad, H. de Thé, and V. Lallemand-Breitenbach, "Oxidative stress-induced assembly of PML nuclear bodies controls sumoylation of partner proteins.," *The Journal of cell biology*, vol. 204, pp. 931–945, Mar. 2014.

[206] X. Cheng and H.-Y. Kao, "Post-translational modifications of PML: consequences and implications.," *Frontiers in oncology*, vol. 2, p. 210, 2012.

[207] U. Sahin, H. de Thé, V. L.-B. Nucleus, and 2014, "PML nuclear bodies: assembly and oxidative stress-sensitive sumoylation," *Taylor & Francis*.

[208] M. L. Schmitz and I. Grishina, "Regulation of the tumor suppressor PML by sequential post-translational modifications.," *Frontiers in oncology*, vol. 2, p. 204, 2012.

[209] E. Van Damme, K. Laukens, T. D. I. j. of, and 2010, "A manually curated network of the PML nuclear body interactome reveals an important role for PML-NBs in SUMOylation dynamics," *ncbi.nlm.nih.gov*.

[210] D. Guan and H.-Y. Kao, "The function, regulation and therapeutic implications of the tumor suppressor protein, PML.," *Cell & bioscience*, vol. 5, p. 60, 2015.

[211] R. Bernardi and P. P. Pandolfi, "A Dialog on the First 20 Years of PML Research and the Next 20 Ahead.," *Frontiers in oncology*, vol. 4, p. 23, 2014.

[212] U. Sahin, V. Lallemand-Breitenbach, and H. de Thé, "PML nuclear bodies: regulation, function and therapeutic perspectives.," *The Journal of pathology*, vol. 234, pp. 289–291, Nov. 2014.

[213] H. Zakaryan, T. S. C. microbiology, and 2011, "Nuclear remodelling during viral infections," *Wiley Online Library*.

[214] M. Stadler, M. K. Chelbi-Alix, M. H. Koken, L. Venturini, C. Lee, A. Saïb, F. Quignon, L. Pelicano, M. C. Guillemin, and C. Schindler, "Transcriptional induction of the PML growth suppressor gene by interferons is mediated through an ISRE and a GAS element.," *Oncogene*, vol. 11, pp. 2565–2573, Dec. 1995.

[215] U. Sahin, O. Ferhi, X. Carnec, A. Z. Nature, and 2014, "Interferon controls SUMO availability via the Lin28 and let-7 axis to impede virus replication," *nature.com*.

[216] T. Grötzinger, K. Jensen, and H. Will, "The interferon (IFN)-stimulated gene Sp100 promoter contains an IFN-gamma activation site and an imperfect IFN-stimulated response element which mediate type I IFN inducibility.," *The Journal of biological chemistry*, vol. 271, pp. 25253–25260, Oct. 1996.

[217] H. H. Guldner, C. Szostecki, T. Grötzinger, and H. Will, "IFN enhance expression of Sp100, an autoantigen in primary biliary cirrhosis.," *Journal of immunology (Baltimore, Md. : 1950)*, vol. 149, pp. 4067–4073, Dec. 1992.

[218] Y.-E. Kim and J.-H. Ahn, "Positive role of promyelocytic leukemia protein in type I interferon response and its regulation by human cytomegalovirus.," *PLoS pathogens*, vol. 11, p. e1004785, Mar. 2015.

[219] Y. Chen, J. Wright, X. Meng, and K. N. Leppard, "Promyelocytic Leukemia Protein Isoform II Promotes Transcription Factor Recruitment To Activate Interferon Beta and Interferon-Responsive Gene Expression.," *Molecular and cellular biology*, vol. 35, pp. 1660–1672, May 2015.

[220] A. Lunardi, M. Gaboli, M. Giorgio, R. Rivi, A. Bygrave, M. Antoniou, D. Drabek, E. Dzierzak, M. Fagioli, L. Salmena, M. Botto, C. Cordon-Cardo, L. Luzzatto, P. G. Pelicci, F. Grosveld, and P. P. Pandolfi, "A Role for PML in Innate Immunity.," *Genes & cancer*, vol. 2, pp. 10–19, Jan. 2011.

[221] R. D. Everett, "DNA viruses and viral proteins that interact with PML nuclear bodies.," *Oncogene*, vol. 20, pp. 7266–7273, Oct. 2001.

[222] M. Scherer and T. Stamminger, "Emerging Role of PML Nuclear Bodies in Innate Immune Signaling.," *Journal of virology*, vol. 90, pp. 5850–5854, July 2016.

[223] N. Tavalai and T. Stamminger, "New insights into the role of the subnuclear structure

ND10 for viral infection.," *Biochimica et biophysica acta*, vol. 1783, pp. 2207–2221, Nov. 2008.

[224] N. Tavalai, P. Papior, S. Rechter, and T. Stamminger, "Nuclear domain 10 components promyelocytic leukemia protein and hDaxx independently contribute to an intrinsic antiviral defense against human cytomegalovirus infection.," *Journal of virology*, vol. 82, pp. 126–137, Jan. 2008.

[225] N. Tavalai, M. Adler, M. Scherer, Y. Riedl, and T. Stamminger, "Evidence for a dual antiviral role of the major nuclear domain 10 component Sp100 during the immediate-early and late phases of the human cytomegalovirus replication cycle.," *Journal of virology*, vol. 85, pp. 9447–9458, Sept. 2011.

[226] J. Berscheminski, P. Wimmer, J. Brun, W. H. Ip, P. Groitl, T. Horlacher, E. Jaffray, R. T. Hay, T. Dobner, and S. Schreiner, "Sp100 isoform-specific regulation of human adenovirus 5 gene expression.," *Journal of virology*, vol. 88, pp. 6076–6092, June 2014.

[227] S. Schreiner, P. Wimmer, H. Sirma, R. D. Everett, P. Blanchette, P. Groitl, and T. Dobner, "Proteasome-dependent degradation of Daxx by the viral E1B-55K protein in human adenovirus-infected cells.," *Journal of Virology*, vol. 84, pp. 7029–7038, July 2010.

[228] P. Wimmer, S. Schreiner, and T. Dobner, "Human pathogens and the host cell SUMOylation system.," *Journal of virology*, vol. 86, pp. 642–654, Jan. 2012.

[229] R. T. Hay, "SUMO: a history of modification.," *Molecular cell*, vol. 18, pp. 1–12, Apr. 2005.

[230] H. Saitoh and J. Hinchey, "Functional heterogeneity of small ubiquitin-related protein modifiers SUMO-1 versus SUMO-2/3.," *Journal of Biological Chemistry*, vol. 275, pp. 6252–6258, Mar. 2000.

[231] Y. Wang and M. Dasso, "SUMOylation and deSUMOylation at a glance.," *Journal of cell science*, vol. 122, pp. 4249–4252, Dec. 2009.

[232] K. M. Bohren, V. Nadkarni, J. H. Song, K. H. Gabbay, and D. Owerbach, "A M55V polymorphism in a novel SUMO gene (SUMO-4) differentially activates heat shock transcription factors and is associated with susceptibility to type I diabetes mellitus.," *The Journal of biological chemistry*, vol. 279, pp. 27233–27238, June 2004.

[233] D. Owerbach, E. M. McKay, E. T. H. Yeh, K. H. Gabbay, and K. M. Bohren, "A proline-90 residue unique to SUMO-4 prevents maturation and sumoylation.," *Biochemical and biophysical research communications*, vol. 337, pp. 517–520, Nov. 2005.

[234] Y.-C. Liang, C.-C. Lee, Y.-L. Yao, C.-C. Lai, M. L. Schmitz, and W.-M. Yang, "SUMO5, a Novel Poly-SUMO Isoform, Regulates PML Nuclear Bodies.," *Scientific reports*, vol. 6, p. 26509, May 2016.

[235] M. H. Tatham, E. Jaffray, O. A. Vaughan, J. M. P. Desterro, C. H. Botting, J. H. Naismith, and R. T. Hay, "Polymeric Chains of SUMO-2 and SUMO-3 Are Conjugated to Protein Substrates by SAE1/SAE2 and Ubc9," *Journal of Biological Chemistry*, vol. 276, pp. 35368–35374, Sept. 2001.

[236] I. Matic, M. van Hagen, J. Schimmel, B. Macek, S. C. Ogg, M. H. Tatham, R. T. Hay, A. I. Lamond, M. Mann, and A. C. O. Vertegaal, "In vivo identification of human small ubiquitin-like modifier polymerization sites by high accuracy mass spectrometry and an in vitro to in vivo strategy.," *Molecular & cellular proteomics : MCP*, vol. 7, pp. 132–144, Jan. 2008.

[237] H. A. Blomster, S. Y. Imanishi, J. Siimes, J. Kastu, N. A. Morrice, J. E. Eriksson, and L. Sistonen, "In vivo identification of sumoylation sites by a signature tag and cysteine-targeted affinity purification.," *The Journal of biological chemistry*, vol. 285, pp. 19324–19329, June 2010.

[238] F. Galisson, L. Mahrouche, M. Courcelles, E. Bonneil, S. Meloche, M. K. Chelbi-Alix, and P. Thibault, "A novel proteomics approach to identify SUMOylated proteins and their modification sites in human cells.," *Molecular & cellular proteomics : MCP*, vol. 10, p. M110.004796, Feb. 2011.

[239] I. Matic, J. Schimmel, I. A. Hendriks, M. A. van Santen, F. van de Rijke, H. van Dam, F. Gnad, M. Mann, and A. C. O. Vertegaal, "Site-specific identification of SUMO-2 targets in cells reveals an inverted SUMOylation motif and a hydrophobic cluster SUMOylation motif.," *Molecular cell*, vol. 39, pp. 641–652, Aug. 2010.

[240] *Functional Analysis of Cellular STUbLs in the Replication Cycle of Human Adenovirus Type 5 Functional Analysis of Cellular STUbLs in the Replication Cycle of Human Adenovirus Type 5 Functional analysis of cellular STUbLs in the replication cycle of human adenovirus type 5*. PhD thesis, 2017.

[241] R. T. Hay, "SUMO-specific proteases: a twist in the tail.," *Trends in cell biology*, vol. 17, pp. 370–376, Aug. 2007.

[242] D. Mukhopadhyay and M. Dasso, "Modification in reverse: the SUMO proteases.," *Trends in biochemical sciences*, vol. 32, pp. 286–295, June 2007.

[243] J. M. Desterro, M. S. Rodriguez, G. D. Kemp, and R. T. Hay, "Identification of the enzyme required for activation of the small ubiquitin-like protein SUMO-1.," *The Journal of biological chemistry*, vol. 274, pp. 10618–10624, Apr. 1999.

[244] E. S. Johnson, I. Schwienhorst, R. J. Dohmen, and G. Blobel, "The ubiquitin-like protein Smt3p is activated for conjugation to other proteins by an Aos1p/Uba2p heterodimer.," *The EMBO journal*, vol. 16, pp. 5509–5519, Sept. 1997.

[245] L. M. Lois and C. D. Lima, "Structures of the SUMO E1 provide mechanistic insights into SUMO activation and E2 recruitment to E1.," *The EMBO journal*, vol. 24, pp. 439–451, Feb. 2005.

[246] J. M. Desterro, J. Thomson, and R. T. Hay, "Ubch9 conjugates SUMO but not ubiquitin.," *FEBS Letters*, vol. 417, pp. 297–300, Nov. 1997.

[247] T. Okuma, R. Honda, G. Ichikawa, N. Tsumagari, and H. Yasuda, "In vitro SUMO-1 modification requires two enzymatic steps, E1 and E2.," *Biochemical and biophysical research communications*, vol. 254, pp. 693–698, Jan. 1999.

[248] M. S. Rodriguez, C. Dargemont, and R. T. Hay, "SUMO-1 Conjugation in VivoRequires Both a Consensus Modification Motif and Nuclear Targeting," *Journal of Biological Chemistry*, vol. 276, pp. 12654–12659, Apr. 2001.

[249] V. Bernier-Villamor, D. A. Sampson, M. J. Matunis, and C. D. Lima, "Structural basis for E2-mediated SUMO conjugation revealed by a complex between ubiquitin-conjugating enzyme Ubc9 and RanGAP1.," *Cell*, vol. 108, pp. 345–356, Feb. 2002.

[250] J.-S. Seeler and A. Dejean, "Nuclear and unclear functions of SUMO.," *Nature reviews. Molecular cell biology*, vol. 4, pp. 690–699, Sept. 2003.

[251] F. Melchior, M. Schergaut, and A. Pichler, "SUMO: ligases, isopeptidases and nuclear pores.," *Trends in biochemical sciences*, vol. 28, pp. 612–618, Nov. 2003.

[252] L. Gong and E. T. H. Yeh, "Characterization of a family of nucleolar SUMO-specific proteases with preference for SUMO-2 or SUMO-3.," *The Journal of biological chemistry*, vol. 281, pp. 15869–15877, June 2006.

[253] J. Hang and M. Dasso, "Association of the human SUMO-1 protease SENP2 with the nuclear pore.," *The Journal of biological chemistry*, vol. 277, pp. 19961–19966, May 2002.

[254] L. Texari and F. Stutz, "Sumoylation and transcription regulation at nuclear pores.," *Chromosoma*, vol. 124, pp. 45–56, Mar. 2015.

[255] A. Di Bacco, J. Ouyang, H.-Y. Lee, A. Catic, H. Ploegh, and G. Gill, "The SUMO-specific protease SENP5 is required for cell division.," *Molecular and cellular biology*, vol. 26, pp. 4489–4498, June 2006.

[256] I. A. Hendriks and A. C. O. Vertegaal, "A comprehensive compilation of SUMO proteomics.," *Nature reviews. Molecular cell biology*, vol. 17, pp. 581–595, Sept. 2016.

[257] C.-M. Hecker, M. Rabiller, K. Haglund, P. Bayer, and I. Dikic, "Specification of SUMO1- and SUMO2-interacting motifs.," *The Journal of biological chemistry*, vol. 281, pp. 16117–16127, June 2006.

[258] K. Keusekotten, V. N. Bade, K. Meyer-Teschendorf, A. M. Sriramachandran, K. Fischer-Schrader, A. Krause, C. Horst, G. Schwarz, K. Hofmann, R. J. Dohmen, and G. J. K. Praefcke, "Multivalent interactions of the SUMO-interaction motifs in RING finger protein 4 determine the specificity for chains of the SUMO.," *The Biochemical journal*, vol. 457, pp. 207–214, Jan. 2014.

[259] J. Song, L. K. Durrin, T. A. Wilkinson, T. G. Krontiris, and Y. Chen, "Identification of a SUMO-binding motif that recognizes SUMO-modified proteins.," *Proceedings of the National Academy of Sciences of the United States of America*, vol. 101, pp. 14373–14378, Oct. 2004.

[260] D.-Y. Lin, Y.-S. Huang, J.-C. Jeng, H.-Y. Kuo, C.-C. Chang, T.-T. Chao, C.-C. Ho, Y.-C. Chen, T.-P. Lin, H.-I. Fang, C.-C. Hung, C.-S. Suen, M.-J. Hwang, K.-S. Chang, G. G. Maul, and H.-M. Shih, "Role of SUMO-interacting motif in Daxx SUMO modification, subnuclear localization, and repression of sumoylated transcription factors.," *Molecular cell*, vol. 24, pp. 341–354, Nov. 2006.

[261] K. S. Sung, Y.-A. Lee, E. T. Kim, S.-R. Lee, J.-H. Ahn, and C. Y. Choi, "Role of the SUMO-interacting motif in HIPK2 targeting to the PML nuclear bodies and regulation of p53.," *Experimental cell research*, vol. 317, pp. 1060–1070, Apr. 2011.

[262] I. A. Hendriks, R. C. J. D'Souza, B. Yang, M. Verlaan-de Vries, M. Mann, and A. C. O. Vertegaal, "Uncovering global SUMOylation signaling networks in a site-specific manner.," *Nature structural & molecular biology*, vol. 21, pp. 927–936, Oct. 2014.

[263] I. A. Hendriks, L. W. Treffers, M. Verlaan-de Vries, J. V. Olsen, and A. C. O. Vertegaal, "SUMO-2 Orchestrates Chromatin Modifiers in Response to DNA Damage.," *Cell reports*, vol. 10, pp. 1778–1791, Mar. 2015.

[264] D. Nathan, D. S. P. o. the, and 2003, "Histone modifications: Now summoning sumoylation," *National Acad Sciences*.

[265] Y. Shiio and R. N. Eisenman, "Histone sumoylation is associated with transcriptional repression.," *Proceedings of the National Academy of Sciences of the United States of America*, vol. 100, pp. 13225–13230, Nov. 2003.

[266] D. A. Sampson, M. Wang, and M. J. Matunis, "The small ubiquitin-like modifier-1 (SUMO-1) consensus sequence mediates Ubc9 binding and is essential for SUMO-1 modification.," *The Journal of biological chemistry*, vol. 276, pp. 21664–21669, June 2001.

[267] S. Salinas and E. J. Kremer, "Virus induced and associated post-translational modifications.," *Biology of the cell*, vol. 104, pp. 119–120, Mar. 2012.

[268] W. H. Tsai, C. W. Chang, Y. S. Lin, W. C. I. and, and 2008, "Streptococcal pyrogenic exotoxin B-induced apoptosis in A549 cells is mediated through αvβ3 integrin and Fas," *Am Soc Microbiol*.

[269] N.-H. Zhang, L.-B. Song, X.-J. Wu, R.-P. Li, M.-S. Zeng, X.-F. Zhu, D.-S. Wan, Q. Liu, Y.-X. Zeng, and X.-S. Zhang, "Proteasome inhibitor MG-132 modifies coxsackie and adenovirus receptor expression in colon cancer cell line lovo.," *Cell cycle (Georgetown, Tex.)*, vol. 7, pp. 925–933, Apr. 2008.

[270] M. Y. Balakirev, M. Jaquinod, A. L. Haas, and J. Chroboczek, "Deubiquitinating function of adenovirus proteinase.," *Journal of Virology*, vol. 76, pp. 6323–6331, June 2002.

[271] A. F. Yousef, G. J. Fonseca, P. Pelka, J. N. G. Ablack, C. Walsh, F. A. Dick, D. P. Bazett-Jones, G. S. Shaw, and J. S. Mymryk, "Identification of a molecular recognition feature in the E1A oncoprotein that binds the SUMO conjugase UBC9 and likely interferes with polySUMOylation.," *Oncogene*, vol. 29, pp. 4693–4704, Aug. 2010.

[272] A. Ledl, D. Schmidt, and S. Müller, "Viral oncoproteins E1A and E7 and cellular LxCxE proteins repress SUMO modification of the retinoblastoma tumor suppressor.," *Oncogene*, vol. 24, pp. 3810–3818, May 2005.

[273] C. Endter, J. Kzhyshkowska, R. Stauber, and T. Dobner, "SUMO-1 modification required for transformation by adenovirus type 5 early region 1B 55-kDa oncoprotein.," *Proceedings of the National Academy of Sciences*, vol. 98, pp. 11312–11317, Sept. 2001.

[274] P. Wimmer, P. Blanchette, S. Schreiner, W. Ching, P. Groitl, J. Berscheminski, P. E. Branton, H. Will, and T. Dobner, "Cross-talk between phosphorylation and SUMOylation regulates transforming activities of an adenoviral oncoprotein.," *Oncogene*, vol. 32, pp. 1626–1637, Mar. 2013.

[275] C. Bürck, A. Mund, J. Berscheminski, L. Kieweg, S. Müncheberg, T. Dobner, and S. Schreiner, "KAP1 Is a Host Restriction Factor That Promotes Human Adenovirus E1B-55K SUMO Modification.," *Journal of Virology*, vol. 90, pp. 930–946, Jan. 2016.

[276] S. Müncheberg, R. T. Hay, W. H. Ip, T. Meyer, C. Weiß, J. Brenke, S. Masser, K. Hadian, T. Dobner, and S. Schreiner, "E1B-55K-Mediated Regulation of RNF4 SUMO-Targeted Ubiquitin Ligase Promotes Human Adenovirus Gene Expression.," *Journal of Virology*, vol. 92, p. 7029, July 2018.

[277] S.-Y. Sohn and P. Hearing, "Adenovirus regulates sumoylation of Mre11-Rad50-Nbs1 components through a paralog-specific mechanism.," *Journal of Virology*, vol. 86, pp. 9656–9665, Sept. 2012.

[278] S.-Y. Sohn and P. Hearing, "The adenovirus E4-ORF3 protein functions as a SUMO E3 ligase for TIF-1γ sumoylation and poly-SUMO chain elongation.," *Proceedings of the National Academy of Sciences of the United States of America*, vol. 113, pp. 6725–6730, June 2016.

[279] N. A. Forrester, R. N. Patel, T. Speiseder, P. Groitl, G. G. Sedgwick, N. J. Shimwell, R. I. Seed, P. Ó. Catnaigh, C. J. McCabe, G. S. Stewart, T. Dobner, R. J. A. Grand,

A. Martin, and A. S. Turnell, “Adenovirus E4orf3 targets transcriptional intermediary factor 1γ for proteasome-dependent degradation during infection.,” *Journal of Virology*, vol. 86, pp. 3167–3179, Mar. 2012.

[280] Q. Lin, Y. Kim, R. M. Alarcon, and Z. Yun, “Oxygen and Cell Fate Decisions.,” *Gene regulation and systems biology*, vol. 2, pp. 43–51, Feb. 2008.

[281] A. Sendoel and M. O. Hengartner, “Apoptotic cell death under hypoxia.,” *Physiology (Bethesda, Md.)*, vol. 29, pp. 168–176, May 2014.

[282] G. L. Semenza, “HIF-1 and human disease: one highly involved factor.,” *Genes & Development*, vol. 14, pp. 1983–1991, Aug. 2000.

[283] H. Tian, S. L. McKnight, and D. W. Russell, “Endothelial PAS domain protein 1 (EPAS1), a transcription factor selectively expressed in endothelial cells.,” *Genes & development*, vol. 11, pp. 72–82, Jan. 1997.

[284] S.-K. Park, A. M. Dadak, V. H. Haase, L. Fontana, A. J. Giaccia, and R. S. Johnson, “Hypoxia-induced gene expression occurs solely through the action of hypoxia-inducible factor 1alpha (HIF-1alpha): role of cytoplasmic trapping of HIF-2alpha.,” *Molecular and cellular biology*, vol. 23, pp. 4959–4971, July 2003.

[285] C.-J. Hu, L.-Y. Wang, L. A. Chodosh, B. Keith, and M. C. Simon, “Differential roles of hypoxia-inducible factor 1alpha (HIF-1alpha) and HIF-2alpha in hypoxic gene regulation.,” *Molecular and cellular biology*, vol. 23, pp. 9361–9374, Dec. 2003.

[286] Y. Z. Gu, S. M. MORAN, J. B. HOGENESCH, T. J. o. Liver, and 1998, “Molecular characterization and chromosomal localization of a third α-class hypoxia inducible factor subunit, HIF3α,” *ingentaconnect.com*.

[287] WHO, “Fact sheets/detail/cancer.”

[288] G. L. Wang, B. H. Jiang, E. A. Rue, and G. L. Semenza, “Hypoxia-inducible factor 1 is a basic-helix-loop-helix-PAS heterodimer regulated by cellular O2 tension.,” *Proceedings of the National Academy of Sciences of the United States of America*, vol. 92, pp. 5510–5514, June 1995.

[289] C. W. Pugh, J. F. O’Rourke, M. Nagao, J. G. J. o. Biological, and 1997, “Activation of hypoxia-inducible factor-1; definition of regulatory domains within the α subunit,” *ASBMB*.

[290] M. Ema, K. Hirota, J. Mimura, H. Abe, J. Y. T. EMBO, and 1999, "Molecular mechanisms of transcription activation by HLF and HIF1α in response to hypoxia: their stabilization and redox signal-induced interaction with CBP/p300," *embopress.org*.

[291] B. H. Jiang, J. Z. Zheng, S. W. Leung, R. Roe, and G. L. Semenza, "Transactivation and inhibitory domains of hypoxia-inducible factor 1alpha. Modulation of transcriptional activity by oxygen tension.," *The Journal of biological chemistry*, vol. 272, pp. 19253–19260, Aug. 1997.

[292] J. L. Ruas, L. Poellinger, T. P. J. o. B. Chemistry, and 2002, "Functional Analysis of Hypoxia-inducible Factor-1α-mediated Transactivation IDENTIFICATION OF AMINO ACID RESIDUES CRITICAL FOR TRANSCRIPTIONAL . . . ," *ASBMB*.

[293] L. E. Huang, J. Gu, M. Schau, and H. F. Bunn, "Regulation of hypoxia-inducible factor 1alpha is mediated by an O2-dependent degradation domain via the ubiquitin-proteasome pathway.," *Proceedings of the National Academy of Sciences of the United States of America*, vol. 95, pp. 7987–7992, July 1998.

[294] E. Y. Dimova and T. Kietzmann, "Hypoxia-inducible factors: post-translational crosstalk of signaling pathways.," *Methods in molecular biology (Clifton, N.J.)*, vol. 647, no. Chapter 13, pp. 215–236, 2010.

[295] P. J. Kallio, K. Okamoto, S. O'Brien, P. Carrero, Y. Makino, H. Tanaka, and L. Poellinger, "Signal transduction in hypoxic cells: inducible nuclear translocation and recruitment of the CBP/p300 coactivator by the hypoxia-inducible factor-1alpha.," *The EMBO journal*, vol. 17, pp. 6573–6586, Nov. 1998.

[296] S. S. Hong, H. Lee, K. K. Korean, treatment official journal of, and 2004, "HIF-1α: a valid therapeutic target for tumor therapy," *ncbi.nlm.nih.gov*.

[297] A. C. Epstein, J. M. Gleadle, L. A. McNeill, K. S. Hewitson, J. O'Rourke, D. R. Mole, M. Mukherji, E. Metzen, M. I. Wilson, A. Dhanda, Y. M. Tian, N. Masson, D. L. Hamilton, P. Jaakkola, R. Barstead, J. Hodgkin, P. H. Maxwell, C. W. Pugh, C. J. Schofield, and P. J. Ratcliffe, "C. elegans EGL-9 and mammalian homologs define a family of dioxygenases that regulate HIF by prolyl hydroxylation.," *Cell*, vol. 107, pp. 43–54, Oct. 2001.

[298] R. K. Bruick and S. L. McKnight, "A conserved family of prolyl-4-hydroxylases that modify HIF.," *Science*, vol. 294, pp. 1337–1340, Nov. 2001.

[299] P. Jaakkola, D. R. Mole, Y. M. Tian, M. I. Wilson, J. Gielbert, S. J. Gaskell, A. von Kriegsheim, H. F. Hebestreit, M. Mukherji, C. J. Schofield, P. H. Maxwell, C. W. Pugh, and P. J. Ratcliffe, "Targeting of HIF-alpha to the von Hippel-Lindau ubiquitylation complex by O2-regulated prolyl hydroxylation.," *Science*, vol. 292, pp. 468–472, Apr. 2001.

[300] F. Yu, S. B. White, Q. Zhao, and F. S. Lee, "HIF-1alpha binding to VHL is regulated by stimulus-sensitive proline hydroxylation.," *Proceedings of the National Academy of Sciences*, vol. 98, pp. 9630–9635, Aug. 2001.

[301] R. H. Wenger, D. P. Stiehl, and G. Camenisch, "Integration of oxygen signaling at the consensus HRE.," *Science's STKE : signal transduction knowledge environment*, vol. 2005, pp. re12–re12, Oct. 2005.

[302] G. K. Wilson, D. A. Tennant, and J. A. McKeating, "Hypoxia inducible factors in liver disease and hepatocellular carcinoma: Current understanding and future directions," *Journal of Hepatology*, vol. 61, pp. 1397–1406, Dec. 2014.

[303] S.-H. Bae, J.-W. Jeong, J. A. Park, S.-H. Kim, M.-K. Bae, S.-J. Choi, and K.-W. Kim, "Sumoylation increases HIF-1alpha stability and its transcriptional activity.," *Biochemical and biophysical research communications*, vol. 324, pp. 394–400, Nov. 2004.

[304] X. Han, X.-L. Wang, Q. Li, X.-X. Dong, J.-S. Zhang, and Q.-C. Yan, "HIF-1α SUMOylation affects the stability and transcriptional activity of HIF-1α in human lens epithelial cells.," *Graefe's archive for clinical and experimental ophthalmology = Albrecht von Graefes Archiv fur klinische und experimentelle Ophthalmologie*, vol. 253, pp. 1279–1290, Aug. 2015.

[305] J. Cheng, X. Kang, S. Zhang, E. Y. Cell, and 2007, "SUMO-specific protease 1 is essential for stabilization of HIF1α during hypoxia," *Elsevier*.

[306] M. Yee Koh, T. R. Spivak-Kroizman, and G. Powis, "HIF-1 regulation: not so easy come, easy go.," *Trends in biochemical sciences*, vol. 33, pp. 526–534, Nov. 2008.

[307] A. Naldini, F. Carraro, W. R. Fleischmann, and V. Bocci, "Hypoxia enhances the antiviral activity of interferons.," *Journal of interferon research*, vol. 13, pp. 127–132, Apr. 1993.

[308] I. I. L. Hwang, I. R. Watson, S. D. Der, and M. Ohh, "Loss of VHL confers hypoxia-inducible factor (HIF)-dependent resistance to vesicular stomatitis virus: role of HIF in antiviral response.," *Journal of virology*, vol. 80, pp. 10712–10723, Nov. 2006.

[309] Y.-G. Yoo, S. H. Oh, E. S. Park, H. Cho, N. Lee, H. Park, D. K. Kim, D.-Y. Yu, J. K. Seong, and M.-O. Lee, "Hepatitis B virus X protein enhances transcriptional activity of hypoxia-inducible factor-1alpha through activation of mitogen-activated protein kinase pathway.," *Journal of Biological Chemistry*, vol. 278, pp. 39076–39084, Oct. 2003.

[310] P. Birner, M. Schindl, A. Obermair, C. Plank, G. Breitenecker, and G. Oberhuber, "Over-expression of hypoxia-inducible factor 1alpha is a marker for an unfavorable prognosis in early-stage invasive cervical cancer.," *Cancer research*, vol. 60, pp. 4693–4696, Sept. 2000.

[311] M. Höckel, K. Schlenger, B. Aral, M. Mitze, U. S. C. research, and 1996, "Association between tumor hypoxia and malignant progression in advanced cancer of the uterine cervix," *AACR*.

[312] X. Tang, Q. Zhang, J. Nishitani, J. Brown, S. Shi, and A. D. Le, "Overexpression of human papillomavirus type 16 oncoproteins enhances hypoxia-inducible factor 1 alpha protein accumulation and vascular endothelial growth factor expression in human cervical carcinoma cells.," *Clinical cancer research : an official journal of the American Association for Cancer Research*, vol. 13, pp. 2568–2576, May 2007.

[313] N. Wakisaka, S. Kondo, T. Yoshizaki, S. Murono, M. Furukawa, and J. S. Pagano, "Epstein-Barr virus latent membrane protein 1 induces synthesis of hypoxia-inducible factor 1 alpha.," *Molecular and cellular biology*, vol. 24, pp. 5223–5234, June 2004.

[314] S. Kondo, S. Y. Seo, T. Yoshizaki, N. Wakisaka, M. Furukawa, I. Joab, K. L. Jang, and J. S. Pagano, "EBV latent membrane protein 1 up-regulates hypoxia-inducible factor 1alpha through Siah1-mediated down-regulation of prolyl hydroxylases 1 and 3 in nasopharyngeal epithelial cells.," *Cancer research*, vol. 66, pp. 9870–9877, Oct. 2006.

[315] W.-C. Yuan, Y.-R. Lee, S.-F. Huang, Y.-M. Lin, T.-Y. Chen, H.-C. Chung, C.-H. Tsai, H.-Y. Chen, C.-T. Chiang, C.-K. Lai, L.-T. Lu, C.-H. Chen, D.-L. Gu, Y.-S. Pu, Y.-S. Jou, K. P. Lu, P.-W. Hsiao, H.-M. Shih, and R.-H. Chen, "A Cullin3-KLHL20 Ubiquitin ligase-dependent pathway targets PML to potentiate HIF-1 signaling and prostate cancer progression.," *Cancer cell*, vol. 20, pp. 214–228, Aug. 2011.

[316] D. Hanahan, "Studies on transformation of Escherichia coli with plasmids," *Journal of Molecular Biology*, vol. 166, pp. 557–580, June 1983.

[317] P. Gripon, S. Rumin, S. Urban, J. Le Seyec, D. Glaise, I. Cannie, C. Guyomard, J. Lucas, C. Trepo, and C. Guguen-Guillouzo, "Infection of a human hepatoma cell line by hepatitis B virus.," *Proceedings of the National Academy of Sciences of the United States of America*, vol. 99, pp. 15655–15660, Nov. 2002.

[318] T. Mitsudomi, S. M. Steinberg, M. M. Nau, D. Carbone, D. D'Amico, S. Bodner, H. K. Oie, R. I. Linnoila, J. L. Mulshine, and J. D. Minna, "p53 gene mutations in non-small-cell lung cancer cell lines and their correlation with the presence of ras mutations and clinical features.," *Oncogene*, vol. 7, pp. 171–180, Jan. 1992.

[319] B. P. Lucey, W. A. Nelson-Rees, and G. M. Hutchins, *Henrietta Lacks, HeLa cells, and cell culture contamination.*, vol. 133. Sept. 2009.

[320] A. C. O. Vertegaal, S. C. Ogg, E. Jaffray, M. S. Rodriguez, R. T. Hay, J. S. Andersen, M. Mann, and A. I. Lamond, "A proteomic study of SUMO-2 target proteins.," *Journal of Biological Chemistry*, vol. 279, pp. 33791–33798, Aug. 2004.

[321] F. L. Graham, J. Smiley, W. C. Russell, and R. Nairn, "Characteristics of a human cell line transformed by DNA from human adenovirus type 5.," *Journal of General Virology*, vol. 36, pp. 59–74, July 1977.

[322] R. B. DuBridge, P. Tang, H. C. Hsia, P. M. Leong, J. H. Miller, and M. P. Calos, "Analysis of mutation in human cells by using an Epstein-Barr virus shuttle system.," *Molecular and cellular biology*, vol. 7, pp. 379–387, Jan. 1987.

[323] K. Kindsmüller, P. Groitl, B. Härtl, P. Blanchette, J. Hauber, and T. Dobner, "Intranuclear targeting and nuclear export of the adenovirus E1B-55K protein are regulated by SUMO1 conjugation.," *Proceedings of the National Academy of Sciences*, vol. 104, pp. 6684–6689, Apr. 2007.

[324] P. Blanchette, C. Y. Cheng, Q. Yan, G. Ketner, D. A. Ornelles, T. Dobner, R. C. Conaway, J. W. Conaway, and P. E. Branton, "Both BC-box motifs of adenovirus protein E4orf6 are required to efficiently assemble an E3 ligase complex that degrades p53.," *Molecular and Cellular Biology*, vol. 24, pp. 9619–9629, Nov. 2004.

[325] T. Speiseder, "Herstellung und Charakterisierung von E4orf3-und E4orf6-defekten Virusmutanten von Adenovirus Serotyp 5," 2006.

[326] S. A. Stewart, D. M. Dykxhoorn, D. Palliser, H. Mizuno, E. Y. Yu, D. S. An, D. M. Sabatini, I. S. Y. Chen, W. C. Hahn, P. A. Sharp, R. A. Weinberg, and C. D. Novina, "Lentivirus-delivered stable gene silencing by RNAi in primary cells.," *RNA (New York, N.Y.)*, vol. 9, pp. 493–501, Apr. 2003.

[327] T. Dull, R. Zufferey, M. Kelly, R. J. Mandel, M. Nguyen, D. Trono, and L. Naldini, "A third-generation lentivirus vector with a conditional packaging system.," *Journal of virology*, vol. 72, pp. 8463–8471, Nov. 1998.

[328] N. C. Reich, P. Sarnow, E. Duprey, and A. J. Levine, "Monoclonal antibodies which recognize native and denatured forms of the adenovirus DNA-binding protein.," *Virology*, vol. 128, pp. 480–484, July 1983.

[329] M. J. Marton, S. B. Baim, D. A. Ornelles, and T. Shenk, "The adenovirus E4 17-kilodalton protein complexes with the cellular transcription factor E2F, altering its DNA-binding properties and stimulating E1A-independent accumulation of E2 mRNA.," *Journal of virology*, vol. 64, pp. 2345–2359, May 1990.

[330] J. Sambrook and D. W. Russell, *Molecular cloning*. a laboratory manual, 2001.

[331] M. M. Bradford, "A rapid and sensitive method for the quantitation of microgram quantities of protein utilizing the principle of protein-dye binding.," *Analytical biochemistry*, vol. 72, pp. 248–254, May 1976.

[332] S. A. P. Jessica A. Bertout and M. C. Simon, "The impact of O," pp. 1–9, Nov. 2008.

[333] S. Gao, J. Zhou, Y. Zhao, P. Toselli, and W. Li, "Hypoxia-Response Element (HRE)–Directed Transcriptional Regulation of the Rat Lysyl Oxidase Gene in Response to Cobalt and Cadmium," *Toxicological Sciences*, vol. 132, pp. 379–389, Nov. 2012.

[334] F. Yu, S. B. White, Q. Zhao, and F. S. Lee, "Dynamic, site-specific interaction of hypoxia-inducible factor-1alpha with the von Hippel-Lindau tumor suppressor protein.," *Cancer research*, vol. 61, pp. 4136–4142, May 2001.

[335] A. Sparks, S. Dayal, J. Das, P. Robertson, S. Menendez, and M. K. Saville, "The degradation of p53 and its major E3 ligase Mdm2 is differentially dependent on the proteasomal ubiquitin receptor S5a.," *Oncogene*, vol. 33, pp. 4685–4696, Sept. 2014.

[336] F. D. Araujo, T. H. Stracker, C. T. Carson, D. V. Lee, and M. D. Weitzman, "Adenovirus Type 5 E4orf3 Protein Targets the Mre11 Complex to Cytoplasmic Aggresomes," *Journal of Virology*, vol. 79, pp. 11382–11391, Aug. 2005.

[337] R. N. Shepard and D. A. Ornelles, "E4orf3 Is Necessary for Enhanced S-Phase Replication of Cell Cycle-Restricted Subgroup C Adenoviruses," *Journal of Virology*, vol. 77, pp. 8593–8595, Aug. 2003.

[338] T. H. Stracker, D. V. Lee, C. T. Carson, F. D. Araujo, D. A. Ornelles, and M. D. Weitzman, "Serotype-Specific Reorganization of the Mre11 Complex by Adenoviral E4orf3 Proteins," *Journal of Virology*, vol. 79, pp. 6664–6673, May 2005.

[339] J. D. Evans and P. Hearing, "Relocalization of the Mre11-Rad50-Nbs1 complex by the adenovirus E4 ORF3 protein is required for viral replication.," *Journal of Virology*, vol. 79, pp. 6207–6215, May 2005.

[340] R. Bernardi and P. P. Pandolfi, "Role of PML and the PML-nuclear body in the control of programmed cell death," *Oncogene*, vol. 22, pp. 9048–9057, Dec. 2003.

[341] M. A. Berta, N. Mazure, M. Hattab, J. Pouysségur, and M. C. Brahimi-Horn, "SUMOylation of hypoxia-inducible factor-1alpha reduces its transcriptional activity.," *Biochemical and biophysical research communications*, vol. 360, pp. 646–652, Aug. 2007.

[342] S.-Y. Sohn and P. Hearing, "Mechanism of Adenovirus E4-ORF3-Mediated SUMO Modifications.," *mBio*, vol. 10, Feb. 2019.

[343] C. Y. Cheng, T. Gilson, P. Wimmer, S. Schreiner, G. Ketner, T. Dobner, P. E. Branton, and P. Blanchette, "Role of E1B55K in E4orf6/E1B55K E3 Ligase Complexes Formed by Different Human Adenovirus Serotypes," *Journal of Virology*, vol. 87, pp. 6232–6245, June 2013.

[344] J. Biddlestone, D. Bandarra, and S. Rocha, "The role of hypoxia in inflammatory disease (review).," *International journal of molecular medicine*, vol. 35, pp. 859–869, Apr. 2015.

[345] D. F. Balkovetz and J. Katz, "Bacterial invasion by a paracellular route: divide and conquer.," *Microbes and infection*, vol. 5, pp. 613–619, June 2003.

[346] A. C. Koong, E. Y. Chen, and A. J. Giaccia, "Hypoxia causes the activation of nuclear factor kappa B through the phosphorylation of I kappa B alpha on tyrosine residues.," *Cancer research*, vol. 54, pp. 1425–1430, Mar. 1994.

[347] J. A. St George, "Gene therapy progress and prospects: adenoviral vectors.," *Gene Therapy*, vol. 10, pp. 1135–1141, July 2003.

[348] L. A. Nash, R. P. G. T. w. A. B. V. Ng, P, and 2016, "Adenovirus Biology and Development as a Gene Delivery Vector."

[349] F. F. Lang, J. M. Bruner, G. N. Fuller, K. Aldape, M. D. Prados, S. Chang, M. S. Berger, M. W. McDermott, S. M. Kunwar, L. R. Junck, W. Chandler, J. A. Zwiebel, R. S. Kaplan, and W. K. A. Yung, "Phase I trial of adenovirus-mediated p53 gene therapy for recurrent glioma: biological and clinical results.," *Journal of clinical oncology : official journal of the American Society of Clinical Oncology*, vol. 21, pp. 2508–2518, July 2003.

[350] S. Kizaka-Kondoh, M. Inoue, H. Harada, and M. Hiraoka, "Tumor hypoxia: a target for selective cancer therapy.," *Cancer science*, vol. 94, pp. 1021–1028, Dec. 2003.

[351] S. Kizaka-Kondoh, S. Tanaka, H. Harada, and M. Hiraoka, "The HIF-1-active microenvironment: an environmental target for cancer therapy.," *Advanced drug delivery reviews*, vol. 61, pp. 623–632, July 2009.

[352] D. E. Post, N. S. Devi, Z. Li, D. J. Brat, B. Kaur, A. Nicholson, J. J. Olson, Z. Zhang, and E. G. Van Meir, "Cancer therapy with a replicating oncolytic adenovirus targeting the hypoxic microenvironment of tumors.," *Clinical cancer research : an official journal of the American Association for Cancer Research*, vol. 10, pp. 8603–8612, Dec. 2004.

[353] W.-K. Cho, Y. R. Seong, Y. H. Lee, M. J. Kim, K.-S. Hwang, J. Yoo, S. Choi, C.-R. Jung, and D.-S. Im, "Oncolytic effects of adenovirus mutant capable of replicating in hypoxic and normoxic regions of solid tumor.," *Molecular therapy : the journal of the American Society of Gene Therapy*, vol. 10, pp. 938–949, Nov. 2004.

[354] T. Sieber and T. Dobner, "Adenovirus Type 5 Early Region 1B 156R Protein Promotes Cell Transformation Independently of Repression of p53-Stimulated Transcription," *Journal of Virology*, vol. 81, pp. 95–105, Dec. 2006.

[355] P. E. Branton, S. T. Bayley, and F. L. Graham, "Transformation by human adenoviruses.," *Biochimica et biophysica acta*, vol. 780, no. 1, pp. 67–94, 1985.

[356] C. Endter and T. Dobner, "Cell transformation by human adenoviruses.," *Current topics in microbiology and immunology*, vol. 273, pp. 163–214, 2004.

[357] B. Tauber and T. Dobner, “Adenovirus early E4 genes in viral oncogenesis.,” *Oncogene*, vol. 20, pp. 7847–7854, Nov. 2001.

[358] M. Echavarría, “Adenoviruses in immunocompromised hosts.,” *Clinical microbiology reviews*, vol. 21, pp. 704–715, Oct. 2008.

[359] N. Tatsis and H. C. J. Ertl, “Adenoviruses as vaccine vectors.,” *Molecular therapy : the journal of the American Society of Gene Therapy*, vol. 10, pp. 616–629, Oct. 2004.

[360] G. P. Kobinger, H. Feldmann, Y. Zhi, G. Schumer, G. Gao, F. Feldmann, S. Jones, and J. M. Wilson, “Chimpanzee adenovirus vaccine protects against Zaire Ebola virus.,” *Virology*, vol. 346, pp. 394–401, Mar. 2006.

[361] A. T. Catanzaro, R. A. Koup, M. Roederer, R. T. Bailer, M. E. Enama, Z. Moodie, L. Gu, J. E. Martin, L. Novik, B. K. Chakrabarti, B. T. Butman, J. G. D. Gall, C. R. King, C. A. Andrews, R. Sheets, P. L. Gomez, J. R. Mascola, G. J. Nabel, B. S. Graham, and Vaccine Research Center 006 Study Team, “Phase 1 safety and immunogenicity evaluation of a multiclade HIV-1 candidate vaccine delivered by a replication-defective recombinant adenovirus vector.,” *The Journal of infectious diseases*, vol. 194, pp. 1638–1649, Dec. 2006.

Appendix A

Addendum

A.1 Publications and Conferences

A.1.1 Publications

Masser S, Mai J, Hofmann S, Groitl P, Maaz J, McKeating J, Schreiner S. Modulation of hypoxia by HAdV (manuscript in preparation)

Hofmann S, Mai J, **Masser S**, Groitl P, Herrmann A, Sternsdorf T, Brack.Werner R, Schreiner S, ATO (Arsenic Trioxide) effects on PML nuclear bodies reveals antiviral intervention capacity. Adv. Sci. 2020

Müncheberg S, Hay RT, Ip WH, Meyer T, WeißC, Brenke J, **Masser S**, Hadian K, Dobner T, Schreiner S. E1B-55K mediated regulation of RNF4 STUbL promotes HAdV gene expression. J Virol. 2018

Kluth M, Jung S, Habib O, Eshagzaiy M, Heinl A, Amschler N, **Masser S**, Mader M, Runte F, Barow P, Frogh S, Omari J, Möller-Koop C, Hube-Magg C, Weischenfeldt J, Korbel J, Steurer S, Krech T, Huland H, Graefen M, Minner S, Sauter G, Schlomm T, Simon R. Deletion lengthening at chromosomes 6q and 16q targets multiple tumor suppressor genes and is associated with an increasingly poor prognosis in prostate cancer. Oncotarget 2017

Tennstedt P, Strobel G, Bölch C, Grob T, Minner S, **Masser S**, Simon R. Patterns of ALK expression in different human cancer types. J Clin Pathol. 2014 Jun

Tennstedt P, Bölch C, Strobel G, Minner S, Burkhardt L, Grob T, **Masser S**, Sauter G, Schlomm T, Simon R. Patterns of TPD52 overexpression in multiple human solid tumor types analyzed by quantitative PCR. Int J Oncol. 2014

Burkhardt L, Fuchs S, Krohn A, **Masser S**, Mader M, Kluth M, Bachmann F, Huland H, Steuber T, Graefen M, Schlomm T, Minner S, Sauter G, Sirma H, Simon R. CHD1 is a 5q21 tumor suppressor required for ERG rearrangement in prostate cancer. Cancer Res. 2013 May

Weischenfeldt J, Simon R, Feuerbach L, Schlangen K, Weichenhan D, Minner S, Wuttig D, Warnatz HJ, Stehr H, Rausch T, Jäger N, Gu L, Bogatyrova O, Stütz AM, Claus R, Eils J, Eils R, Gerhäuser C, Huang PH, Hutter B, Kabbe R, Lawerenz C, Radomski S, Bartholomae CC, Fälth M, Gade S, Schmidt M, Amschler N, HaßT, Galal R, Gjoni J, Kuner R, Baer C, **Masser S**, von Kalle C, Zichner T, Benes V, Raeder B, Mader M, Amstislavskiy V, Avci M, Lehrach H, Parkhomchuk D, Sultan M, Burkhardt L, Graefen M, Huland H, Kluth M, Krohn A, Sirma H, Stumm L, Steurer S, Grupp K, S"ultmann H, Sauter G, Plass C, Brors B, Yaspo ML, Korbel JO, Schlomm T. Integrative genomic analyses reveal an androgen-driven somatic alteration landscape in early-onset prostate cancer. Cancer Cell. 2013 Feb

A.1.2 Conferences

Oral presentations

2019 - DNA Tumour Virus Conference 2019 July 9 – July 14 Stazione Marittima Congress Centre, Trieste, Italy Oral presentation: Modulation of hypoxia by HAdV

2019 - Retreat of the Institute of Virology 2019 June 18 – June 19 2019, Herrsching, Germany Oral presentation: Modulation of hypoxia by HAdV

2018 - DNA Tumour Virus Conference 2018 July 31 – August 4 2018, Madison, Wisconsin, USA Oral presentation: E4orf3 dependent modulation of hypoxia

Poster presentations

29th annual Meeting of the Society of Virology March 20 - March 23 2019, Heinrich-Heine-Universität, Düsseldorf, Germany

2016 - Retreat of the Institute of Virology 2016 June 2 – June 3 2016, Spitzingsee, Germany

A.2 Acknowledgments

First i want to thank my first supervisor PD Dr. Sabrina Schreiner, not only for the possibility to work on this fascinating project, but also for her constant guidance and support throughout a very difficult time in my life. Without her support this work wouldn't have been finished. I also want to thank her for never giving up and believing in the abilities of people.

I also want to thank my second supervisor Prof. Dr. Arnd Kieser and Dr. Tanja Bauer for their valuable discussion of my thesis.

Additionally i would like to thank all lab members of the Virology, specially our group: Peter Groitl, Miona Stubbe, Christina Weiß, Verena Plank, Lilian Goöttig, Maryam Karimi, Johanna Markert and Ute Finkel for their open discussions and constant help in the lab. Particularly i want to thank Johanna Götz, Alexander Herrmann, Christine Kunze, Samuel Hofmann, Julia Mai and Nathalie Skvorc. Besides the good lab work, they also supported a life outside the lab. I don't think there are a lot of people you can spend more than 15 hours a day and thanks to you i started to like Munich a bit more!
Extra shout out to Julia and Samuel for proof reading my thesis!

Furthermore i want to thank Jessica Schnellert, even with the distance you were always there for me and didn't hesitate to support me at the most difficult time of my life. I don't think i would have been able to do everything, if you wouldn't have supported me. Thank you for always enduring my quirks as well.

Um grande obrigado vai ao meu marido Rodrigo. Você sempre me ajudou e cuidou de mim. Sem você, eu não estaria inteira. Você me mostrou a vida e o amor.

List of Figures

List of Tables